

Tsunami Assessment Method for Nuclear Power Plants in Japan 2016

September 2016

The Tsunami Evaluation Subcommittee,
The Nuclear Civil Engineering Committee,
JSCE (Japan Society of Civil Engineers)

Preface

The 2011 Tohoku earthquake (the 2011 off the Pacific coast of Tohoku Earthquake), which struck off the Pacific coast of the Tohoku region on March 11, 2011, possessed the greatest amount of energy ever observed in an area around Japan. The earthquake recorded a moment magnitude of 9.0 with an extensive hypocentral region measuring 200km east to west and 500km north to south. Damage was of an unprecedented scale. However, the extent of the damage attributable to ground vibration was relatively small, and most of the human and economic damage resulted from the tsunami, which has been described as being of a scale occurring once every thousand years. Among the damage inflicted, the accident at Tokyo Electric Power Company's Fukushima Daiichi Nuclear Power Station developed into a severe accident that led to failure of the primary containment vessel, the first such experience in Japan. The resulting variance of radioactive materials forced the evacuation of many people and left a sizable scar on the land such that even today five years after the earthquake there are areas to which people are not permitted to return.

The direct cause of this accident lies in the seawalls, which had been erected, not being able to perform their function against the strike of a tsunami that reached a height exceeding any previous rendered assumptions and the resulting station blackout caused by inundation of seawater throughout the site. In devising the assumptions that had been worked out for tsunami height at the Fukushima Daiichi Nuclear Power Station, the "Tsunami Assessment Method for Nuclear Power Plants in Japan", published by the Japan Society of Civil Engineers in 2002, was utilized. Consequently, the engineers, researchers and the Japan Society of Civil Engineers involved in putting together this publication were subjected to criticism.

We, engineers and researchers, need to sincerely face the fact that we were unable to estimate the scale of the earthquake and tsunami that actually occurred, and to accept that our knowledge and judgments were not insufficient. It is true that improvement of our geophysical knowledge waits upon the development of various types of observation instruments, and that empirical research on mechanisms generating earthquakes only just began in the late 1960s. With respect to tsunami, the mechanism for such occurrences is thought to depend significantly on the mechanism of earthquake generation, and full-scale research in this field merely entered the initial phase in the late 1970s.

At the time of the release of the previously published "Tsunami Assessment Method for Nuclear Power Plants in Japan", the tsunami estimation technology was still under development, so the largest ever recorded tsunami was used as the benchmark on the assumption that new knowledge would subsequently be proactively incorporated. Of course, although this system took into account uncertainty to a certain extent, the end result was that a variety of phenomena were not able to be taken into account that occur in nuclear power plant systems when such a facility is struck by a tsunami exceeding all previous expectations.

Academic advances with respect to tsunami are truly progressing at a rapid rate. Even since 2002, much new knowledge has been gained and remarkable progress made in the numerical analysis technology for predicting tsunami height. Unfortunately, before these developments were sufficiently utilized, the 2011 Tohoku earthquake occurred. However, over the five years since the earthquake occurred, we have been able to conduct detailed analyses of the conditions of this tsunami to verify our previous knowledge, and we have also been able to raise the level of scholarship addressing tsunami. These results have been compiled here in this publication “Tsunami Assessment Methods for Nuclear Power Plants in Japan: 2016”. Our goal has not been to present the state of research and technology achievements accomplished up to a certain point, but to provide a starting point for advancing scholarship the next step. We hope that this publication will lead to further development of technology for assessing tsunami.

We wish to express our deepest gratitude to Tomoyuki Takahashi, Chairman of the Tsunami Evaluation Subcommittee as well as the committee members and Chief Secretary for their dedicated efforts in putting together this publication.

September 2016

Kyuichi Maruyama, Chairman
The Nuclear Civil Engineering Committee

Usage of This Publication

- This publication is comprised of main volume and appendix volume, and these are a compilation of assessment approaches for configuring hypothetical tsunami with respect to a nuclear power plant, available elementary technologies and examples of such applications. The assessment approaches and examples of such applications presented in this publication do not imply a universal maximum scale of the various types of anticipated tsunami with the goal of preventing or reducing damage inflicted by a tsunami on society, nor do they indicate a minimum required level for a hypothetical tsunami. The Tsunami Evaluation Subcommittee under the auspices of the Japan Society of Civil Engineers' Nuclear Civil Engineering Committee believes that the various conditions necessary for estimating tsunami should be configured for each individual case based on relevant knowledge in keeping with the design objectives, use and other factors.
- Any responsibility for damage or other harm to a third-party as well as damage that occurs from the use of methods and procedures for assessing hypothetical tsunami as well as applicable case studies presented in this publication lies with the user, and the Tsunami Evaluation Subcommittee under the auspices of the Japan Society of Civil Engineers' Nuclear Civil Engineering Committee as well as any other person involved with the preparation of this publication shall assume no liability whatsoever.

Chapter 1 Preface

The 2011 Tohoku earthquake (the 2011 off the Pacific coast of Tohoku Earthquake), which struck on March 11, 2011, inflicted enormous human loss and economic damage on Japan. A large part of this damage was due to the tsunami that far exceeded expectations. The tsunami, which battered coastal regions, extended beyond those areas, where flooding had been anticipated and announced by local municipalities, to swallow up thousands of people and homes. This tsunami disaster was a vivid display of how an external force exceeding what has been anticipated considerably intensifies the damage. Moreover, the tsunami flooded the site of the Fukushima Daiichi Nuclear Power Station, and was the principal factor causing a major accident there. The damage from the nuclear accident has extended across a very broad area and will continue to affect this area for a very long period of time. We must seriously confront this grave accident and clarify the mechanisms that gave rise to it as well as endeavor to prevent any such recurrence.

Although this accident involved a variety of factors, there is no mistake that the direct and proximate cause was the strike of a tsunami that far exceeded expectations. Put another way, the fact that the tsunami had been underestimated was a major cause of the accident. An equivalent or perhaps even greater issue was that insufficient assumptions had been made about what condition the nuclear power plant might lapse into when a tsunami that exceeded expectations hit, and preparations for such a contingency were insufficient. In other words, the fact that the perspective of defense in depth was lacking also brought about even more extensive damage. We must earnestly address these two points so that the lessons learned from the 2011 Tohoku earthquake may be put to good use in preventing nuclear disasters in the future.

The Headquarters for Earthquake Research Promotion, Central Disaster Management Council, local governments and other public institutions have already prepared several tsunami estimates, and these tsunamis have been considered in assessments with respect to nuclear power plants. However, many of the estimates prior to the 2011 Tohoku earthquake were principally reproductions of the largest recorded tsunami based on historical records, which were set as the standard even in considerations of uncertainty. However, the information about past tsunami that we have is not sufficient, and the 2011 Tohoku earthquake showed that there are even larger tsunamis that we did not know about. We need to humbly accept this fact, and not depend only on deterministic methods, but also, in the future, articulate assessments of tsunami hazard based on probabilistic methods.

A lot of material has already been created on methods for assessing tsunami. Among these, the “Guide to Strengthening Tsunami Countermeasures in Regional Disaster Prevention Plans”, which was published by seven government agencies concerned with coastal areas (National Land Agency, Ministry of Agriculture, Forestry and Fisheries’ Agricultural Structure Improvement Bureau, Ministry of Agriculture, Forestry and Fisheries’ Fisheries Agency, Ministry of Transport, Japan Meteorological

Agency, Ministry of Construction, and the Fire and Disaster Management Agency) in March 1998, provides a compilation of methods for surveying and assessing relevant tsunami, and constructed a foundation upon which tsunami damage is currently estimated. Moreover, the “Guide to Configuration of Tsunami Inundation Estimates”, which was published by the Ministry of Land, Infrastructure, Transport and Tourism’s Water and Disaster Management Bureau’s Seacoast Office and the National Institute for Land and Infrastructure Management’s River Department’s Coast Division in February 2012 after the 2011 Tohoku earthquake, provides a detailed compilation of methods and other techniques for simulating tsunami inundation that is necessary when local governments undertake efforts to estimate tsunami damage. These guides are applicable to general disaster prevention, but to address nuclear disaster prevention, the “Tsunami Assessment Method for Nuclear Power Plants in Japan”, the precursor to this publication, was released as a report issued by the Tsunami Evaluation Subcommittee (then), the Nuclear Civil Engineering Committee, Japan Society of Civil Engineers in February 2002. This report compiles a variety of knowledge obtained from previous research on earthquakes and tsunami into a single work, and assembles methods available for configuring design tsunami with respect to nuclear power plants. In addition, so that the publication may also be used in the field where disaster prevention is practiced, analytical methods are explained in detail. As such, it has been extensively utilized also in general disaster prevention. Subsequently, the publication “Methods of Probabilistic Tsunami Hazard Analysis” (Japan Society of Civil Engineers, 2011), which provides techniques for assessing tsunami hazards based upon probability theory, was compiled. This method has been incorporated into a technological standard (Atomic Energy Society of Japan, 2011) that sets forth the specifications and standards to serve as technical guidelines established by the Atomic Energy Society of Japan.

More than 10 years have passed since the previous publication was released (in 2002), and much new knowledge about earthquakes and tsunami has been gained. In addition, estimation methods and analytical methods have also become more advanced and cover a broader range of events. The Tsunami Assessment Panel changed its name to the Tsunami Evaluation Subcommittee in September 2013, but it has continued to study tsunami assessment technology for nuclear power plants. Accordingly, the previous publication has been wholly revised, and knowledge about the 2011 Tohoku earthquake has furthermore been taken into account in the release of this new publication. Along with assessments from the aforementioned perspective of defense in depth and probabilistic tsunami hazard analyses, numerous items have been newly added, including methods for assessing non-earthquake factors causing tsunami as well as methods for analyzing complex phenomena that arise along with a tsunami strike, including tsunami force, sediment transport and flotsam. Just as with the previous publication, this document brings together the most up-to-date available knowledge into a single volume, compiling technologies for assessing tsunami with respect to nuclear power plants.

This publication includes assessment technology that may also be used for tsunami

countermeasures other than those specific to nuclear power plants. However, it is desirable to give sufficient consideration also to the fact that tsunami countermeasure methods and approaches differ depending on their purpose, role and scale.

[Chapter 1 References]

Atomic Energy Society of Japan (2011): Implementation Standard Concerning the Tsunami Probabilistic Risk Assessment Due to Tsunami on Nuclear Power Plants, 2011(AESJ-SC-RK004E:2011).

Japan Society of Civil Engineers Nuclear Civil Engineering Committee (2002): Tsunami Assessment Method for Nuclear Power Plants in Japan.

Japan Society of Civil Engineers Nuclear Civil Engineering Committee (2011): Methods of Probabilistic Tsunami Hazard Analysis, <http://committees.jsce.or.jp/ceofnp/node/39> (Accessed on August 2016).

Ministry of Land, Infrastructure, Transport and Tourism's Water and Disaster Management Bureau's Seacoast Office and the National Institute for Land and Infrastructure Management's River Department's Coast Division (2012): Guide to Configuration of Tsunami Inundation Estimates.

National Land Agency, Ministry of Agriculture, Forestry and Fisheries' Agricultural Structure Improvement Bureau, Ministry of Agriculture, Forestry and Fisheries' Fisheries Agency, Ministry of Transport, Japan Meteorological Agency, Ministry of Construction, and the Fire and Disaster Management Agency (1998): Guide to Strengthening Tsunami Countermeasures in Regional Disaster Prevention Plans.

Chapter 2 Overview of Tsunami Assessments

2.1 Lessons of the 2011 Tohoku Earthquake

At least when it occurred, the 2011 Tohoku earthquake was the most massive earthquake with a magnitude 9.0 or higher believed to have ever been encountered in Japan's history, and the tsunami that it brought about was enormous inflicting damage across a broad swath of the country. This tsunami was gigantic, reaching a maximum run-up height of 40m, and the length of coastline where the tsunami reached a height of 5m or greater spread across an extensive area of more than 500km. The tsunami's enormity and broad area of impact was on an unprecedented scale exceeding the tsunami caused by the 1707 Hiei earthquake, which had been believed to have been the largest tsunami on record in Japan. The 2011 Tohoku earthquake and subsequent tsunami had a tremendous impact on nuclear power stations along the Pacific coast, and brought about the accident at the Fukushima Daiichi Nuclear Power Station where radioactive materials were released (hereinafter referred to as the "Fukushima Daiichi accident"). The principal cause of this accident is held to be inundation of the reactor building by seawater that ran up onto the site from the tsunami. This flooding resulted in a station blackout and the loss of safety system functions (Atomic Energy Society of Japan, 2014).

Following the Fukushima Daiichi accident, the Japan Society of Civil Engineers' Nuclear Civil Engineering Committee organized the Committee on Specific Topics Concerning Civil Engineering Technology for Nuclear Safety, which held a series of deliberations that resulted in the presentation of proposals on how nuclear safety should be structured against earthquakes, tsunami and other external natural events (Committee on Specific Topics Concerning Civil Engineering Technology for Nuclear Safety, 2013). The proposals first presented a concept that extends across the five tiers set out by the International Atomic Energy Agency ("IAEA") regarding defense in depth, which is the basic approach for nuclear safety (Figure 2.1-1). Next, the principal factor leading to the Fukushima Daiichi accident was the breakdown of the third level of defense in depth "control of accidents in design basis" due to the tsunami that exceeded the level serving as the standard for design. Furthermore, it has been pointed out that there were no effective safety functions corresponding to the fourth level of defense in depth "accident management and confinement of impact" in response to inundation by a tsunami within the site or inside buildings. Accordingly, in the awareness of the possibility that an event might occur exceeding the seismic ground motion and tsunami that serve as the benchmark, a new capability known as "Anti-Catastrophe" was proposed so that the fourth level of defense in depth is able to function effectively against such events. Resilience is the capability to sufficiently reduce the possibility that a crisis situation may result across the entire nuclear power plant system by means of emergency measures or other such means, even in situations where the external force set as the standard has been exceeded. In order to ensure this "Anti-Catastrophe", an understanding of the entire

system comprising a nuclear power plant is necessary as well as discussions transcending the barriers between various engineering fields related to each system.

The Atomic Energy Society of Japan's Investigation Committee on the Nuclear Accident at the Fukushima Daiichi Nuclear Power Plant was organized for the purpose of analyzing the Fukushima Daiichi accident and the actual circumstances of the subsequent nuclear disaster from a scientific and specialized perspective to clarify the underlying and root causes as well as to propose an approach to safety that would formulate measures, a foundation for ensuring nuclear safety and the achievement of continual safety improvements. The final report indicated that there were three direct accident causes: inadequate response to a natural disaster, inadequate severe accident management measures, and confusion during the emergency response.

Based upon the aforementioned, the following two lessons were cited in hindsight with respect to ensuring the safety of a nuclear power plant against a tsunami.

A) Preparations against a tsunami exceeding the design basis were insufficient.

B) The height of the tsunami water level which formed the design basis was insufficient.

In the Nuclear Reactor Regulation Act revised in 2013, additions were incorporated providing for a shift to safety regulations that also take into account major accidents and a shift to regulations that also reflect the latest knowledge for existing facilities (backfit) (Nuclear Regulation Authority, 2013a). The new regulatory requirements, which were reviewed and drafted following this legal revision, have enshrined (1) the enhancement of measures against events, including those exceeding the design basis so that a major accident will not result, and (2) the enhancement of measures against large-scale natural disasters so that safety functions are not lost simultaneously. In addition to earthquakes and tsunami, natural phenomena anticipated also included volcanic eruptions, tornadoes and other such events, and, with respect to tsunami, the measures also cover tsunami resulting from factors other than fault movement. Numerals (1) and (2) corresponded respectively to the previously presented lessons learned (A) and (B), and are in harmony with the approach of ensuring anti-catastrophe.

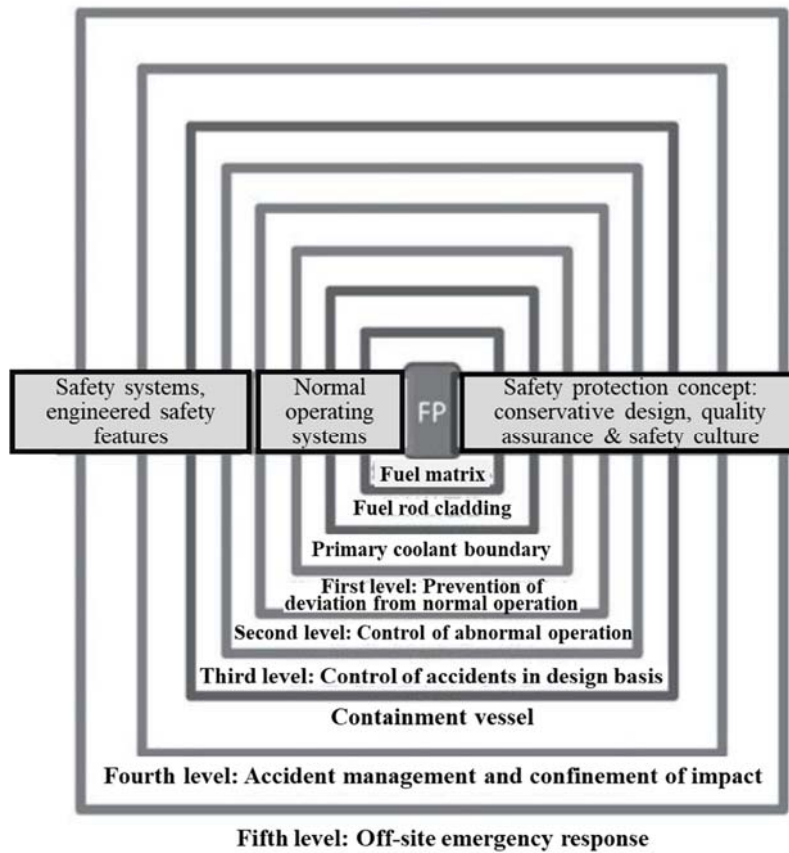


Figure 2.1-1 IAEA defense in depth (Yamaguchi, 2012)

2.2 Background and Objectives of this Publication

Endeavoring to manage and reduce risks due to tsunamis from the perspective of defense in depth is a practical method for ensuring anti-catastrophe, in other words, ensuring nuclear safety. Table 2.2-1 provides an example of how design standards are situated in relation to defense in depth. Based on this, three points are noted: (1) protection and control through the original design against events within the design basis, and, furthermore, (2) prevention of escalation of an accident attributable to events exceeding the design basis, and (3) mitigation of the impact of a major accident. Specific examples of responses at each of these levels (1) through (3) are, with respect to (1): tide embankments and other tsunami protection facilities that reduce potential flooding accompanying a tsunami; with respect to (2): the prevention of inundation of buildings by improving the water tightness of building openings in preparation for cases where the tsunami inundates a site as well as impact mitigation with alternatives in cases where electrical equipment or power supplies are impaired; and, with respect to (3): evacuation of residents and other nuclear disaster prevention measures.

With respect to examples (1) and (2) of the responses presented above, it is necessary to assess

the action of the tsunami, such as inundation, tsunami force, tsunami pressure and other properties and their impact on the respective pieces of equipment and machinery. To that end, in addition to a civil engineering field assessment of such actions, the knowledge of experts in a wide variety of fields, including nuclear, mechanical and electrical, is necessary to assess such effects. In addition, the approach to improving safety against earthquakes and tsunami with respect to nuclear power plants and the course of such assessments has also been presented in the new regulatory standards, by scholarly societies and others (Atomic Energy Society of Japan, 2014; Kameda, 2011; Joint Editorial Committee for the Reports on the Great East Japan Earthquake Disaster, 2013; Japan Association for Earthquake Engineering, 2014). These deliberations are ongoing and will likely be updated in the future as well. The IAEA has proposed the “Integrated Risk Informed Decision-Making (IRIDM)” to serve as the system for making decisions about measures addressing such issues. In so doing, deterministic tsunami hazards and probabilistic tsunami risk hazards are utilized to provide information about risks, which is necessary for rendering decisions about tsunami countermeasures (Figure 2.2-1, IAEA, 2011; Narumiya, 2014).

Accordingly, the objective of this publication is to compile deterministic tsunami hazard analysis, probabilistic tsunami hazard analysis, methods for assessing the action of inundation, tsunami force, tsunami pressure and other properties attributable to tsunami, as well as the elemental technology necessary for such methods, which are considered necessary when formulating an approach to improving safety and constructing a course for assessments that will be updated as well in the future to reflect the latest knowledge.

It is hoped that these elemental technologies will be utilized in the continuing enhancement of assessments for improving safety as indicated in the Nuclear Reactor Regulation Act (Nuclear Regulation Authority, 2013b), such as, for example, in probabilistic external event risk assessments as well as assessments of safety margins with respect to tsunami.

Table 2.2-1 IAEA’s approach to defense in depth and examples of design standard positioning
(Atomic Energy Society of Japan, 2014)

| | Defense-in-Depth Level | Objective of design | Application for Tsunami Measures |
|---------------------|-------------------------|---|--|
| Plant Design Bases | Level 1 First layer | Prevention of failure | Feasibility to maintain the normal operation Prevention of tsunami Dry-site Tsunami Height for Design standard |
| | Level2 Second layer | Detection of failure | Emergency measures for operation limiting, automatic shut-off, etc. Detection of tsunami Detection of water level |
| | Level3 Third layer | Control of accident within design basis | Automatic. Safety Process for DBA Prevention of tsunami Tsunami Height for DBA (Accident-Control Tsunami) |
| Beyond Design Basis | Level 4 Fourth layer | Management to mitigate consequence after core damage | Beyond Design Base Events or BDBA Accident Management Measures Tsunami Height for Accident Conditions (Severe-Accident Tsunami) (prevention escalating, mitigations) |
| Emergency Response | Level5 Fifth layer | Management to mitigate consequence after containment failure | Coexistence with local public Assessment of tsunami impact Minimization Risk of Radiological Consequence Disaster Prevention and Mitigation |

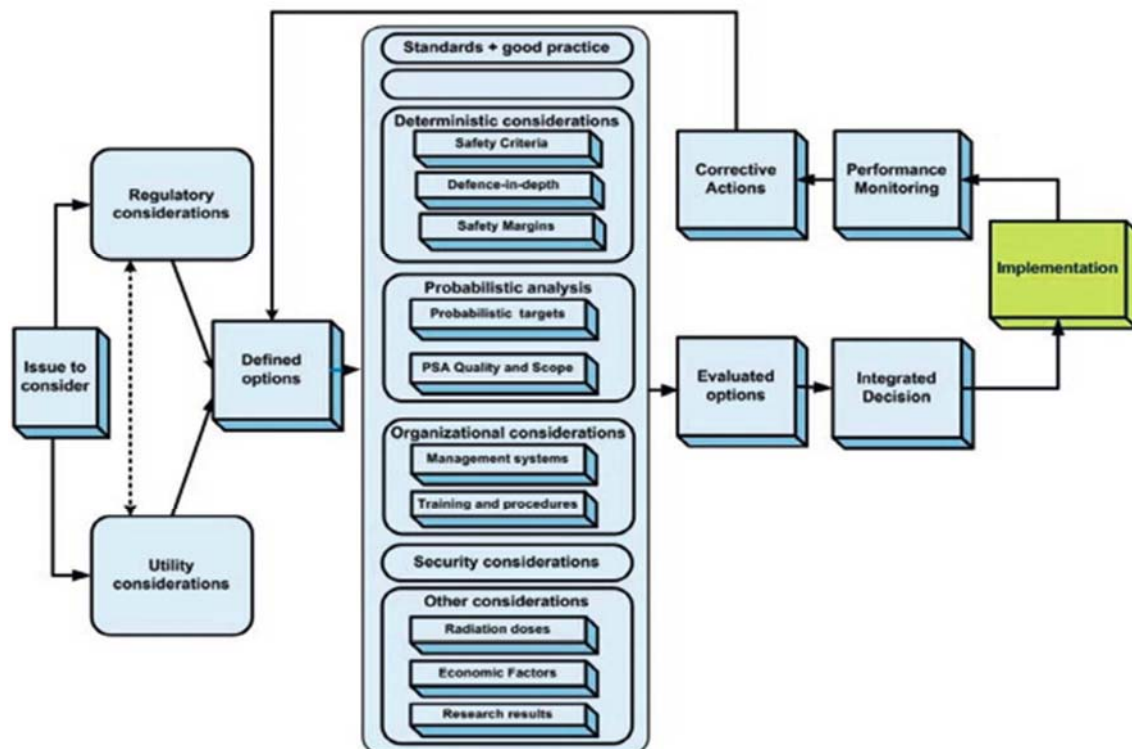


Figure 2.2-1 Key elements of the integrated risk informed decision making process (IAEA, 2011; Narumiya, 2014)

2.3 Tsunami Sources for Assessment

2.3.1 Tsunami Causal Factors

As presented in Section 2.1 of the main volume, when considering the safety of nuclear power plants in the future, many natural phenomena will be subject to consideration. With respect to tsunami as well, we need to take account of the fact that it is not just fault motions but other factors that also cause tsunami. In addition, as necessary, multiple factors should be considered as necessary for assessment selection, which are anticipated to have a significant impact on the site of a nuclear power plant. The factors causing tsunami which are regarded as subject to assessment are given below.

[Fault motions]

- Earthquakes along plate boundary
- Inland crustal earthquakes

[Non-fault motions]

- Submarine landslides
- Slope failures
- Volcanic phenomena (sector collapse, caldera collapse, etc.)

2.3.2 Combinations of Causal Factors

Taking into account the relationship between causal factors and the geological context of the area surrounding a site that is related to tsunami causal factors, consideration is given to earthquakes along plate boundary and as other earthquakes as well as combinations of earthquakes and submarine landslides or slope failures on the premise that there is a cause-and-effect relationship. Volcanic phenomena (sector collapse, caldera collapse, etc.) are understood to be independent events and mainly regarded not as being subject to combination.

2.4 Tsunami Action for Assessment

The water rise and water fall due to tsunami is subject to assessment. Moreover, as necessary, fluid force, sediment transport, flotsam and other actions resulting from tsunami at a site or in the area surrounding a site are subject to assessment.

In order to put in place a design so that important facilities are not impaired from the perspective of the impact of a tsunami on a nuclear power plant, it is important to assess the maximum water rise for the purpose of assessing any inundation of the site accompanying the water rise, and the maximum water fall to assess the impact on important safety functions involved in water intake capability or the

amount of time affecting water intake. Moreover, from the perspective of defense in depth, it is necessary to consider the impact on important facilities that actions resulting from a tsunami other than water level change have when considering the design of a nuclear power plant. Typical actions attributable to a tsunami are given below.

- Inundation, flood damage and submersion due to a rise in the water level
- Water fall affecting water intake
- Generation of fluid force (tsunami pressure, tsunami force, buoyancy force, etc.)
- Topography change due to sediment transport (erosion, sedimentation, and scouring)
- Generation, floating and collision of flotsam

2.5 Composition of this Publication

Figure 2.5-1 presents an overview of tsunami assessment and a flowchart showing the relationship of the chapters of the main volume. First, the necessary surveys (Chapter 3) are conducted and detailed assessments are then conducted. The assessment methods employed at such time may be classified into two types: Deterministic tsunami hazard analysis and Probabilistic tsunami hazard analysis.

- Deterministic tsunami hazard analysis (DTHA): For the target nuclear power plant, a tsunami source is configured that takes into account the necessary uncertainty, and action in the area surrounding the plant due to a tsunami generated by this source is computed using numerical simulation and other methods.
- Probabilistic tsunami hazard analysis (PTHA): For the target nuclear power plant, multiple tsunami causal factors are selected that are thought to have a certain impact on the target nuclear power plant, and the probability of a tsunami occurring is computed in relation to the tsunami water level, taking into account any necessary uncertainty.

Generally speaking, DTHA is mainly considered for assessments of tsunami water level in the design of outdoor facilities and soundness assessments. On the other hand, PTHA results may be linked to Probabilistic Tsunami Fragility Analysis (PTFA) and accident sequence analysis, thereby making it possible to compute core damage frequency and other tsunami risks (Tsunami PRA*).

Core damage frequency is one index showing the safety of a nuclear power plant when considering measures for quantitatively reducing tsunami risk.

*PRA: Probabilistic Risk Assessment

As with the IRIDM approach described in Section 2.2 of the main volume, DTHA, Tsunami PRA and other methods may be appropriately combined to assess risks attributable to tsunami as well as changes in risks resulting from countermeasures to determine more appropriate proposals for

countermeasures. In this publication, Chapter 4 and 5 respectively describe DTHA and PTHA with respect to Tsunami PRA. Also, assessments of the action of inundation, tsunami force and other properties attributable to tsunami necessary for assessing such tsunami risks are described in Chapter 6.

An appendix volume have been compiled to supplement this main volume. The appendix volume is a compilation of tsunami propagation calculations as well as specific methods for assessing tsunami force, seafloor topography change, flotsam collision force and so on as well as seismological and geophysical knowledge that may be utilized for configuring fault models. There are also case studies showing the application of DTHA and PTHA.

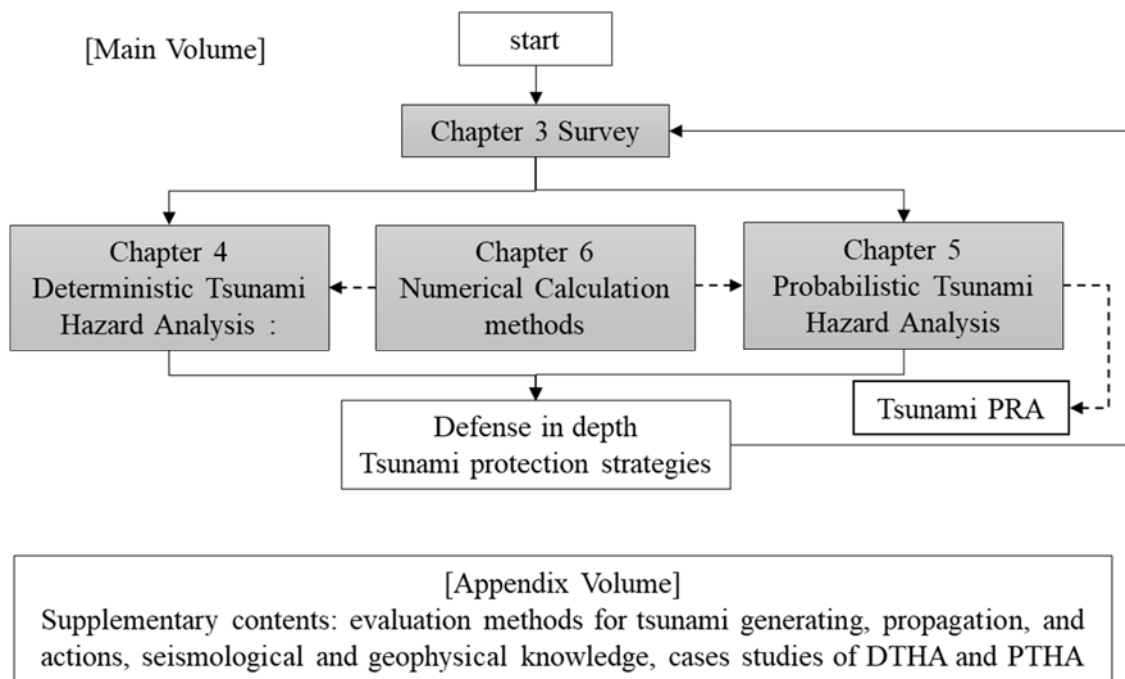


Figure 2.5-1 Overview of nuclear safety assessments with respect to tsunami and relationship of chapters

2.6 Definition of Terms

The definitions of terms used in this volume are given below.

- Examination-subject tsunami

Of the tsunami that might arise in the future in the seas around Japan including sea areas along the Japan Trench, Kuril Trench, Nankai Trough, eastern margin of the Japan Sea as well as off the coast of Chile or other distant places, tsunamis for which it is appropriate to consider that their impact on the site under examination will be maximum are defined as “examination-subject tsunami”.

- Examination-subject tsunami group

Users may conduct parametric studies using examination-subject tsunamis for the site to be examined. We define a set of those tsunamis as “examination-subject tsunami group”.

- Probable maximum tsunami

From an examination-subject tsunami group, a tsunami for which the maximum water rise or maximum water fall (for time affecting water intake depending upon power station conditions) at assessment points will be maximum is defined as a “probable maximum tsunami”.

- Parametric study

With respect to examination-subject tsunami caused by standard fault model defined with seismological parameters, investigating such parameter sensitivities onto examination-subject tsunami, within reasonable parameter ranges, using a set of numerical simulations is defined as a "parametric study". Such parametric study leads us to estimate how the uncertainty in tsunami causal factors affects a probable maximum tsunami.

- Standard fault model

A fault model for a parametric study is defined as a "standard fault model".

- Maximum water level ascent and maximum water level descent

These terms are defined as follows.

- Maximum water level ascent: The maximum rise in water level measured from the suitable tidal level on which numerical simulation is carried out (Positive value)
- Maximum water level descent: The maximum fall in water level measured from the (suitable) tidal level on which numerical simulation is carried out (Negative value)

[Chapter 2 References]

- Atomic Energy Society of Japan's Investigation Committee on the Nuclear Accident at the Fukushima Daiichi Nuclear Power Plant (2014): Full Picture of the Fukushima Daiichi Nuclear Power Station Accident and Proposals for Tomorrow: Final Report of the Society's Accident Investigation, 448p.
- Committee on Specific Topics Concerning Civil Engineering Technology for Nuclear Safety (2013): Proposal on Optimal Earthquake and Tsunami Resistant Performance of Nuclear Power Plants (Civil Engineering Perspective).
<http://committees.jsce.or.jp/2011quake/node/158> (Accessed on April 2016)
- IAEA (2011): A Framework for an Integrated Risk Informed Decision Making Process (INSAG-25), The International Nuclear Safety Group, 23p.
http://www-pub.iaea.org/MTCD/publications/PDF/Pub1499_web.pdf (Accessed on April 2016)
- Japan Association for Earthquake Engineering (2014): Tsunami Resistant Engineering for Nuclear Safety: Aiming for a Comprehensive System of Technology for Tsunami and Earthquake Defense, 283p.
- Joint Editorial Committee for the Reports on the Great East Japan Earthquake Disaster (2013): Report on the Great East Japan Earthquake Disaster: Mechanical Engineering Volume, 93p.
- Kameda, H. (2011): Earthquake Engineering Issues Pertaining to the Safety of Nuclear Power Plants, Bulletin of the Japan Association for Earthquake Engineering, No. 15, Special Issue on the Great East Japan Earthquake, pp. 97-102.
- Narumiya, Y. (2014): Issues Concerning the Decision-Making Process for Safety Improvement Measures, Atomic Energy Society of Japan 2014 Fall Meeting, 13p.
<http://www.aesj.or.jp/committees/gijiroku/etc/sc2014f-0301.pdf>
(Accessed on April 2016)
- Nuclear Regulation Authority (2013a): New Regulatory Requirements for Commercial Power Reactors, Nuclear Fuel Facilities, etc.
http://www.nsr.go.jp/activity/regulation/tekigousei/shin_kisei_kijyun.html (Accessed on April 2016)
- Nuclear Regulation Authority (2013b): Operation Guide for Safety Improvement Assessments of Commercial Power Reactors, Nuclear Fuel Facilities, p. 37.
<http://www.nsr.go.jp/data/000085457.pdf> (Accessed on April 2016)
- Yamaguchi, A. (2012): Current Status and Future Expectation concerning Probabilistic Risk Assessment of Nuclear Power Plants, Journal of the Atomic Energy Society of Japan, Vol. 54, pp. 184-190.

Chapter 3 Investigations Necessary for Tsunami Assessment

There are a broad variety of factors that cause tsunami including earthquakes along plate boundary, fault motions resulting from inland crustal earthquakes or other such seismic movements in sea areas as well as natural phenomena other than fault motions including submarine landslides, slope failures, volcanic phenomena (flank collapse, caldera collapse, etc.). Accordingly, for tsunami assessments, it is necessary to conduct appropriate investigations that take into account the relationship between tsunami causal factors and the geographic characteristics of the assessment points.

The investigations necessary for tsunami assessment are explained in detail with five classifications broadly divided in accordance to the objective: investigations of past tsunami, investigations of tsunami propagation routes, investigations concerning the configuration of tsunami source models, investigations of sediment transport due to tsunami, and investigations of tsunami debris.

3.1 Investigations of Past Tsunami

3.1.1 Literature Survey

In order to identify past tsunami that may have had a significant impact on an assessment point, a literature survey is conducted of historical records that include evidences of past tsunami, tsunami deposit and oral traditions as well as records of earthquakes that have occurred and other data. The following sorts of publications may be part of a literature survey of past tsunami.

- Watanabe, Hideo (1998): *Comprehensive Survey of Destructive Tsunami in Japan (Second Edition)*, University of Tokyo Press.
- National Astronomical Observatory, Editor: *Chronological Scientific Tables*, Maruzen.
- Usami, Tatsuo et al. (2013): *Comprehensive Survey of Destructive Earthquakes in Japan 599-2012*, University of Tokyo Press.
- Utsu, Tokuji (1982): *Table of M6.0 or Greater Earthquakes and Destructive Earthquakes Near Japan: 1885 to 1980*, *Bulletin of the Earthquake Research Institute of The University of Tokyo*, Vol. 57, pp. 401-463.
- Utsu, Tokuji et al., editors (2001): *Encyclopedia of Earthquakes (Second Edition)*, *Table of Major Earthquakes in Japan*, Asakura Publishing Co., Ltd., pp. 569-641.
- Shuto, Nobuo et al., editors (2007): *Encyclopedia of Tsunami*, *Appendix Table*, Asakura Publishing Co., Ltd., pp. 333-341.
- Abe, Katsuyuki (1988): *Quantification of Earthquake and Tsunami near Japan According to Tsunami Magnitude*, *Bulletin of the Earthquake Research Institute of The University of Tokyo*,

Vol. 63, pp.289-303.

- Abe, Katsuyuki (1999): Determination of Tsunami Magnitude M_t Using Run-up Height, Earthquake Second Compendium, Vol. 52, pp. 369-377.
- Tsunami Deposit Database: https://gbank.gsj.jp/tsunami_deposit_db/
- Trace of past tsunami Database: <http://tsunami-db.irides.tohoku.ac.jp/>
- Investigative reports by universities and other research institutions as well as the Japan Meteorological Agency and other public agencies
- Scholarly publications by researchers (series of research publications on historical tsunami by Hatori and other scholarly publications)

In cases where far-field tsunami are examined, it is conceivable that there may be effects attributable to tsunami mainly following earthquakes that are estimated to occur near plate boundaries off the coast of Chile or the Cascadia region, so data on past tsunami and other information is also collected with respect to such tsunami sources.

Of the various records concerning evidences of past tsunami, the height of traces evidencing tsunami prior to the 1896 Meiji Sanriku earthquake-tsunami have been projected by researchers based on ancient documents and other literature sources as well as oral traditions and other legends, so the reliability of tsunami height traces is closely scrutinized as necessary. With respect to the height of relatively newer traces identified since that time, the methods for investigating tsunami trace height as well as their reliability in individual references are scrupulously examined, and, in cases where reliability is suspected, it is desirable to return to the encyclopedia or other source to conduct a precise review and critically study the pros and cons of adopting such data in assessments.

With respect to past tsunami that have occurred in recent years, there are cases where water levels and waveforms have been observed, so, from tide observation data provided by the Japan Meteorological Agency and other sources with respect to tide levels (high and low water levels, etc.) at assessment points, records from the automatic tide gauge stations may be utilized.

3.1.2 Tsunami Deposit Investigations

In order to obtain information other than from literature surveys of ancient documents and other such sources about the run-up height record of past tsunami, tsunami deposit investigation are conducted as needed.

A tsunami deposit investigation surveys records based on literature surveys and topographical surveys of ancient earthquakes and tsunami that are assumed to have had an impact on the site, terrain where it appears that tsunami deposit may remain, information concerning sources supplying deposit, as well as changes and other alterations to the paleoenvironment. Next, taking into account the results

of literature and topographical surveys, fieldwork is conducted to check for any possibility that tsunami deposit may be remaining as well as examine the sedimentation environment so as to evaluate the effectiveness of on-site surveys.

In the on-site surveys, in order to acquire information about whether or not tsunami deposit is present, the frequency with which tsunami occur, their scale and other such data, exploratory drilling and other such means are employed to collect samples of sediment going back to the Jomon Transgression. With respect to the samples of event sediments obtained through exploratory drilling or other such means, in keeping with the characteristics of the survey points and the condition of the sediment, sedimentological analyses, chronological analyses, paleontological analyses and other such analyses are appropriately combined to analyze and study sedimentary structure, sediment thickness, particle size distribution, distribution elevation and planar sediment distribution, presence of oceanic origins substances, changes in the sediment environment, simultaneity with crustal movements, and other characteristics, and these are contrasted with historical records as well as the results of surveys conducted by various institutions to identify and confirm the tsunami deposit.

The “Guide for Surveying and Assessing Tsunami Deposit” (Japan Nuclear Energy Safety Organization, 2014a) and “Tsunami Deposit Handbook” (Japan Nuclear Energy Safety Organization, 2014b) serve as references for the methods for surveying and assessing tsunami deposit.

3.2 Investigations of Tsunami Propagation Routes

Topographic surveys are conducted in sea and land areas in order to gain an understanding of topographical features and propagation routes from the tsunami source related to the tsunami assessment up to the area around the assessment point (taking into consideration land run-up). As for the currently available material related to topography of marine areas, topographic data concerning the seas around Japan that may be referenced include:

- Japan Hydrographic Association: JTOPO30
- Japan Hydrographic Association: Bathymetric digital data (M7000 and M5000 series)
- Japan Hydrographic Association: Bathymetric and geological survey reports
- Japan Coast Guard: Basic maps of the sea along the coast
- Japan Coast Guard: Basic maps of the sea along the continental shelf
- Japan Coast Guard: Various nautical charts
- Japan Coast Guard: J-EGG500
- National Institute of Advanced Industrial Science and Technology: Various marine geological charts

Material that may serve as references for areas around assessment points includes:

- Coastal administrative authorities: Depth measurement data

- Port administrative authorities: Top views of ports
- Fishing port administrative authorities: Top views of fishing ports
- River administrative authorities: Results of river longitudinal and cross-section measurements

In addition, in cases where the analysis region is extremely broad, topographic data that covers the entire earth may also be used, such as:

- National Geophysical Data Center (NGDC): ETOPO1, ETOPO2 (Global Relief Model)
- International Hydrographic Organization (IHO)
- Intergovernmental Oceanographic Commission of UNESCO (IOC): GEBCO (General Bathymetric Chart of the Oceans)

On the other hand, as for currently available material pertaining to topography of land areas, the basic map data published by the Geographical Survey Institute (digital elevation models, 5m grid, 10m grid) as well as elevation data measured with aerial lasers, which has been carried out by local governments and companies, and basic urban planning maps prepared by local governments as well as other such data may be used.

When performing numerical simulation for past tsunami and assess tsunami deposit surveys, in cases where artificial modifications (structures, etc.), which did not exist when the tsunami struck previously, are reflected in the latest topographical data and cases where there is the likelihood that the impact or other effects of fault motions have significantly altered the topography or elevation around an assessment point, consideration is given to reconstructing past topographical data prior to the modification using ancient maps or other sources as necessary and then utilizing the reconstructed data.

3.3 Investigations on Configuration of Tsunami Source Models

3.3.1 Literature survey

In the configuration of tsunami source models due to earthquakes occurring along plate boundaries, users may utilize information about the earthquakes that are considered to have had an impact on the site in the past, and may collect knowledge about source mechanisms of large earthquakes not only in Japan but also the world as well as their tectonic setting. In particular, with respect to tsunami generated by earthquakes along plate boundary, it is important to utilize knowledge about tsunami generated by great earthquakes that occurred in the world in the past, including the 2011 Tohoku earthquake.

In the configuration of tsunami source models for tsunami that originated from inland crustal earthquakes offshore around the site, ones may collect information from previous literature and other sources about location, geometry, activity, length (between edges), etc. of active faults, and, as

necessary, ones may obtain records of acoustic(seismic) explorations from the Japan Coast Guard, National Institute of Advanced Industrial Science and Technology (NIAIST), Geological Survey of Japan and other such institutions, and then may reanalyze them to re-interpret acoustic profiles.

Ones may take into account reports prepared by earthquake model review committees and working groups which have been established by institutions such as the Central Disaster Prevention Council, Cabinet Office, and Ministry of Land, Infrastructure, Transport and Tourism, as references for basic information about the configuration of tsunami source models for tsunami attributable to large-scale fault motions.

In addition to referencing assessments of earthquakes and tsunami as well as long-term assessments of active faults and subduction-zone earthquakes by the Headquarters for Earthquake Research Promotion, a framework for seismotectonic divisions, which is presented in the assessment methods for earthquakes whose hypocenter parameters is difficult to identify in advance, may also be referenced for the probabilistic assessments described in Chapter 5.

In the assessment of tsunami generated from submarine landslides, slope failures, volcanic phenomena (flank collapse, caldera collapse, etc.), it is necessary to configure the tsunami source model appropriately, by referring current knowledge and surveys by businesses. Previous case studies of tsunami generated from such non-seismic events are mentioned in Section 4.6.4 of the appendix volume.

With respect to the distribution of submarine landslides, ones may reference traces of submarine landslides are indicated on submarine geological maps, made by the NIAIST/ Geological Survey of Japan. With respect to the distribution of slope failures and other such phenomena on land, ones may reference landslide topographical distribution maps and earthquake hazard stations (including landslide topographical distribution map databases) published by the National Research Institute for Earth Science and Disaster Resilience. In addition, with respect to volcanic phenomena, the NIAIST has publicly released a database of active volcanoes, and the Japan Meteorological Agency has released information on the distribution of active volcanoes in Japan. Ones may utilize these sources.

There are also cases where tsunami at the assessment point or in the surrounding area have been assessed by government institutions, in addition to tsunami source models that have been proposed in scientific literature by researchers. In the configuration of tsunami source models, ones may collect such information about the approach adopted for tsunami source model configuration as well as analysis conditions and others, and may utilize these information as necessary.

3.3.2 Offshore surveys

In the assessment of tsunami originating from crustal earthquakes, ones may conduct surveys in offshore around the power plant area, as necessary, to investigate submarine topography, geologic

stratigraphy, stratigraphic distribution, geological structures and other such features for the purpose of clarifying the location, geometry, activity, length (between edges) and other characteristics of active faults.

There are cases where it is useful to conduct offshore surveys to estimate the location, size, and ranges of collapse and sedimentation with past submarine landslides.

3.3.3 Collection and Analysis of Other Information and Knowledge

There are seismic observations, crustal movement observations and other such observations which have been conducted by businesses. Ones may utilize the observation data.

3.4 Investigations of Sediment Transport Caused by Tsunami

In assessing the impact that sediment transport caused by tsunami have on water intake at a power plant, the distribution and characteristics of bottom sediment are ascertained by means of on-site surveys and other such investigations of sea areas in front of assessment points as well as by means of literature surveys for the purpose of obtaining parameters to be used in the calculation of sediment transport employing models for forecasting topography change.

In cases where it has been determined that bottom sediment is comprised of sand and other deposits that tsunamis have likely swirled up, samples are taken to obtain data on particle size distribution, specific gravity and other properties.

In the literature available on bottom sediment, there are, for example, bottom sediment (surface deposits) distribution maps, basic maps of the sea (Japan Coast Guard), and data detailing sediment that has been collected. In addition, the methods employed in field surveys of bottom sediment include boring and side-scan sonar.

3.5 Investigations of Tsunami debris

In assessing the soundness of tsunami protection facilities and other such structures, objects are anticipated that may become tsunami debris and their physical quantities are estimated for the purpose of assessing such impact following collision of tsunami debris with a facility.

Objects that may become tsunami debris include fishing boats and other vessels navigating the areas around the power station, some of the structures installed in the tsunami run-up area around a power plant, various types of wood and lumber, as well as structures, vehicles and other such objects in the area where flooding is anticipated at a site. From among these, objects that may conceivably have an impact on power station facilities due to collisions are identified, and the physical quantities

estimated as necessary for calculating the size, weight, specific gravity and other such data necessary for calculating the impact force of debris.

[Chapter 3 References]

Japan Nuclear Energy Safety Organization (2014a): Guide for Surveying and Assessing Tsunami Deposits.

Japan Nuclear Energy Safety Organization (2014b): Tsunami Deposits Handbook.

National Research Institute for Earth Science and Disaster Resilience: Landslide Topographical Distribution Map.

http://dil-opac.bosai.go.jp/publication/nied_tech_note/

(Accessed on August 2016).

National Research Institute for Earth Science and Disaster Resilience: Seismic Hazard Stations.

<http://www.j-shis.bosai.go.jp/map/> (Accessed on August 2016)

Chapter 4 Deterministic Tsunami Hazard Analysis

4.1 Basic Matters

4.1.1 Flowchart of Deterministic Tsunami Hazard Analysis

The basic flow of a deterministic tsunami hazard analysis is shown in Figure 4.1.1-1.

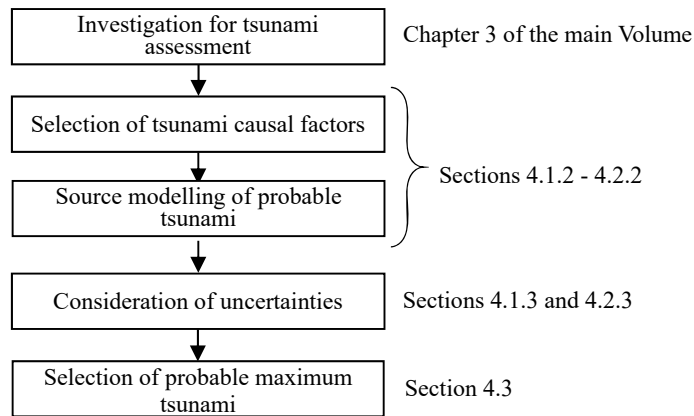


Figure 4.1.1-1. Basic flow of a deterministic tsunami hazard analysis

4.1.2 Selection of Tsunami Causal Factors

Of those tsunamis that have possibility to occur in the future, the tsunamis that are appropriately regarded as being likely to have the greatest impact on the site are set as probable tsunami. Also, the aggregate of probable tsunamis is referred to as a probable tsunami group.

In the selection of tsunami causal factors, of those tsunami causal factors listed in Section 2.3 of the main volume as well as such combinations, multiple causal factors are selected that are believed to have a significant impact on the site on the basis of survey results. In so doing, there are simplified prediction techniques, which are given below, that serve as methods for selecting causal factors with a significant impact.

- tsunami by fault motion: Abe (1989), etc.
- tsunami by slope failure: Huber and Hager (1997) (see Section 4.2.2 of the the main volume)

4.1.3 Consideration of Uncertainties

The uncertainties of the tsunami sources are taken into account in the assessment of tsunami impact on a site.

For tsunami attributable to fault motion, it is conceivable that a parametric study of fault parameters (described in Section 4.2.3.1 of the main volume) may be conducted using the standard fault model as well as the possibility examined of multiple seismically-active areas being active simultaneously.

For tsunami for which the primary cause is not fault movement, case studies are taken into account that indicate the possibility of a tsunami amplifying due to submarine landslides or earthquakes such as the 1998 Papua New Guinea earthquake (Japan Society of Civil Engineers, 2002) to also examine the likelihood that fault motion and tsunami attributable to other factors may occur almost simultaneously, and, in cases where there is the possibility of simultaneous occurrence, a review is conducted also of the superposition of such events. The following cases are examples of such occurrences.

- Superposition of tsunami resulting from submarine landslide and resulting from fault motion
- Superposition of tsunami resulting from slope failure and tsunami resulting from fault motion

The focus is on the maximum water level ascent and descent (time affecting water intake dependent upon power station conditions), and, as necessary, an examination may also be conducted of wave period, impact on geomorphic change, etc.

4.2 Preparation of Probable Tsunami

4.2.1 Fault Motion-Caused Tsunami

4.2.1.1 Basic Policy for Configuration of Tsunami Source for Probable Tsunami Caused by Fault Motion

(1) Earthquake Occurrence Patterns

The patterns of earthquake occurrence that may turn into factors causing a tsunami are taken into account in configuring the default fault parameters for the wave source of a probable tsunami.

The following is a list of examples of patterns of earthquake occurrence that may turn into factors causing a tsunami around Japan.

- 1) Earthquake along the plate boundaries
 - 1-1) Inter-plate earthquake resulting from plate subduction
 - 1-1-a) Archetypical inter-plate reverse fault earthquake
 - 1-1-b) Tsunami earthquake
 - 1-2) Intraplate earthquake within a subducting plate
 - 1-2-a) Normal fault earthquake
 - 1-2-b) Reverse fault earthquake

- 2) Inland crustal earthquake
 - 2-1) Earthquake along the eastern margin of the Japan Sea
 - 2-2) Earthquake due to a submarine active fault

And, as necessary, combinations of the aforementioned 1) and 2) may also be taken into account.

In the majority of coastal regions, a near-field tsunami will be used as the target for the wave source of a probable tsunami, but, in some cases, it is conceivable that a far-field tsunami may have a greater impact on the assessment points. For this reason, as necessary, the impact is also added, which results from a tsunami occurring off the coast of Chile or the Cascadia region or other far-field tsunami have, in configuring the wave source of a probable tsunami.

(2) Location and Scale

The occurrence region and scale of the earthquake are appropriately configured taking into account current stress conditions and other factors, which are based on the crustal structure, distribution of active faults, state of asperities, conditions in which past earthquakes occurred, and other such data.

(3) Configuration of Fault Parameter

In the configuration of fault parameter for the wave source of a probable tsunami, a scaling law may be applied that is appropriate in keeping with the crustal structure, characteristics of the sea area, patterns of earthquake occurrence that give rise to tsunami, and other factors.

Three approaches are shown below with respect to scaling laws for fault parameters that are relevant to moment magnitude.

- 1) Method that does not set a limit for fault length L , fault width W or average slip amount D
- 2) Method setting a limit only for fault width W
- 3) Method setting a limit for average slip amount D and fault width W

With respect to inter-plate earthquakes, a typical example of numeral 1) is the relational

expression described by Murotani et al. (2013) that yields a relationship among seismic moment, fault area and average slip for earthquakes having a moment magnitude up to 9. Other representative scaling laws are shown in Sections 2.1.2 and 2.4.1 of the appendix volume.

(4) Heterogeneity of Slip

In cases where heterogeneous slip may be configured for the fault plane on the basis of knowledge about slip distribution and calculations reproducing past tsunami, it is desirable to take such facts into account.

In cases where heterogeneous slip is taken into account, the slip amount, area and position may be configured for a large slip region using inversion calculations for past tsunami as well as knowledge about inter-plate earthquakes, which is available from the Cabinet Office (2012), Japan Nuclear Energy Safety Organization (2014), and other references.

4.2.1.2 Configuration of Tsunami Source Caused by Earthquakes along Plate Boundary

(1) Assessment Objects

On the basis of knowledge about plate tectonics in the area surrounding Japan, characteristics of earthquakes that have occurred and characteristics of fault models rendering these, the area around Japan is believed to be divided into the two types of sea areas indicated below. For this reason, assessments are conducted of tsunami originating in earthquakes along plate boundary included within these sea areas.

- Sea area associated with subduction of the Pacific Plate
- Sea area associated with subduction of the Philippine Sea Plate

Moreover, in addition to the aforementioned sea areas, as indicated in Section 4.2.1.1 of the main volume, as necessary, the assessment may also cover far-field tsunami occurring off the coast of Chile, Cascadia region or other such areas.

(2) Standard Fault Model

Taking into account the location and pattern of earthquake occurrence, a fault model that is in keeping with the moment magnitude and other characteristics of anticipated tsunami is configured as the standard fault model.

Examples of methods for configuration of standard fault models for each sea area are shown in Section 2.2.5 of the appendix volume. In addition, details about the basis for configuration of standard fault model for specific sea area and other such particulars are given in Sections 2.2.1 through 2.2.4 of the appendix volume.

In the sea area along the Japan Trench and Kuril Trench (southern part) as well as the sea

area along the Nankai Trough, tsunamis have repeatedly occurred in the past, and there is a relative wealth of knowledge about plate boundary profiles and other such characteristics, so such knowledge may also be utilized in configuring a standard fault model that reflects the distinguishing features of each sea area. Modeling is carried out with consideration given to information about the profile of plate boundaries and motion direction. However, as necessary, faults near the trench axis on the Pacific side which are believed to be bifurcated from the plate boundary surface are subject to modeling, taking into account the impact and other characteristics on tsunami that occur as well as the activity of target faults.

When assessing probable tsunami in sea areas other than the aforementioned, a standard fault model is configured based on scaling laws and other knowledge of tsunami accompanying earthquakes near plate boundaries as well as the profile of plate boundaries.

(3) Tsunami Source Location

The location of the standard fault model is set in keeping with the pattern of tsunami occurring at locations considered to be reasonable, taking into account the conditions in which past earthquakes have occurred and other seismological knowledge and information. In addition, with respect to the division of regions for wave source configuration, divisions are appropriately configured based on crustal structure, pattern of earthquake occurrence and other data. However, as necessary, an examination is also conducted of the possibility that the region near a trench axis and the zone for a typical interplate thrust earthquake may be active at the same time, taking into account knowledge acquired about the 2011 Tohoku earthquake.

4.2.1.3 Configuration of Tsunami Source Caused by an Earthquake Anticipated near the Eastern Margin of the Japan Sea

(1) Assessment Objects

With respect to the eastern margin of the Japan Sea, it is believed that a mature plate boundary surface has not formed, but from the area off the western part of Hokkaido extending to the area off the western part of Niigata Prefecture, there are regions where strain has concentrated due to crustal movements (strain concentration zones), and, in the surrounding areas, large earthquakes and tsunami caused by such have almost continually occurred in a spatial manner. Taking into account to this fact, separate from assessments of tsunami following earthquakes anticipated in sea-area active faults, tsunamis following earthquakes for which it is appropriate to assume might occur along the eastern margin of the Japan Sea are regarded as subject to assessment.

(2) Standard Fault Model

Taking into account the location and pattern of earthquake occurrence, a fault model that is in keeping with the moment magnitude and fault length of anticipated tsunami is configured as the standard fault model. Methods and other information about configuring standard fault models for the eastern margin of the Japan Sea are given in Section 2.3.2 of the appendix volume. Also, details about the basis for configuration of standard fault models and other such particulars are given in Section 2.3.1 of the appendix volume.

Along the eastern margin of the Japan Sea, because it is believed that a mature plate boundary surface has not formed, uncertainty about the parameters including the dip angle is reflected as derived from the fact that earthquakes have occurred having different dip directions, and limitations on the thickness of the seismogenic layer are taken into account in applying the scaling law indicated in Section 2.4.1 of the appendix volume.

(3) Tsunami Source Location

The location for the standard fault model is set in keeping with the pattern of tsunami occurring at locations considered to be reasonable, taking into account the conditions in which past earthquakes have occurred and other seismological knowledge and information. The standard fault model may take into account knowledge about the conditions in which past earthquake have occurred, strain concentration zones and other data to work out a configuration in keeping with the pattern of tsunami occurrence at a location which is considered reasonable and has been divided up in more detail.

4.2.1.4 Configuration of Tsunami Source Caused by an Earthquake in Submarine Active Fault

(1) Assessment Object

Although there are not known cases of large-scale damage due to a tsunami originating from activity in a submarine active fault, tsunami resulting from earthquakes anticipated in submarine active faults where there is a possibility of activity in the future are subject to assessment.

The tsunamis following an earthquake anticipated in a submarine active fault, which are addressed here, are different from those pertaining to the sea area division indicated in Section 4.2.1.2 (1) and 4.2.1.3 (1) of the main volume, as they refer to the entire sea area around Japan.

Simplified prediction techniques are utilized to compare approximate estimations of tsunami height at assessment points, thereby making it possible to identify tsunami to be subject to detailed assessment from among multiple active faults. The method using the M_t equation by Abe (1989) and other such methods serve as simplified prediction techniques for identifying what should be subject to assessment. However, assessments using simplified prediction techniques

are rough estimations based on a statistical relationship found among earthquake magnitude, propagation distance and tsunami height, and the impact of water depth at the tsunami source location and the coastal topography are not directly taken into account. For this reason, in cases where the results of a narrowing down of objects to be assessed using simplified prediction techniques provides multiple tsunami resulting from earthquakes anticipated in submarine active faults considered to have a significant impact at the assessment points, it is desirable to perform a detailed assessment employing numerical simulations with respect to these.

(2) Standard Fault Model

Taking into account the characteristics of individual submarine active faults, a standard fault model is configured in keeping with such characteristics. Configuration methods are given in Section 2.4.2 of the appendix volume. Also, specific details about the basis for configuration of the standard fault model and other particulars are given in Section 2.4.1 of the appendix volume.

With respect to tsunami originating from earthquakes anticipated in submarine active faults, limitations on the thickness of the seismogenic layer are taken into account in configuring the standard fault model by applying a scaling law similar to that for the eastern margin of the Japan Sea reflecting uncertainty about parameters, including dip angle.

(3) Fault Location, etc.

The fault location, fault length and strike direction of submarine active faults are configured based on literature surveys, surveys of submarine active faults for individual assessment points and other data. Similarly, with respect to inclination angle and other parameters as well, cases where it is clear, based on literature surveys, surveys of submarine active faults for individual assessment points and other data, that the dip angle and other such parameters may also be treated in a definite manner similar to fault length and strike direction.

It is also possible to configure the slip angle of a fault based on the relationship of wide-area stress field and fault plane angles as well as other data (see Section 2.4.3 of the appendix volume).

4.2.2 Non-Fault Motion-Caused Tsunami

4.2.2.1 Basic Policy for Preparation of Probable Tsunami Not Caused by Fault Motion

There are tsunamis that occur due to submarine landslides, slope failures or volcanic phenomena (flank collapse, caldera collapse, etc.) that cause move of ocean water. In cases where such topography or traces are observable, tsunami that are believed to have an impact on a site may be subject to assessment based on information about such scale and location of occurrence obtained from surveys.

Past examples comprising such phenomena include the tsunami that originated from the 1741 Oshima-Oshima flank collapse.

4.2.2.2 Selection of Tsunami Source

(1) Examination Objects

Based on the scale of the phenomenon, positional relationship with the site and other factors as well as simplified prediction techniques, it is possible to identify targets for detailed assessment from multiple assessment objects. For example, the following formula is given, which has been derived from tests employing hydraulic models using slope failure in Huber and Hager (1997) as a simplified formula relating to water level during the initial period of a tsunami resulting from slope failure.

$$\frac{H}{d} = 2 \cdot 0.88 \sin \alpha \cos^2 \left(\frac{2\gamma}{3} \right) M^{1/2} \left(\frac{\rho_s}{\rho_w} \right)^{1/4} \left(\frac{r}{d} \right)^{-2/3}$$

$$M = V_s / bd^2$$

where, H : Total tsunami amplitude, d : Water depth at the slide location, α : Inclination of the slip plane, γ : Incident angle, ρ_s : Slide density, ρ_w : Seawater density, r : Propagation distance, V_s : Slide volume, and b : Slide width.

In identifying the objects to be assessed, slope inclination, landslide scale, water depth and other data necessary using simplified prediction techniques are appropriately configured based on surveys.

(2) Tsunami Source Location, etc.

In accordance with the results of investigations as described in Chapter 3 of the main volume, location and scale are configured, and the tsunami source that is thought to have a significant impact on the site is selected.

It is generally known that tsunami following a submarine landslide, slope failure or volcanic phenomenon (flank collapse, etc.) has high directionality of energy in the incident direction compared to a tsunami originating in a fault motion. For this reason, after appropriately configuring the location and other characteristics for the tsunami source based on surveys, the relationship of the tsunami source's position with the site is taken into account in selecting a tsunami source that is regarded as having a significant impact.

4.2.3 Consideration of Uncertainties

4.2.3.1 Uncertainty Related to Tsunami Caused by Fault Motion

Conducting a parametric study of a standard fault model is one method of considering uncertainty. In a parametric study, numerical calculations are conducted by modifying parameters for important factors within the parameters of a standard fault model where uncertainty is present (location, length, width, strike direction, dip angle, slip amount, slip angle, slip distribution, upper edge depth, failure initiation point, failure propagation velocity, etc.) to assess a probable tsunami group. In assessing a probable tsunami group, it is important that the factors used to conduct the parametric study be appropriately selected, and their scope reasonably prescribed.

As for other uncertainties, it is also conceivable that multiple seismically-active areas may be active simultaneously, as discussed in Section 4.1.3 of the main volume. In this section, the basic approach to parametric study will be addressed.

(1) Parametric Study Procedures

Of the parameters of the standard fault model, after a parametric study is conducted of those factors regarded as relatively more dominant, it is fundamental that a fault model be used that sets parameters having the greatest impact on the site from among such factors so as to conduct a perimeter study of other subordinate factors.

Parametric study are carried out on each water level rise and fall.

(2) Parametric study Factors

In principle, a standard fault model is utilized to conduct a parametric study of factors determined to have relatively significant uncertainty. In so doing, consideration is given to whether or not tsunami source uncertainty is expressed by any of the parameters. Typical factors are given in Section 3.1 of the appendix volume.

Moreover, with respect to inter-plate earthquakes for which the expansion of the tsunami source is very broad, consideration is also given to dynamic parameters (failure propagation velocity, failure initiation point, etc.) which represent chronological change of the fault motion in keeping with the extent of the impact.

(3) Scope of Parametric study

With respect to the scope of the parametric study, the scope for modifying the parameters regarded as reasonable is appropriately configured by taking into account the degree of uncertainty. In addition, with respect to factors that may be statistically processed based on data

about past earthquakes, the extent of the standard deviation may serve as a yardstick for the scope.

With respect to the tsunami sources of tsunami resulting from earthquakes anticipated along the eastern margin of the Japan Sea or submarine active faults, the scope is indicated in the standard fault model with regard to factors considered to have relatively large uncertainty (see Section 3.2 of the appendix volume). In such a case, a parametric study may be conducted using such scope as the standard.

4.2.3.2 Other Uncertainties

(1) Consideration of Combinations of Tsunami Causal Factors

In cases where tsunami, which are caused by multiple factors that have a cause-and-effect relationship, occur almost simultaneously, the superposition of these is taken into consideration. For example, in a case where the possibility is recognized that a both a tsunami resulting from fault motion and a tsunami resulting from a submarine landslide may occur, the phenomenon is assessed in which both are superimposed. In so doing, in cases where the locations where the anticipated tsunami are to occur are away from each other as well as cases where a tsunami having a small scale is included, the tsunami to be superimposed are selected after reviewing the possibility that superposition may have a significant impact on the site.

(2) Consideration of Time Differences

From the perspective of impact on the site, differences in the time when tsunami resulting from various factors occur are taken into consideration. For example, in a case where seismic ground motion induces a submarine landslide, time differences may be taken into consideration within such scope when the difference in time is able to be configured within a reasonable scope, such as taking into consideration the duration over which seismic ground motion, whose the primary factor is a submarine landslide, continues.

4.3 Selection of Probable Maximum Tsunami

(1) Selection of Probable Maximum Tsunami

Of the probable tsunamis, those for which the maximum water level ascent or descent (time affecting water intake dependent upon power station conditions) at the assessment points is the greatest are selected as probable maximum tsunami. In so doing, it is fundamental that the mean high tide level is taken into account for water level rise, and the mean low tide level for water level fall. Moreover, in cases where vertical displacement of the site is anticipated accompanying fault motion, it is necessary to select the probable tsunami for which the relative amount of the

water level change is the maximum in relation to the site level.

(2) Necessary Conditions

With respect to probable maximum tsunami it is to be verified that at least one of the following conditions “(A)” or “both (B-1) and (B-2)” is satisfied. However, the “vicinity of the assessment point” is appropriately configured after studying similarities between the coastal and submarine topography and the assessment points, number and distribution of the heights of traces evidencing past tsunami which are regarded as having a significant impact on the assessment points.

- (A) There is evidence of the height of past tsunami regarded as having a significant impact on the assessment point, and the results of calculations of probable maximum tsunami exceed such heights.
- (B-1) The results of calculations of probable maximum tsunami exceed the results of calculations of past tsunami at the assessment point.
- (B-2) The envelope curve of the results of calculations of the probable tsunami group exceeds tracing evidencing of the height of past tsunami in the vicinity of the assessment points.

The intent is to have the conditions set for (A), (B-1) and (B-2) confirm that the rise in water level of a probable maximum tsunami selected after estimating for a variety of types of uncertainty exceeds the evidence of the height of traces of past tsunami at least at the assessment points. Accordingly, in cases where there is evidence of the height of past tsunami believed to have a significant impact on an assessment point, it is sufficient to verify only (A). In cases where there are no records of traces of past tsunami at an assessment point, then it is desirable to satisfy both (B-1) and (B-2), but if there are limits on the amount of information that may be acquired about the evidence of the height of past tsunami, then it is sufficient that either (B-1) or (B-2) be verified. In so doing, past tsunami of a small-scale for which it is clearly evident that the level was below the scenario tsunami at the assessment point may be omitted from confirmation.

Although probable maximum tsunami does not need to have an occurrence profile or location that is identical to past tsunami for which records of such traces have been produced, attention does need to be given to the fact that satisfying “(A)” or “both (B-1) and (B-2)” is the minimum requirement for a determination probable maximum tsunami. In addition, in cases where tsunami deposits are able to provide information about the range of tsunami inundation, it is desirable to closely examine the reliability of tsunami deposits in obtaining the results of calculations for inundation that comprise these distribution ranges.

[Chapter 4 References]

- Abe, Katsuyuki (1989): Estimate of tsunami heights from magnitudes of earthquake and tsunami, Bulletin of the Earthquake Research Institute, The University of Tokyo, Vol. 64, pp. 51-69 (in Japanese with English abstract).
- Cabinet Office Study Group on Models for Massive Earthquakes in the Nankai Trough (2012): Study Group on Models for Massive Earthquakes in the Nankai Trough (Second Report) Tsunami Fault Model Volume: Tsunami Fault Models and Tsunami Height, Inundation, etc. (in Japanese).
http://www.bousai.go.jp/jishin/nankai/model/pdf/20120829_2nd_report01.pdf (Accessed on August 2016)
- Huber, A. and W. H. Hager (1997): Forecasting impulse waves in reservoirs, in Dix-neuvieme Congres des Grands Barrages, Florence, Commission Internationale des Grands Barrages, pp. 993-1005.
- Japan Nuclear Energy Safety Organization (2014): Guidelines for Developing Design Basis Tsunami Based on Probabilistic Approach, JNES-RE-Report Series, JNES-RE-2013-2041, 193p.
- Japan Society of Civil Engineers Nuclear Civil Engineering Committee (2002): Tsunami Assessment Method for Nuclear Power Plants in Japan.
- Murotani, S., K. Satake and Y. Fujii (2013): Scaling relations of seismic moment, rupture area, average slip, and asperity size for M~9 subduction-zone earthquakes, Geophysical Research Letters, Vol. 40, pp. 1-5.

Chapter 5 Probabilistic Tsunami Hazard Analysis

5.1 Overview of Probabilistic Tsunami Hazard Analysis

5.1.1 Basic Flow of Probabilistic Tsunami Hazard Analysis

Probabilistic tsunami hazard analysis is a method for obtaining the relationship between tsunami height and the exceedance probability during a specific period of time, and current methods for probabilistic tsunami hazard analysis have been proposed for such references (Annaka et al., 2006; Annaka et al., 2007; Geist and Parsons, 2006; Sugino et al., 2008; Japan Society of Civil Engineers, 2011; Japan Nuclear Energy Safety Organization, 2014; etc.).

The purpose of probabilistic tsunami hazard analyses, which are premised on the presence of uncertainty, is to systematically process a variety of types of uncertainty related to estimation so as to find the relationship between tsunami height and the exceedance probability during a specific period of time and thereby provide data for making an engineering determination. Important differences from the deterministic method are that probabilistic tsunami hazard analyses reflect all conceivable events in the assessment and specifically take into account time (occurrence frequency).

In the assessment, a logic tree is configured that takes into account uncertainty upon the basis of past earthquake data and other factors for the region around a nuclear power plant to compute the exceedance (occurrence frequency) probability of the tsunami water level, which is likely to attack in the future. The basic flow of probabilistic tsunami hazard analysis is shown in Figure 5.1.1-1.

With a probabilistic hazard analysis of the earthquake and tsunami, one must be mindful that, in cases where a change occurs in the understanding of earthquakes and tsunami, the configured logic tree also changes.

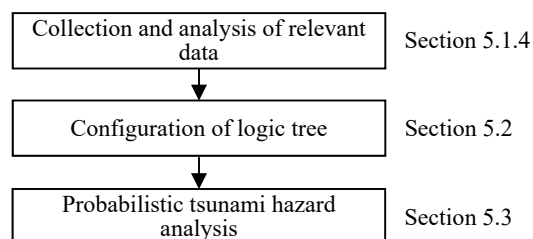


Figure 5.1.1-1 Basic flow of probabilistic tsunami hazard analysis

5.1.2 Two Types of Uncertainty and Logic Tree Approach

A probabilistic tsunami hazard analysis is premised on the presence of uncertainty and provides

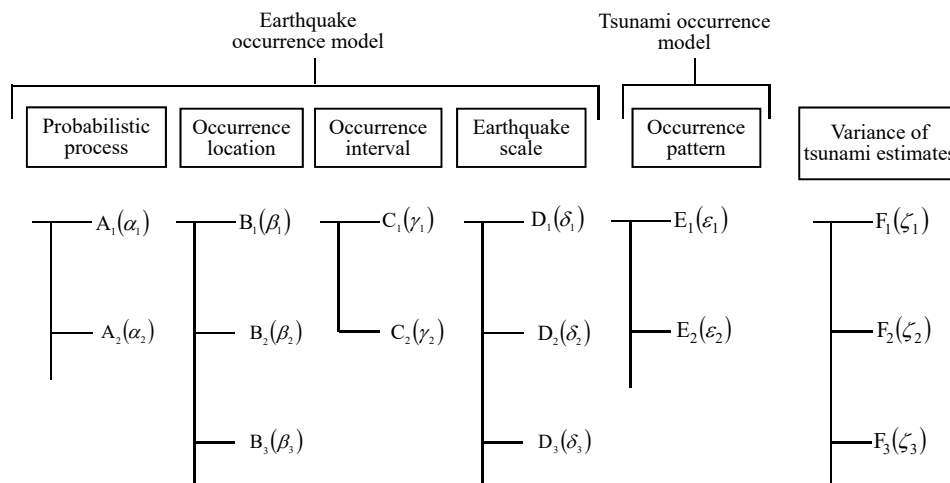
data for making an engineering decision under such conditions. This uncertainty is generally divided into two types for consideration: aleatory uncertainty and epistemic uncertainty.

Aleatory uncertainty is uncertainty that is attributable to randomness inherent in a physical phenomenon and is regarded as unpredictable. In a probabilistic tsunami hazard analysis, aleatory uncertainty is taken into account within one tsunami hazard curve.

Epistemic uncertainty is uncertainty that is attributable to insufficient knowledge or awareness, such as the problem of whether or not there is an active faults or the range of magnitude that might occur, a solution to the problem may be finalized if research is advanced, but, currently, the issue is unpredictable, and it is taken into consideration as branches of logic tree and expressed by multiple tsunami hazard curves.

To take into account epistemic uncertainty is to create a tsunami hazard curve group with weights based on multiple combinations corresponding to epistemic uncertainty. The logic tree approach is a method for systematically conducting this, and the results are mainly expressed as a fractile. A fractile hazard curve (percentile hazard curve) indicates the level of equal non-exceedance probability for a set of hazard curves. An illustration of a logic tree is shown in Figure 5.1.2-1.

The logic tree approach is generally utilized in probabilistic hazard analysis of earthquakes and tsunami in order to quantitatively reflect in assessments the likelihood of each opinion at the current point in time with respect to individual issues where there are multiple opinions, even among experts. Accordingly, in this publication, descriptions are provided on the assumption that the logic tree approach is utilized. However, if there are other methods where epistemic uncertainty is able to be treated quantitatively, then such methods may serve as an alternative for the logic tree approach.



$\alpha_i, \beta_j, \gamma_k$ and other such symbols indicate the weight of each branch component.

Figure 5.1.2-1 Illustration of a logic tree

5.1.3 Assessment Objects

In this publication, the object of probabilistic tsunami hazard analyses is tsunami for which the direct cause is a fault motion. The reflection of tsunami arising due to submarine landslides, slope failures, volcanic phenomena (flank collapse, caldera collapse, etc.) and other factors that are not fault motion is regarded as an issue to be pursued in future research. However, if there are objects for which the scope of uncertainty relating to the occurrence frequency, scale or occurrence pattern is able to be appropriately configured, then it is also possible to reflect such in the assessment.

The probabilistic tsunami hazard analysis is a method for obtaining the long-term average hazard and the hazards during a particular period of time beginning at the current point in time. The former assesses the long-term average annual exceedance probability. The latter assesses the exceedance probability during a specific period of time beginning from the point in time subject to assessment. Information about the earthquake occurrence probability (frequency) found in the former forms the foundation for assessment of the latter. In the former assessment, as part of the earthquake occurrence probability, data about the average activity interval (occurrence frequency) is used to obtain the earthquake occurrence probability by means of a stationary process (ex. Poisson process). On the other hand, in the latter assessment, data about the time of the most recent occurrence (last event) in addition to the average recurrence interval is used to assess the exceedance probability during a specific period of time by means of a renewal process (ex. BPT (Brownian Passage Time) distribution).

5.1.4 Collection and Analysis of Relevant Information

Information is collected about the occurrence pattern of earthquakes which give rise to tsunami that may impact a power plant (active fault data, data about past earthquakes, etc.). The collection of information from experts is also effective for expressing epistemic uncertainty in branches of logic tree.

When the latest knowledge or other such information has been announced that may have a very significant impact on a probabilistic tsunami hazard analysis, such a data needs to be appropriately reflected.

5.2 Basic Approach to Modeling

This chapter shows in detail the modeling of earthquakes necessary for probabilistic tsunami hazard analyses apply to nuclear power plants, which are described in Section 5.3 of the main volume, procedures for assessment of tsunami height distribution, and the methods of setting up branches and

weights on logic trees for a tsunami assessment.

5.2.1 Modeling of Earthquakes of which Source Parameters can be Expected Seismologically

The components that must be modeled for earthquakes of which source parameters can be expected seismologically are listed below.

- What is the region over which earthquakes occur? (Occurrence region)
- What magnitude earthquakes occur at what rate? (Magnitude distribution)
- What is the frequency at which earthquakes occur? (Average recurrence interval and uncertainty)

It is sufficient that the aforementioned three components be configured in cases where one type of earthquake occurs within one region of activity. But, in cases where there are multiple segments and where rupture of single segment connected rupture of multiple segments or other such situations are intermingled, the following components are taken into account in modeling.

- What frequency does each segment rupture?
- What kind of combination of segments will be ruptured simultaneously?
- What are the respective frequencies that combinations of segments, which rupture simultaneously, occur?
- What kind of magnitude of earthquakes occur at what rate for each combination of segments that ruptures simultaneously?

(1) Source Region

The identification of source regions for earthquakes that may occur in the future on the basis of past earthquakes has generally been undertaken for regions where earthquakes have occurred in the past. However, although these are tectonically similar environment, the identification of the appropriate region is not easy in cases where there are regions where earthquakes have occurred and regions where they have not. Such an example may be seen in the case of tsunami earthquakes and normal fault earthquakes along the Japan Trench. Addressing this kind of issue using a logic tree is regarded as effective.

With tsunami earthquakes and normal fault earthquakes along the Japan Trench as well as earthquakes along the eastern margin of the Japan Sea and other such seismic events, it is argued whether the regions where earthquakes occur are completely separate (there is no fault across the region) or continuous. Addressing this kind of issue also using a logic tree is regarded as effective.

In addition, the source region of a submarine active fault may be configured based on literature surveys and surveys of submarine active faults relating to individual assessment points.

(2) Magnitude Distribution

The distribution width of the magnitude of characteristic earthquakes is considered because, in reality, the characteristic earthquake magnitude is believed not to be limited to one value and to have a significant impact on tsunamis.

The magnitude range of past characteristic earthquakes where it is believed that almost the same region ruptured are shown in Table 5.2.1-1. The magnitude width is distributed across a range from 0.3 to 0.5, so 0.3 and 0.5 are set as the magnitude distribution width.

In order to determine the magnitude distribution width, the specific M_W which is basis for the scenario of each sea region (hereinafter referred to in this section as “ M_c (central magnitude)”)), is required to be assumed, and the position of M_c in the M_W distribution have to be defined. In so doing, M_c is determined by taking into account the characteristics of each sea region (crustal structure, distribution of active faults, state of asperities, conditions in which past earthquakes occurred, etc.). The possibilities that M_c may take with respect to the distribution width are shown in Figure 5.2.1-1. There is a possibility of eight patterns in all and it is difficult to make a definite determination, so addressing this situation using a logic tree is regarded as effective. In such a case, if M_c is appropriately expected taking into account the characteristics of each sea region, then it is considered sufficient for M_c to omit the three patterns near the lower limit of the distribution width and consider the five patterns shown in Figure 5.2.1-1. Also, for inter-plate earthquakes, seismic moment may also be computed based on stress drop and the active region area. In such a case, the results of examining the stress drop of inter-plate earthquakes around the world can be used. The results of the investigation conducted by the Cabinet Office (2012) came up with an average value of 1.2MPa as shown in Figure 5.2.1-2, and, according to the scaling law provided by Murotani et al. (2013), the mean value is 1.6MPa (see Section 2.1.2 of the appendix volume). In cases where $+1\sigma$ is taken into account as the variance 2.2MPa was obtained in the study by the Cabinet Office (2012) and 3.0MPa by Murotani et al. (2013). Based on the aforementioned results, stress drop may also be considered on branches of logic tree.

(3) Average Recurrence Interval and Uncertainty

The average recurrence interval is required in hazard analyses of long-term averages (time independent hazard analysis) as well as instantaneous (time dependent hazard analysis) hazard analyses, but variance is required only for instantaneous hazard analyses.

1) Logarithmic Normal Distribution and Brownian Passage Time (BPT) Distribution

The recurrence interval for characteristic earthquakes is modeled using the logarithmic normal distribution or Brownian Passage Time (BPT) distribution.

BPT distribution is a model that takes into account a physical process (Brownian relaxation

oscillator process) where “in the stationary process of stress accumulation due to plate motion, the stress accumulation reaches a certain threshold and the fault becomes active (earthquake occurs) within a context where disturbance of the stress field is added which is expressed as Brownian motion, which includes the occurrence of an earthquake and a slow event near the targeted hypocentral region”, and is expressed using the following formula (Ellsworth et al., 1999; Matthews et al., 2002).

$$Y(t) = \lambda \cdot t + \delta \cdot W(t)$$

where, $Y(t)$ is the state variable, and t is the elapsed time since the last time it reached Y_f , and, when $Y(t)$ reaches Y_f , then an earthquake occurs and a state is fallen into Y_0 . λt is a term derived from stationary stress accumulation, and $\delta W(t)$ is a term derived from disturbance of the stress field. $W(t)$ is standard Brownian motion, and δ is a nonnegative constant, and δ^2 is referred to as a diffusion coefficient.

The distribution function for time t that elapsed from the time when Y_f was last reached (since the earthquake occurred) until Y_f is reached next (an earthquake occurs) is called the BPT distribution. The density function of the distribution is given using the following formula.

$$f(t; \mu, \alpha) = \left\{ \mu / (2\pi\alpha^2 t^3) \right\}^{1/2} \exp \left\{ - (t - \mu)^2 / (2\mu\alpha^2 t) \right\}$$

The mean of this distribution is μ , and the variance is $(\mu\alpha)^2$. Also there is the following relationship with λ and δ .

$$\mu = (Y_f - Y_0) / \lambda$$

$$\alpha = \delta / \left\{ (Y_f - Y_0) \lambda \right\}^{1/2}$$

$$\text{Variance} = (Y_f - Y_0) \delta^2 / \lambda^3$$

The BPT distribution is also called the inverse Gaussian distribution or Wald distribution in the field of statistics, and has been applied to stock price fluctuations, product life, etc.

An overview of the BPT distribution has been given above, and, in practice, there is no significant difference between the BPT distribution and logarithmic normal distribution. An example is given in Figure 5.2.1-3.

In a case where there are n units of data regarding the recurrence interval of characteristic earthquakes, the m (median value) of the logarithmic normal distribution is:

$$m = \sum_{i=1}^n \frac{\ln T_i}{n}$$

and the μ (mean value) of the BPT distribution is:

$$\mu = \sum_{i=1}^n \frac{T_i}{n}$$

Both are calculated using the arithmetic mean. The logarithmic standard deviation σ_{\ln}

expresses variance across the average recurrence interval in a logarithmic normal distribution, and α in the BPT distribution, and the logarithmic standard deviation σ_{ln} is calculated using:

$$\sigma_{ln} = \sqrt{\frac{\sum_{i=1}^n (\ln T_i - m)^2}{n}}$$

and α in the BPT distribution is calculated using:

$$\alpha^2 = \mu \sum_{i=1}^n \frac{1/T_i}{n} - 1$$

An example of an assessment conducted in the Headquarters for Earthquake Research Promotion (2001) is shown in Table 5.2.1-2. Although σ_{ln} is slightly smaller, both values are almost equal. Based on this table, the variance value is at the level of 0.2 to 0.4.

2) Error in Average Recurrence Interval of Characteristic Earthquakes

In cases where the average recurrence interval of a characteristic earthquake is based on data, it is natural to set branches of logic tree that are based upon error.

If the true value of the distribution mean is x and the arithmetic mean x_o , then the mean value of $x_o - x$ is zero and the standard deviation (standard error for the distribution of true value x) is:

$$\frac{\sigma}{\sqrt{n}}$$

σ is the standard deviation of x . Because the number of data about the average recurrence interval is small, if the value previously described is used as the standard deviation, then the degree of reliability (error) of the estimated value corresponding to the amount of data may be assessed.

3) Error in Cases of Poisson Process

Even in cases where the average recurrence interval is given as a Poisson process, it is possible to assess the confidence interval on the basis of an assessment of standard deviation determined by the number of data. The variance of Poisson variables will be equivalent to the average occurrence frequency when the occurrence frequency is large, and the confidence interval for occurrence frequency X is expressed as:

$$X \pm \sqrt{X}$$

Error in cases where X is small is given by Weichert (1980). This is shown in Figure 5.2.1-4 and Table 5.2.1-3.

(4) Modeling of Multi-segment Rupture

The combinations of multi-segments in earthquakes that have previously occurred along the

Nankai Trough have changed. Such a phenomenon has also been observed in earthquakes that occurred off the coast of Miyagi Prefecture as well as those that have occurred off the coast of Tokachi and Nemuro. As for the earthquakes off the coast of Miyagi Prefecture, cases have been reported where land-side earthquakes and earthquakes along trenches have occurred multi-segment rupture as well as cases where these earthquakes have occurred separately. In addition, with respect to the Japan Trench extending from off the coast of Sanriku to off the coast of Boso, 2011 Tohoku tsunami had a source region comprising the area near the Japan Trench in off the coast of southern Sanriku, part of the region near the Japan trench extending from off the coast of northern Sanriku to off the coast of Boso, off the coast of central Sanriku, off the coast of Miyagi Prefecture, off the coast of Fukushima Prefecture, off the coast of Ibaraki Prefecture and other such regions, and this occurrence region is currently still being studied (The Headquarters for Earthquake Research Promotion, 2011). As for the area off the coast of Tokachi and Nemuro, it has been estimated that earthquakes have occurred in which segments off the coast of Tokachi and off the coast of Nemuro have multi-segment rupture at an interval of around 400 to 500 years (ratio of about once in 6 times) (Central Disaster Prevention Council, 2006). With respect to inland active faults as well, based on the different times when activity has occurred in the past in the main part of the Nobi fault zone, it has been estimated that activity has taken place in three separate segments, the Neodani fault zone, Umehara fault zone and Mitahora fault zone, but it has also been said that it is likely that entire main region of the fault zone was active as one activity segment in a more ancient activity (The Headquarters for Earthquake Research Promotion, 2005).

A schematic depiction of this phenomenon is shown in Figure 5.2.1-5. Such a model is called a cascade model (series model) in the study by the Working Group on California Earthquake Probabilities (“WGCEP”) (1995) and a multi-segment model in the study by Odagiri and Shimazaki (2000).

When a historical record of multiple earthquakes that have occurred over a relatively long period of time is available, it is considered feasible to estimate the long-term multi-segment probability based upon actual past events (multi-segment rate), and the following kinds of methods are conceivable in cases where a pattern of multi-segment is anticipated for which the multi-segment rate is not clear or occurrences in the past have not been confirmed.

- [1] Estimation from the multi-segment rate obtained in adjacent sea areas or sea areas that are geo scientifically similar.
- [2] A multi-segment earthquake is considered as an independent characteristic earthquake, and the recurrence interval is set independently based upon estimated slip and strain accumulation rate (back slip).
- [3] The Gutenberg-Richter formula (G-R law; Gutenberg and Richter, 1944), which is applied for

a region, is utilized to extrapolate the frequency of multi-segment earthquakes based upon the frequency of activity of each segment.

Of the aforementioned, [3] is the method that the Headquarters for Earthquake Research Promotion (2014) applied to active faults in Kyushu.

It is conceivable that there are many cases where sufficient information is unable to be obtained to uniquely determine all multi-segment patterns. In such a case, it is desirable to reflect multiple combinations in branches of logic tree.

Currently, in hazard analyses, one issue for future study is to find a method for how to estimate the probability of occurrence for each combination. As the rupture probability for each segment is able to be found based on the average rupture interval and variance of each segment as well as the time of the most recent occurrence, a method is required for converting this into the probability of each segment combination occurring.

With respect to a case where an earthquake off the coast of Tokachi and an earthquake off the coast of Nemuro occurred in a multi-segment manner, the Headquarters for Earthquake Research Promotion (2014) used a method where:

- The probability of the earthquakes occurring multi-segment during the target period is estimated.
- The obtained probability is multiplied by the rate of multi-segment, which is based on actual earthquakes that have occurred in the past and other such data.

WGCEP (1995) presented a method where:

- In the case of multi-segment earthquakes, half of the past occurrence frequency is assumed;
-If an earthquake occurs n times over a period of T years, then $0.5n/T$ is assumed;
- In the case of single segment earthquake, half of the expected occurrence value is assumed.
- So that the number of earthquakes is the minimum, the remaining number is allocated with priority given to large earthquakes.

Annaka et al. (2001) presented a method that partially revises WGCEP (1995) where:

- In the case of multi-segment earthquakes, half of the past occurrence frequency is assumed;
-If an earthquake occurs n times over a period of T years, then $0.5n/T$ is assumed;
- In the case of single segment earthquake, a value is assumed that is found by multiplying the probability at which ruptured in single segment in the past against the expected occurrence value.
- So that the number of earthquakes is the minimum, the remaining portion is allocated with priority given to large earthquakes.

Examples of assessments conducted by Annaka et al. (2001) of the average occurrence frequency for each combination of Boso offshore, the inside of Sagami Bay and West Sagami Bay fractures are shown in Table 5.2.1-4.

Shimazaki et al. (1998) presented an approach that yields constraint conditions. In contrast to determining an allocation so that the aforementioned method satisfies the rupture probability for each segment, the rupture probability of each segment is not always satisfied when specific constraint conditions are given as was done in Shimazaki et al. (1998).

Besides the multi-segment probability, there is the scaling relationship-related issue of how to determine the magnitude for multi-segment earthquakes.

In cases where the slip of each segment is not so dependent on multi-segment, it is possible to add together seismic moments with regard to moment magnitude, so it is regarded as feasible to set the moment magnitude for each segment and add that together, thereby setting the moment magnitude for multi-segment earthquakes.

In cases where the slip of each segment changes significantly due to multi-segment, the range of the moment magnitude requires to be set separately from each segment.

(5) Application of the G-R Model to Megathrust Earthquakes Occurring along Plate Boundaries

With respect to megathrust earthquakes occurring along plate boundaries, there is a method based on the characteristic earthquake model, and a method based on the G-R model that calculates the magnitude and frequency of earthquakes occurring in regional source based on probability and statistics, and these may be regarded as branches of logic tree taking into account epistemic uncertainty. Illustrations of both are shown in Figure 5.2.1-6. Of the graphs shown in Figure 5.2.1-6, (a) shows a G-R model, and (b) shows the relationship between magnitude and the number of earthquakes in one earthquake cycle which includes maximum magnitude M_{max} . In addition, the number of earthquakes at each magnitude is expressed by n , and the cumulative number of earthquakes based on those having a greater magnitude is expressed by N . Although the G-R model shows a sequential distribution up to maximum magnitude, the characteristic earthquake model does not have any earthquakes between maximum magnitude M_{max} and the second greatest earthquake magnitude M_a .

In cases where the G-R model is used, it is necessary to model the magnitude distribution in advance. Illustrations of the logic trees for the G-R model and characteristic earthquake model are shown in Figure 5.2.1-7. Specific details of the investigation are given in Section 7.1.1 of the appendix volume.

Table 5.2.1-1 Range of magnitude of past characteristic earthquakes

| Sea region | Range of M_J |
|---|----------------|
| Miyagi Prefecture offshore: 5 earthquakes | 7.3 ~ 7.5 |
| Northern Sanriku offshore: 4 earthquakes | 7.4 ~ 7.9 |
| Tokachi offshore: 2003, 1952, 1843 | 8.0 ~ 8.2 |
| Nankai Trough: 1946, 1854 | 8.0 ~ 8.4 |

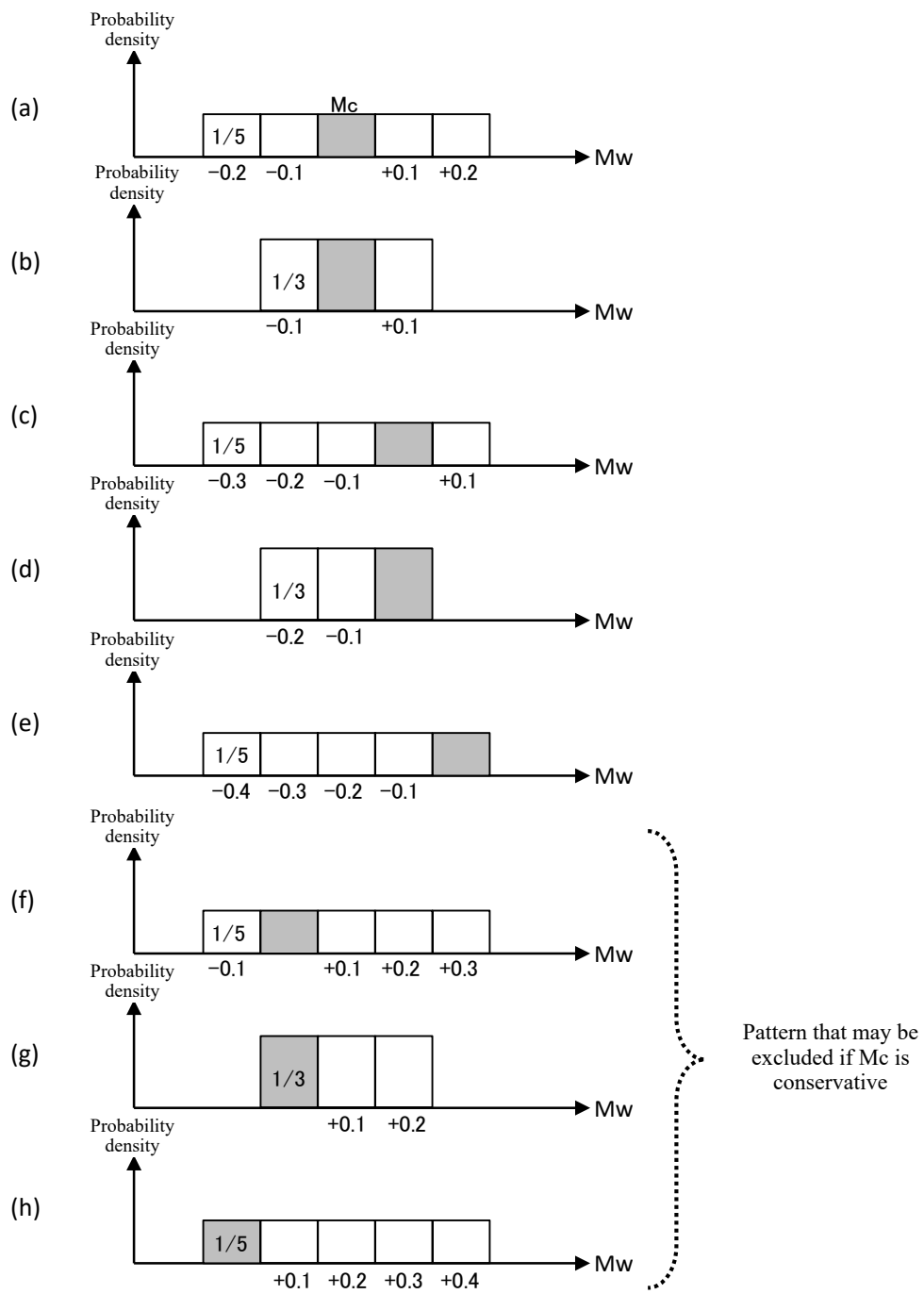
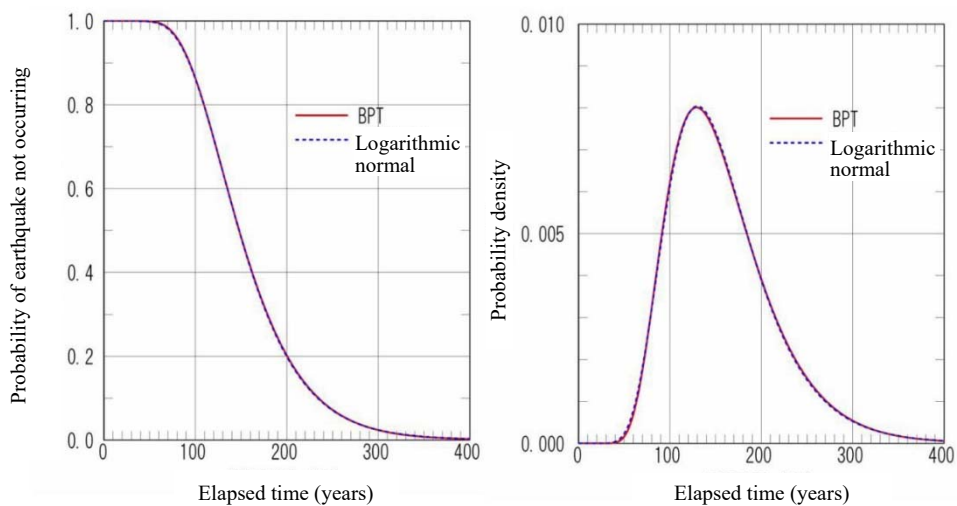


Figure 5.2.1-1 Possibility of position of M_c to distribution width of magnitude

| Eathquake | Reference | data | MO(N m) | M _w | S(km ²) | σ(MPa) | log ₁₀ (Δσ) | Earthquake-specific median value | Earthquake-specific mean value MPa | Residual for each earthquake | Variance for each earthquake | Residual |
|-------------------------|----------------------------|-----------------------|----------|----------------|---------------------|--------|------------------------|----------------------------------|------------------------------------|------------------------------|------------------------------|----------|
| 2003 Tokachi-oki | Tanioka et al. (2004) | Tu | 1.00E+21 | 8 | 9600 | 2.6 | 0.41 | 0.41 | 2.60 | 0.00 | 0.000 | 0.108 |
| 1946 Nankai | Satake (1993) | Tu, G | 3.90E+21 | 8.3 | 59400 | 0.7 | -0.15 | -0.05 | 0.89 | 0.01 | 0.006 | 0.018 |
| | Kato and Ando (1997) | Tu, G | 4.00E+21 | 8.3 | 54000 | 0.8 | -0.10 | | | 0.00 | | |
| | Tanioka and Satake (2001a) | Tu | 5.30E+21 | 8.4 | 52650 | 1.1 | 0.04 | | | 0.01 | | |
| | Baba et al. (2002) | Tu | 4.90E+21 | 8.4 | 52650 | 1 | 0.00 | | | 0.00 | | |
| 1944 Tonankai | Satake (1993) | Tu, G | 2.00E+21 | 8.1 | 48600 | 0.5 | -0.30 | -0.22 | 0.60 | 0.01 | 0.004 | 0.095 |
| | Kato and Ando (1997) | Tu, G | 2.80E+21 | 8.2 | 43200 | 0.8 | -0.10 | | | 0.02 | | |
| | Tanioka and Satake (2001b) | Tu | 2.00E+21 | 8.1 | 42525 | 0.6 | -0.22 | | | 0.00 | | |
| 2011 Tohoku Earthquake | Cabinet Office | Tsunami+GPS | 4.21E+22 | 9.0 | 1.20E+05 | 2.5 | 0.39 | 0.39 | 2.47 | 0.00 | 0.000 | 0.093 |
| 2010 Chili earthquake | Lorito et al. (2011) | GPS+Tsunami+InSAR | 1.55E+22 | 8.8 | 130000 | 0.8 | -0.08 | -0.08 | 0.83 | 0.00 | 0.000 | 0.029 |
| 2004 Sumatra earthquake | Lorito et al. (2010) | GPS+Tsunami+Satellite | 6.63E+22 | 9.15 | 315000 | 0.9 | -0.03 | 0.07 | 1.17 | 0.01 | 0.009 | 0.000 |
| | Fujii and Satake | Tsunami+Satellite | 6.00E+22 | 9.12 | 220000 | 1.5 | 0.16 | | | 0.01 | | |

| | | |
|----------------------|------|--------------------|
| Mean of the median | | Variance |
| log(Δσ) | 0.09 | 0.069 |
| Δσ | 12 | Standard deviation |
| | | 0.26 |
| +Standard deviation | 22 | |
| - Standard deviation | 0.7 | |

Figure 5.2.1-2 Consolidation of mean stress drop based on analysis using tsunami observation data (Cabinet Office, 2012)



(BPT: $\mu=157.8$, $\alpha=0.367$, Logarithmic normal: $m=4.996$, $\sigma=0.358$)

Figure 5.2.1-3 Examples of comparison of BPT distribution and logarithmic normal distribution

Table 5.2.1-2 Examples of assessments of variance

(The Headquarters for Earthquake Research Promotion, 2001)

| Region assessed | σ_{ln} | α |
|------------------------------|---------------|----------|
| Nankai | 0.358 | 0.367 |
| Miyagi Prefecture offshore | 0.176 | 0.177 |
| Atera | 0.287 | 0.293 |
| Tanna | 0.211 | 0.213 |
| Atotsu River | 0.164 | 0.165 |
| Western edge of Nagano basin | 0.247 | 0.250 |

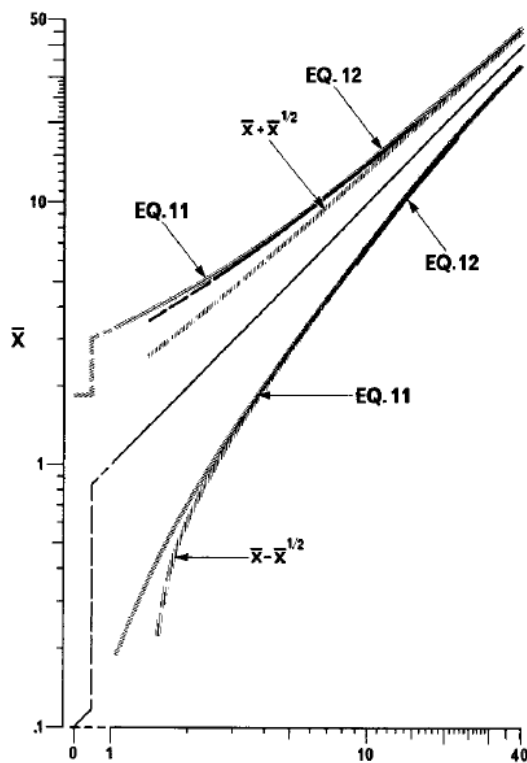


FIG. 1. ± 1 S.D. confidence intervals, 15.9 and 84.1 percentiles, for an estimated average \bar{x} of a Poisson variable, calculated from equations (11) and (12) and from $\bar{x} + \sqrt{x}$.

Figure 5.2.1-4 Confidence intervals for Poisson variables (Weichert, 1980)

Table 5.2.1-3 Confidence intervals for Poisson mean (Weichert, 1980)

| CONFIDENCE INTERVALS FOR POISSON MEAN, N^* | | |
|--|-----|---------|
| μ_U | N | μ_L |
| 1.84 | 0 | 0 |
| 3.30 | 1 | 0.173 |
| 4.64 | 2 | 0.708 |
| 5.92 | 3 | 1.37 |
| 7.16 | 4 | 2.09 |
| 8.38 | 5 | 2.84 |
| 9.58 | 6 | 3.62 |
| 10.8 | 7 | 4.42 |
| 12.0 | 8 | 5.23 |
| 13.1 | 9 | 6.06 |
| 14.3 | 10 | 6.89 |

* Lower and upper ± 1 S.D. confidence intervals, i.e., 15.9 and 84.1 percentiles use μ_L and μ_U from equation (11). Above $N = 9$, use Figure 1 or $N - N^{1/2}$ for the lower bound and $N + 3/4 + (N + 1/2)^{1/2}$ from equation (12).

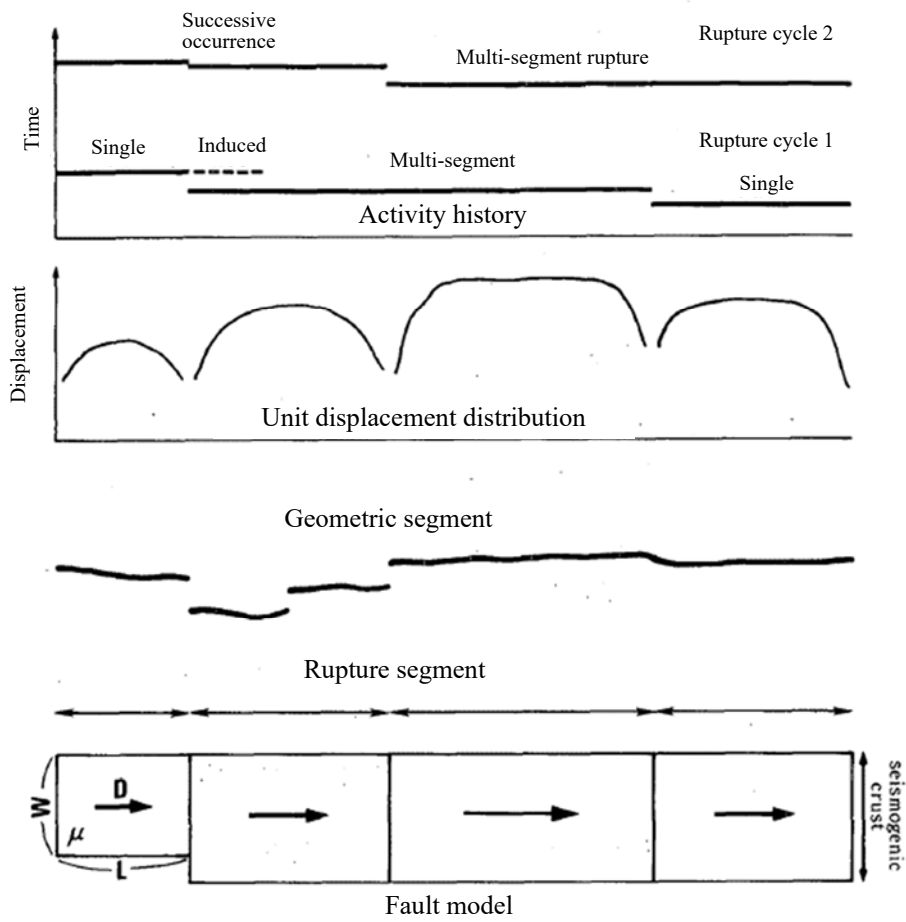


Figure 5.2.1-5 Conceptual diagram of multi-segment model (cascade model) (Sugiyama, 1998)

Table 5.2.1-4 Examples of occurrence frequency in multi-segment model (Annaka et al., 2001)

| | Method 1 (WGCEP method) | | | Method 2 (Revised WGCEP method) | | |
|-------------------|-------------------------|--------------|----------------------------|---------------------------------|--------------|----------------------------|
| Segment | A Boso offshore | B Sagami Bay | C West Sagami Bay fracture | A Boso offshore | B Sagami Bay | C West Sagami Bay fracture |
| Rupture frequency | 0.80 | 4.54 | 13.70 | 0.8 | 4.54 | 13.70 |
| Single rupture | 0.00 | 2.27 | 11.43 | 0.00 | 0.00 | 9.16 |
| A+B | 0.00 | | - | 0.00 | | - |
| B+C | - | 1.47 | | - | 3.74 | |
| A+B+C | 0.80 | | | 0.80 | | |

* Figures indicate the number of earthquakes per 1,000 years

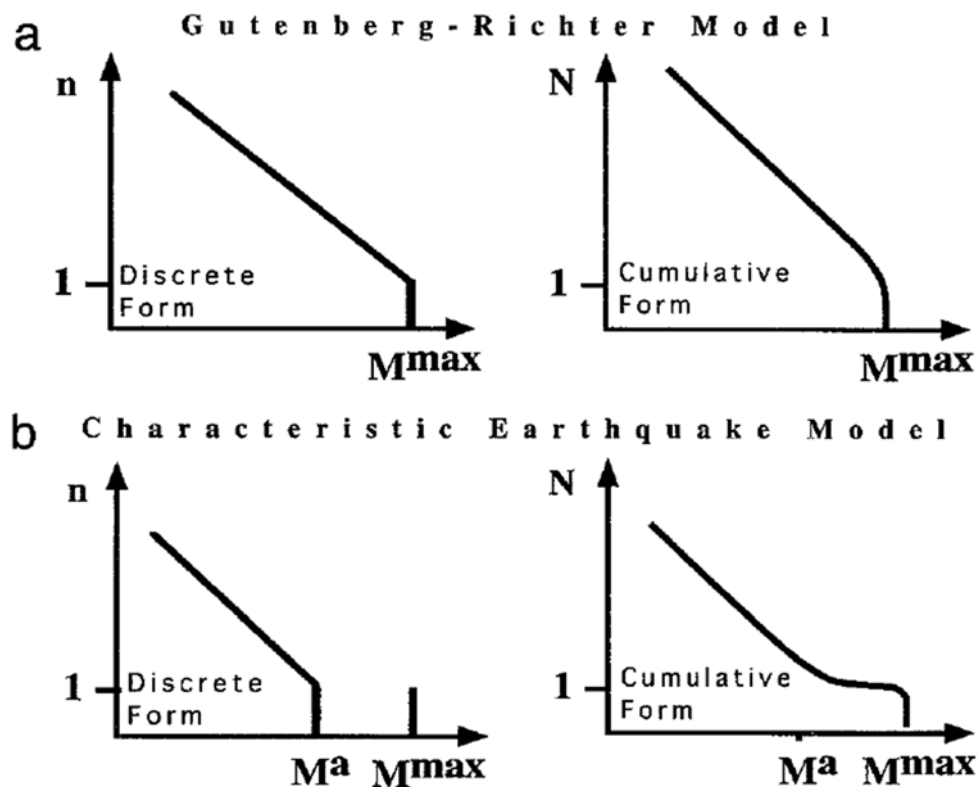


Figure 5.2.1-6 G-R model and characteristic earthquake model (Wesnousky, 1994)

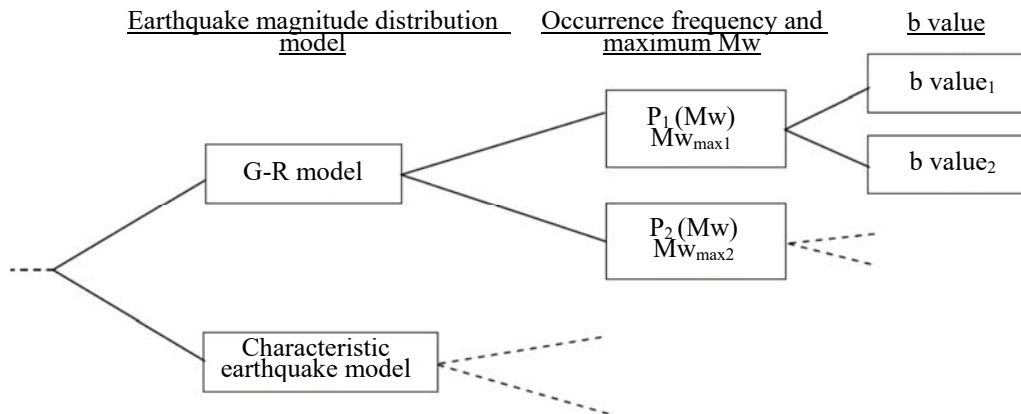


Figure 5.2.1-7 Illustration of logic trees for G-R model and characteristic earthquake model

5.2.2 Modeling of Background Earthquakes

Background earthquakes (earthquakes other than earthquakes of which source parameters can be expected seismologically) are regarded as being sequentially distributed along plate boundaries, within the crust or other regions, so segmentation of active regions and the magnitude frequency distribution of each activity region are required. The basic process for such configuration is shown below.

(1) Segmentation of Active Regions

A segmentation of active regions should be zoned for each target point, and the segmentation may be referenced for assessing earthquakes for which it is difficult to specify in advance the earthquake source fault in the segments given in the models proposed by the Headquarters for Earthquake Research Promotion (e.g. Headquarters for Earthquake Research Promotion, 2014).

(2) Model of Magnitude Frequency Distribution

When the segmentation of active regions are set, the magnitude frequency distribution for each active region is required. The principal methods currently used are the following two.

The first is the truncated Gutenberg-Richter (G-R) law, which truncates the regular G-R law at the maximum magnitude M_{max} . The equation is given as:

$$\log n = a - bM \quad (M \leq M_{max})$$

where n is the number of earthquakes having magnitude M (density, interval frequency).

The other is the modified G-R law (Utsu, 1971). The equation is given as:

$$\log n = a - bM + \log(M_c - M)$$

where M_c is the maximum magnitude.

As shown in Figure 5.2.2-1, in an actual frequency distribution, it is known that the greater M becomes, the lower the curve bends, and the frequency with which large magnitude earthquakes occur decreases compare to the linear relationship with the G-R law. The modified G-R law revises this by having the curved line not exceed the maximum magnitude.

(3) Assessment of Magnitude Frequency Distribution

If a model is determined that is applicable to magnitude frequency distribution, then what remains is to determine the parameters based on data and to appropriately assess error.

1) Exclusion of Non-Independent Earthquakes

Based on earthquake data, it is necessary to exclude earthquakes that are not independent (aftershocks, foreshocks, and earthquakes except for those that are the maximum size in earthquake swarms).

Although simplified methods have been proposed for excluding such non-independent earthquakes (Ministry of Construction's Public Works Research Institute, 1983; Annaka et al., 2002), individual determinations may be made.

2) Assessment of Magnitude Frequency Distribution

There are differences in the range of magnitude of earthquakes, which have been completely recorded over their duration. It is believed that ordinarily all earthquakes of M6.0 or greater have been recorded without omission since 1885, and earthquakes of M5.0 since 1923.

In a case where the truncated G-R law is used, the number of earthquakes (generally, the annual occurrence frequency of those of M5.0 and greater), b values and maximum magnitude should be set based upon data.

A method for assessing error in the magnitude frequency distribution has not been established, but one method has been proposed by Annaka and Yashiro (2000), and a method has been presented where the number of earthquakes of M5.0 or greater is a normal distribution, b value a normal distribution, and maximum magnitude is a uniform distribution (or weighted distribution). In cases where the Monte Carlo method is used, it is possible to generate the necessary sample from such conditions. It is also possible to have discrete branches.

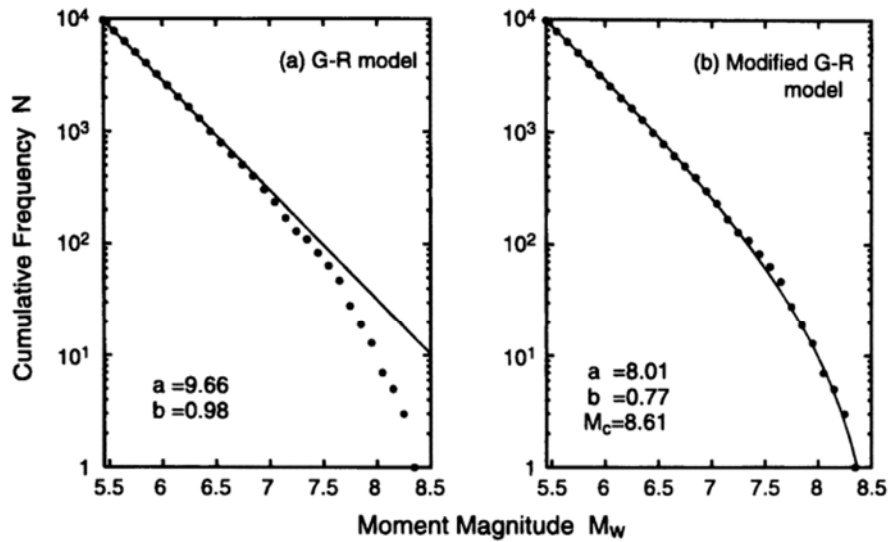


Fig. 4. Fitting of (a) G-R model and (b) modified G-R model to magnitude-frequency distribution of all earthquakes. The figure is shown by using cumulative frequency. Estimated values of model parameters are given in each frame.

Figure 5.2.2-1 Results of fitting G-R law and modified G-R law to earthquakes worldwide (Mabuchi et al., 2002)

* Dots represent data for the period from January 1977 to December 2001 from the Harvard University CMT catalog, and the line is the fitted results.

5.2.3 Assessment of Tsunami Height Distribution

In a tsunami hazard curve assessment, the tsunami height distribution has to be estimated for a case where a specific magnitude of earthquake occurs at a specific location. A logic tree for estimating tsunami height distribution is shown in Figure 5.2.3-1. The background behind each branch components of logic tree is given below.

(1) Setting of Fault Model

A fault model takes into account the characteristics of earthquakes yielding tsunami so as to appropriately create a model of fault motion. Based on a literature survey and other investigation, a fault model is set that is regarded as having an impact on the assessment sites. It is also possible to set a fault model referencing models proposed by public institutions and others.

Besides historical earthquake data, consideration has to also be paid to traces of liquefaction, reviews of tsunami deposits and other geological results.

(2) Whether or Not to Consider Parameter Variation

In estimating tsunami height, the fault model, which was set in the aforementioned numeral

(1), is used, so it is considered necessary to separately take into account “variation in the fault model” or to add “variance due to variation in the fault model” in order to consider uncertainty in the observed and calculated values.

If the model of a fault where earthquakes actually occur varies even in the same location, then the effect attributable to parameter variation is a component that must be taken into consideration. In the deterministic assessments in Chapter 4 of the main volume, this is regarded as the “consideration of uncertainty”. Because there is debate about whether or not it is necessary to take into consideration variances due to variation in fault models in probabilistic assessments, it is currently regarded as effective to treat the question of whether or not to take into consideration this variation as a branch.

Even in cases where parameter studies are conducted that take into consideration variation in fault models, just as with the deterministic assessments presented in Section 4.2.3.1 of the main volume, it is sufficient to assess factors for which it is determined there is relatively great uncertainty.

(3) Error Standard Deviation and Truncated Range

The uncertainty of estimated values is expressed using either logarithmic normal distribution or a truncated logarithmic normal distribution, and logarithmic standard deviation (β) and truncated range (σ) are set as the parameters (specifics concerning the possibility of the variance of estimated values being approximated with the logarithmic normal distribution are shown in Section 5.1.1 of the appendix volume).

Logarithmic standard deviation (β) is expressed by the geometric standard deviation proposed by Aida (1977) (hereinafter referred to in this chapter as “ κ ”), and the relationship in between the two is given in the following formula (specifics details pertaining to κ are given in Section “6.4 Setting of Fault Model Capable of Explaining Run-up Height Record of Past Tsunami”).

$$\ln(\kappa) = \beta$$

where, $\ln(\cdot)$ expresses a natural logarithm.

Table 5.2.3-1 shows the results of an examination of κ in relation to past tsunami. In addition, using the results of an examination that took into account 2011 Tohoku tsunami, Sugino et al. (2014) reported that, in cases where a characterized tsunami source model is used, a logarithmic standard deviation $\beta=0.2 \sim 0.3$ (equivalent to $\kappa=1.22 \sim 1.35$) may be assumed under conditions where the minimum grid size of the area around the site is 5.5m (see Figure 5.2.3-2). On the other hand, from the results of assessments of wide-area variance using several inversion models of 2011 Tohoku tsunami, as shown in Figure 5.2.3-3, results have been obtained where $\kappa=1.3 \sim 1.4$, and both show a variance smaller than that of the results of previous examinations (Table 5.2.3-

1).

When using the examination in this publication where the minimum grid size for coastal areas is set at 50m (Figure 5.2.3-4), all points fall within logarithmic standard deviation (β) of the mean of ± 4 times. Of these, there were very few results exceeding logarithmic standard deviation (β) of the mean ± 3 times, and the effect of local topography, which is unable to be simulated with the grid size used, is revealed. Specific details of the content considered are given in Section 5.1.2 of the appendix volume.

With respect to a truncated range (σ), because it is inconceivable in reality that a value arrived at by dividing the measured value by the calculated value would infinitely increase, the logarithmic normal distribution may be truncated using a finite range.

For example, a case where the range is truncated using a mean $\pm 2.3\beta$ or a mean $\pm 3\beta$ is likened to approximately 1% or approximately 0.1% of one side of the respective logarithmic normal distribution not emerging. The relationship when this is combined with κ is given as follows. A case where $\kappa=1.25 \sim 1.55$ and the truncated range 3β is the equivalent of likening that true values not emerging in excess of $1.25^3=1.95$ to $1.55^3=3.72$ times the results of the numerical simulation. Or, a case where $\kappa=1.25 \sim 1.35$ and the truncated range 3β is the equivalent of likening that true values not emerging in excess of $1.25^3=1.95$ to $1.35^3=2.46$ times the results of the numerical simulation. Details about the truncated range indicated by various institutions are shown in Section 5.1.2 of the appendix volume.

In this way, combinations of logarithmic standard deviation (β) and truncated range (σ) alter the range of true values estimated based on calculation results, so it is desirable to take into consideration the complexity of the topography in areas around points subject to assessment, grid sizes applied, reproducibility of past tsunami and other factors integrated into the branches of logic tree.

(4) Ergodic Hypothesis

κ is an indicator showing the extent to which actual observed values are dispersed in relation to estimated values at multiple points spread out spatially. The variance used in probabilistic tsunami hazard analyses expresses the extent to which the tsunami height at specific points based on the same source (in cases where a specific size earthquake (tsunami) has occurred at a specific location) is dispersed temporally in relation to the estimated values.

In probabilistic tsunami hazard analyses and probabilistic seismic hazard analyses, the aforementioned two are ordinarily assumed to be equal (ergodic hypothesis), but there is debate about the appropriateness of this hypothesis.

Multiple earthquakes along the Nankai Trough have occurred where, although the tsunami sources have not been the same, tsunami sources have overlapped. The appropriateness of the

ergodic hypothesis has been examined by studying the correlation of κ at site points of identical place name in relation to multiple earthquakes.

The relationship between K_i at site points of identical place name in relation to two earthquakes where tsunami sources overlap is shown in Figure 5.2.3-5, and relationship between K_i at site points of identical place name in relation to two earthquakes where tsunami sources do not overlap is shown in Figure 5.2.3-6. The correlation coefficient (ρ) is shown in each figure. However, the correlation coefficient is obtained using 1.0 as the mean for K of each earthquake.

From the two figures, it can be seen that the correlation coefficient in relation to the two earthquakes where tsunami sources overlap displays a greater tendency than the correlation coefficient in relation to the two earthquakes where tsunami sources do not overlap. Finding the mean, the combination of six cases where the tsunami sources overlap is 0.58, and the combination of four cases where the tsunami sources do not overlap is 0.26. The figure of 0.58 shows that there is a correlation with K_i to a certain extent in the two earthquakes where tsunami sources overlap.

The fact that there is a correlation with K_i means that the ergodic hypothesis is not completely correct. In an extreme case, if there were a complete correlation and K were already known in relation to one earthquake, then the K_i of other earthquake occurring there would be the same, and there would be no variance in relation to K_i .

If K_{ij} in relation to tsunami i and point j is expressed using the mean value and the variance (normal distribution) for the point, then:

$$\log(K_{ij}) = K_j + \varepsilon_{ij}$$

The variance related to $\log(K_{ij})$ (standard deviation) is given as σ , variance related to K_j is given as σ_s , and variance related to ε_{ij} is given as σ_o , such that:

$$\sigma^2 = \sigma_s^2 + \sigma_o^2$$

And, the correlation coefficient between the two earthquakes is:

$$\rho = \frac{\sigma_s^2}{\sigma^2}$$

Using a correlation coefficient of 0.58 to calculate the relationship between σ_o and σ gives:

$$\sigma_o^2 = 0.42\sigma^2 = (0.65\sigma)^2$$

This indicates that if K_j is known, then the variance will be even smaller than κ estimated from data about past tsunami.

When σ corresponds to $\kappa=1.45$, then σ_o in the above equation corresponds to $\kappa=1.27$ as the ergodic hypothesis does not hold.

In this assessment, the possibility that the ergodic hypothesis does not hold is given as, $\kappa=1.25$ on the branches of logic tree.

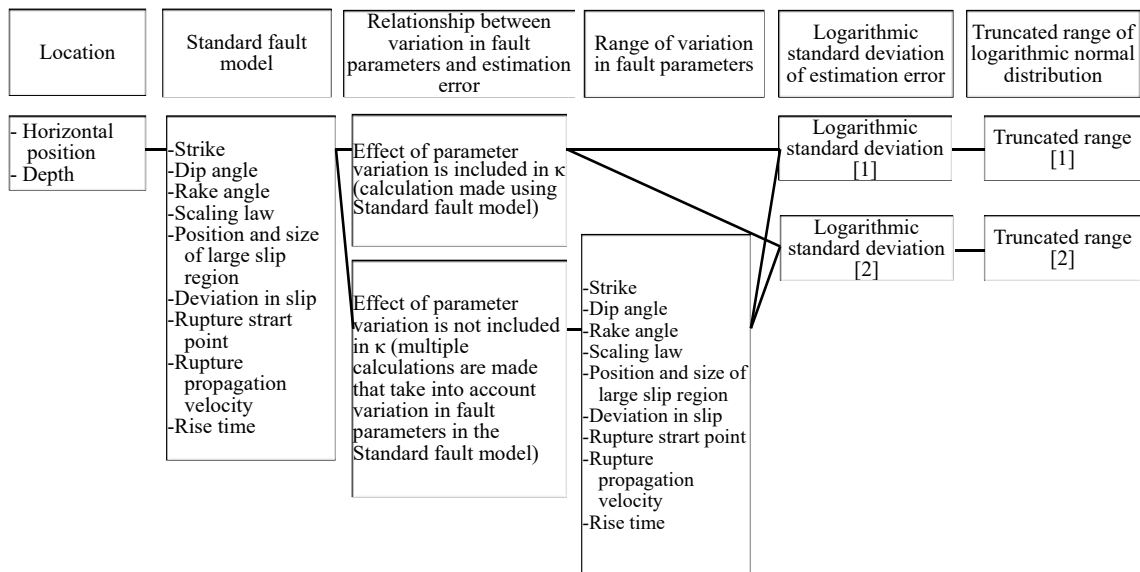


Figure 5.2.3-1 Logic tree for estimation of tsunami height distribution

Table 5.2.3-1(1) κ in cases of uniform slip model*

| Sea region | Earthquake-tsunami | κ | Number of run-up height record points compared |
|---------------------------------|---|----------|--|
| Japan Trench | 1933 Showa Sanriku | 1.40 | 572 |
| | 1896 Meiji Sanriku | 1.45 | 257 |
| | 1968 Tokachi offshore | 1.41 | 273 |
| Nankai Trough | 1946 Nankai | 1.60 | 159 |
| | 1944 Eastern Nankai | 1.58 | 43 |
| | 1854 Ansei Tokai | 1.47 | 89 |
| | 1854 Ansei Nankai | 1.42 | 60 |
| | 1707 Hoei | 1.35 | 61 |
| Eastern margin of the Japan Sea | 1993 Off the shore of Hokkaido southwestern coast | 1.47 | 216 |
| | 1983 Central Japan Sea | 1.48 | 209 |
| Offshore of South America | 1960 Chile | 1.37 | 764 |

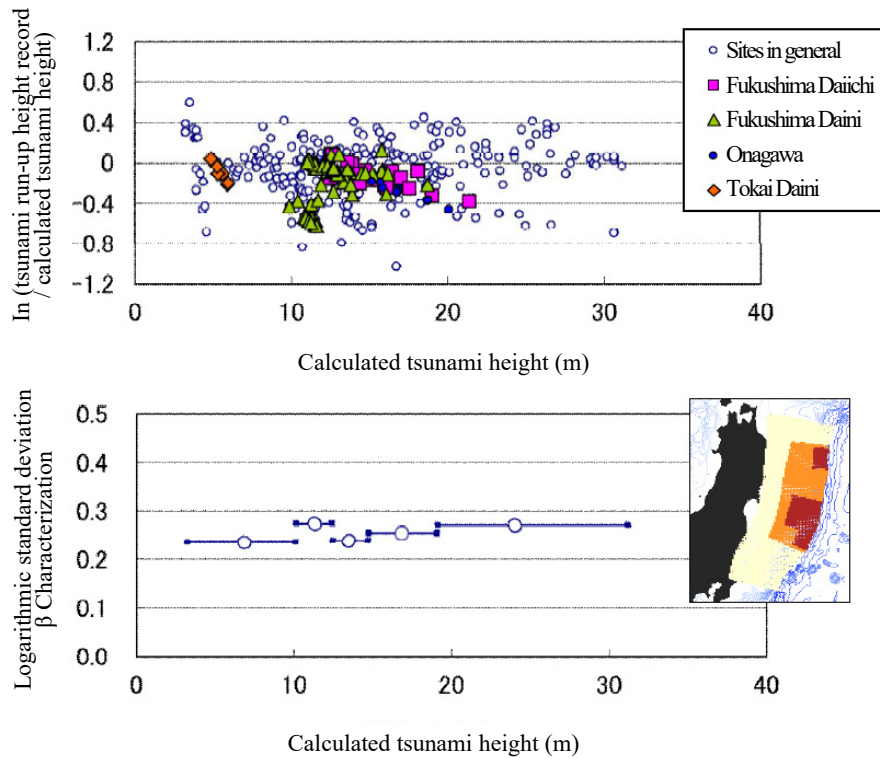
(Median value of the 11 tsunami: 1.453; Median value \pm standard deviation: 1.380 ~ 1.529)

* Uniform slip on the fault plane is considered.

Table 5.2.3-1(2) κ in cases of heterogeneous slip model*

| Sea region | Earthquake-tsunami | κ | Number of run-up height record points compared |
|---------------|-----------------------|----------|--|
| Japan Trench | 1896 Meiji Sanriku | 1.38 | 143 |
| | 1611 Keicho Sanriku | 1.37 | 17 |
| | 1968 Tokachi offshore | 1.38 | 264 |
| | 1856 Ansei Sanriku | 1.45 | 71 |
| Nankai Trough | 1946 Nankai | 1.42 | 96 |
| | 1944 Eastern Nankai | 1.44 | 64 |
| | 1854 Ansei Tokai | 1.48 | 85 |
| | 1854 Ansei Nankai | 1.32 | 42 |
| | 1707 Hiei | 1.37 | 49 |

* Heterogeneous slip on the fault plane is considered.



Note: characterized tsunami source model \times Minimum grid size 5.5m of topography model

Figure 5.2.3-2 Results of examination of variance assessment using characterized tsunami source model (Sugino et al., 2014)

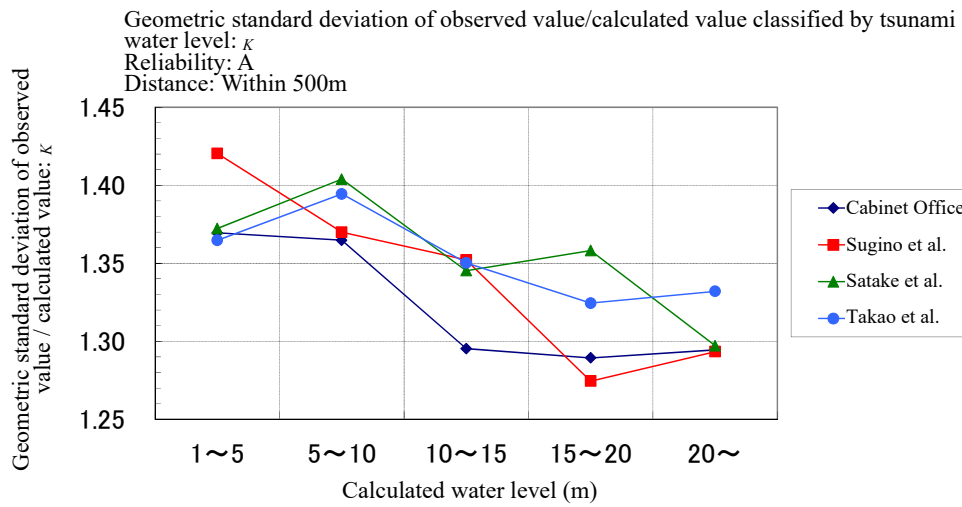


Figure 5.2.3-3 Results of variance assessment using inversion model (Kurita et al., 2013)

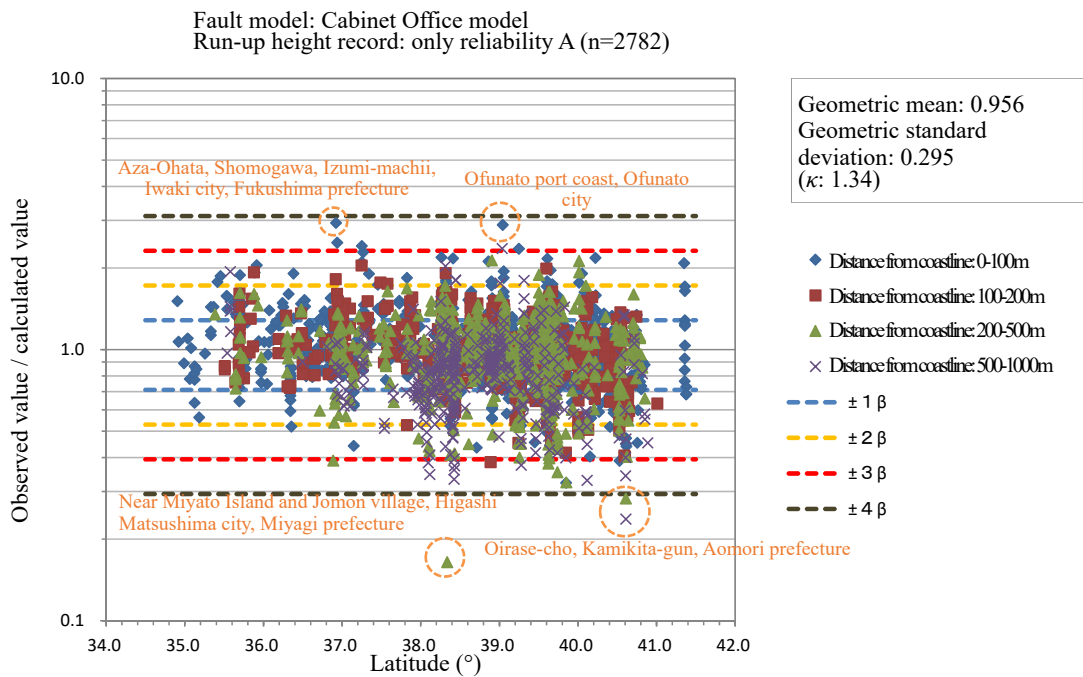


Figure 5.2.3-4 Distribution of observed values/calculated values from results of calculations reproducing 2011 Tohoku Tsunami

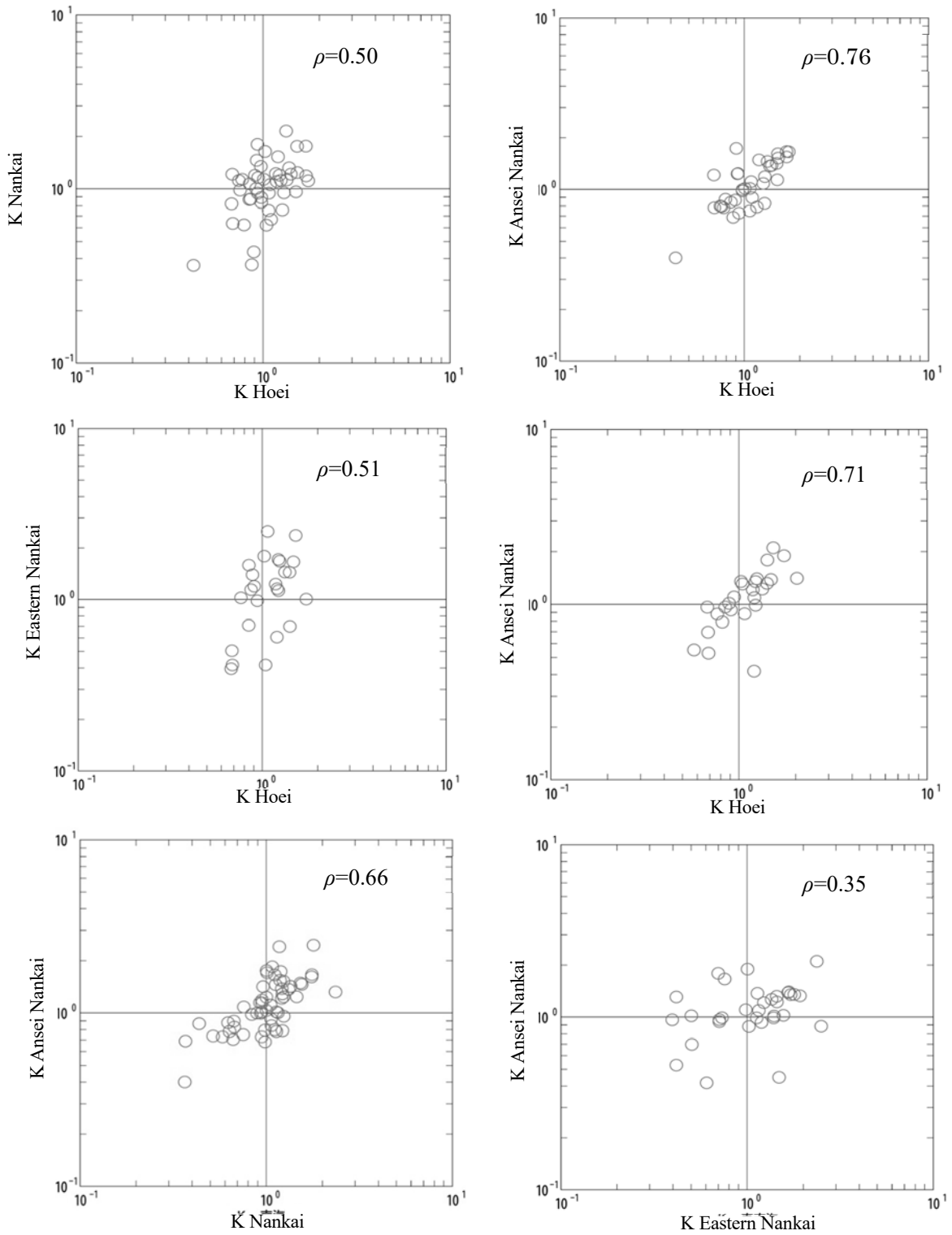


Figure 5.2.3-5 Relationship of K_i at site points of identical place name in relation to two earthquakes (case where tsunami sources overlap)

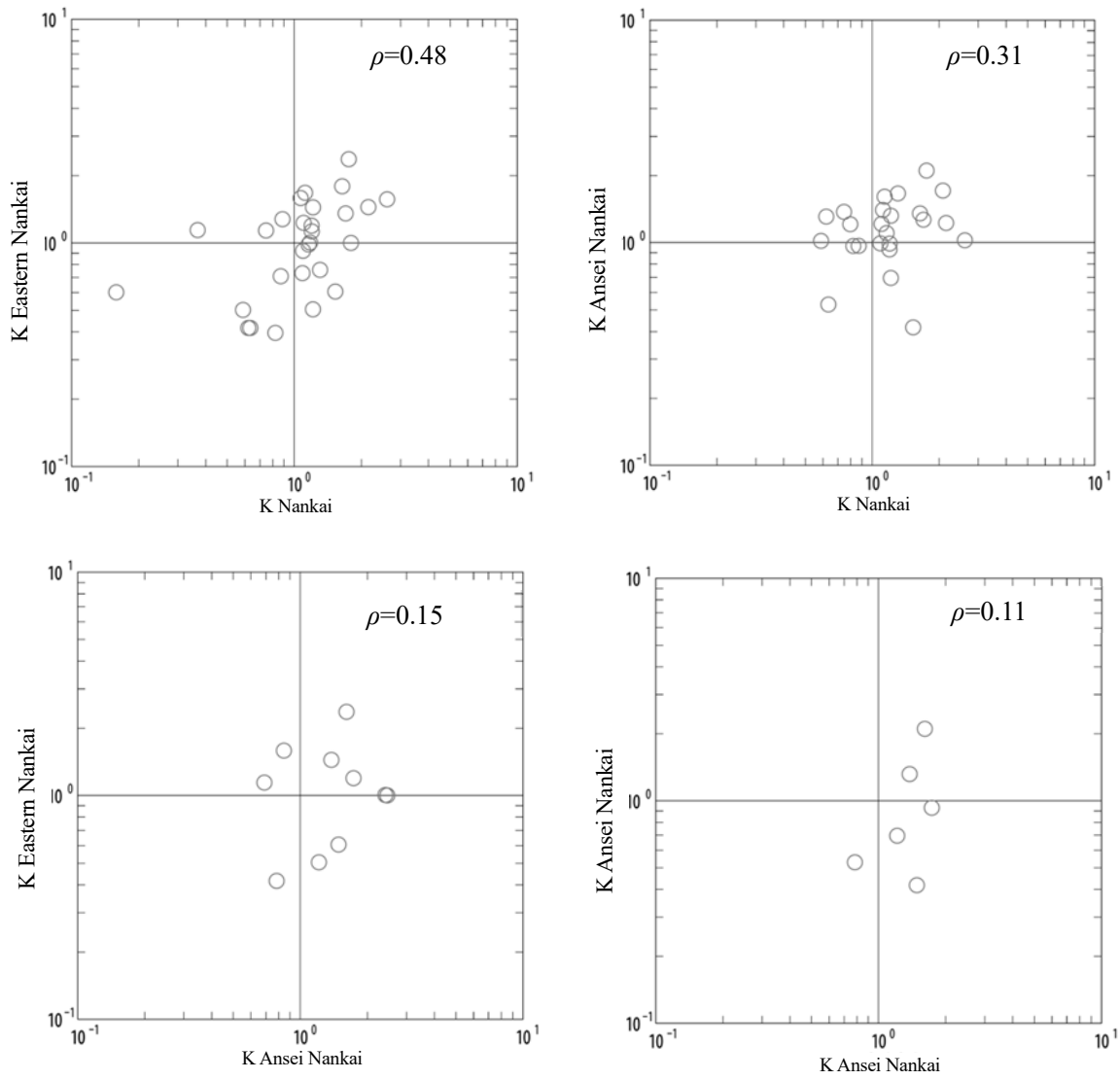


Figure 5.2.3-6 Relationship of K_i at site points of identical place name in relation to two earthquakes (case where tsunami sources do not overlap)

5.2.4 Method for Classification and Weighting of Logic Tree Branches

The purpose in using a logic tree to conduct a probabilistic tsunami hazard analysis is to systematically assess uncertainty at the current time with regard to a hazard assessment as well as any such impact, and to provide information for making an engineering determination under conditions where uncertainty is existing to that end, it is important that branches of logic tree be built that appropriately reflect uncertainty at the current time and that the appropriate weight be set for such branches of logic tree. However, weighting indicates a determination at the current time about the possibility of future accuracy, and it is not regarded as being directly related to accuracy in the natural science sense.

Components of branches of logic tree are able to be divided into two: “components that are branches based mainly on differing judgments and should be regarded as discrete branches” and “components that are branches based mainly on error in values estimated from data and should be regarded as continuous branches”. The former is a component for which a conclusion has been unable to be reached at the current level that research has reached and includes issues such as how to consider source regions of normal fault earthquakes and M8 tsunamigenic earthquakes along the Japan Trench. The latter is essentially determinable based upon data, but is a component for which there are estimation errors resulting from currently insufficient data and other such factors, and includes the average recurrence interval of characteristic earthquakes and other such factors.

Determining the weight of “components that are branches based mainly on differing judgments and should be regarded as discrete branches” is a “distribution of views of a group of experts at the current time”, and a questionnaire or other such survey is a feasible method of determining weight. The approach of the Atomic Energy Society of Japan (2012) and other such research may be referenced with respect to the utilization of “experts”. Such details are given in Section 5.2 of the appendix volume. Also, setting is possible as shown in Table 5.2.4-1, which is a method of allocating weight in cases not based on a questionnaire survey.

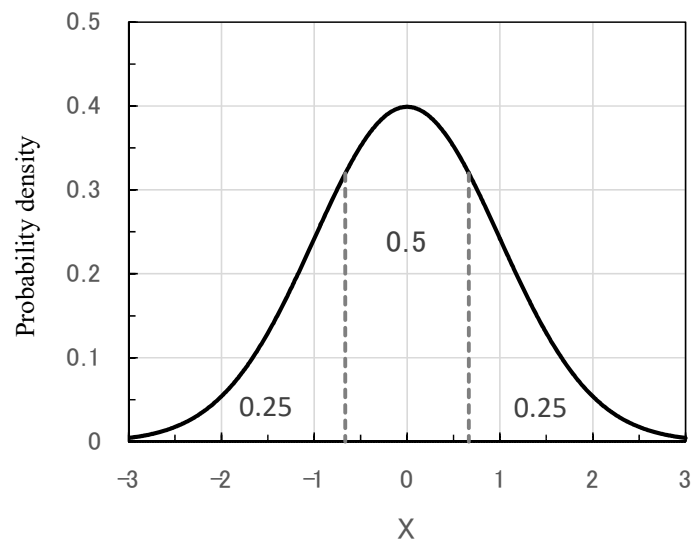
With respect to “components that are branches based mainly on error in values estimated from data and should be regarded as continuous branches”, it is important to appropriately evaluate error based on data. As with the method of evaluating error in relation to the average recurrence interval of characteristic earthquakes as indicated in Section 5.2.1 of the main volume, it is necessary that the method of their evaluation with respect to individual components be clearly defined.

In cases where a continuous distribution is used, it is necessary to utilize the Monte Carlo method which generates samples using random numbers based on the distribution profile, but it is also considered possible to use discrete branches instead of a continuous distribution. In this volume, on the basis of the following approach, the continuous branches (case of normal distribution) have been replaced with discrete branches.

The approach to create branches setting a weight of 0.25:0.50:0.25 in relation to normal distribution is shown in Figure 5.2.4-1. The normal distribution is divided into three so that the areas are 0.25, 0.50 and 0.25, and, when the mean weighting of each region is found, it is -1.27σ , 0.0 , and $+1.27\sigma$. There is also a method where these figures are used directly, but, when consideration is given to the fact that the accuracy of the estimation of σ is not so high and that it is given approximate treatment, 1.0 may be used instead of 1.27.

Table 5.2.4-1 Examples of allocation of weighting in cases not based on questionnaire surveys

| Weighting allocation (case of two branches) | Prerequisites |
|--|--|
| 0.5 : 0.5 | Case where a determination on weighting is difficult using currently available knowledge |
| 0.3 : 0.7 | Case where weight of one side is regarded as high if based on relevant data |
| 0.1 : 0.9 | Case where although the creation of branches is not regarded as necessary if based on relevant data, consideration is given to the feasibility of forming this into a branch |



*Area weighting means are -1.27 , 0.0 and $+1.27$

Figure 5.2.4-1 Illustration of setting up branches in relation to normal distribution

5.3 Probabilistic Tsunami Hazard Analysis Procedures

5.3.1 Calculation Procedures

The procedure of the probabilistic tsunami hazard analysis is given below.

(1) Calculation of Earthquake Occurrence Probability

For each seismic region or active fault, the probability of an earthquake occurrence is calculated. Either of the following methods may be adopted.

- For a hazard analysis in the long-term, the annual occurrence frequency of the earthquake is given. If a Poisson process is assumed, the annual occurrence frequency and annual probability of exceedance will have a 1:1 correspondence.
- For a hazard analysis of the current point, the renewal process is taken into account based on data about the history of earthquake occurrence and the period of time of most recent activity to calculate the probability of occurrence during a specific period of time (ex. 50 years) beginning from the current time.

(2) Calculation of Tsunami Height Distribution

Numerical simulations are used to calculate the water level in front of the site for all scenarios having different calculation configurations. Moreover, error in numerical analysis is taken into account in individual calculation results and converted to a distribution showing the probability of water level exceedance.

(3) Consideration of Tide Level Distribution

In addition to considering tides as a stochastic process, a distribution is prepared with conditions about the probability of water level exceedance when individual scenarios occur.

(4) Creation of Tsunami Water Level Hazard Curve

The probability of an earthquake occurrence is reflected in the distribution of the probability of the water level exceedance in numeral (3) in preparation of multiple tsunami water level hazard curves that indicate the annual probability of water level exceedance in relation to individual scenarios.

(5) Creation of Fractile Hazard Curve

For the group of tsunami hazard curves for each point, the weight of the logic tree branches corresponding to individual scenarios is taken into account in preparing a fractile hazard curve

that indicates the percentage of the consensus that has been obtained among experts who do not think that the probability of exceedance given to a water level will be exceeded.

To create a fractile curve based on the annual probability of exceedance, there are the brute force method which completely expresses all combinations of logic tree branches for each type of fault to find the weighted mean and the Monte Carlo method which generates combinations randomly to approximate the probability.

Expressing the process of the aforementioned numerals (1) to (5) in an equation gives the following.

The results of a calculation (maximum water level) of fault l , magnitude number i , logic tree branch j , and monitoring point k is expressed as:

$$h_{l,i,j,k}^{cal}$$

The probability density function of random variable h where a logarithmic normal distribution is calculated using variance κ and logarithmic mean h^{cal} is:

$$p(h; h^{cal}, \kappa)$$

Also, when the probability density function of tide level h_0 is given as $t(h_0)$, the probability density function $p'_{l,i,j,k}(h')$ of water level $h' = h_{cal} + h_0$, which takes into account the tide level, is:

$$p'_{l,i,j,k}(h') = \int_{h_0=h_0^{\min}}^{h_0^{\max}} p(h' - h_0; h_{l,i,j,k}^{cal}, \kappa) t(h_0) dh_0$$

When variance in the calculation results and the tide level is taking into account for fault l , magnitude number i , logic tree branch j , and monitoring point k , the probability $q_{l,i,j,k}(H^{th})$ of exceeding water level H^{th} is:

$$q_{l,i,j,k}(H^{th}) = \int_{H^{th}}^{\infty} p'_{l,i,j,k}(h') dh'$$

If the earthquake occurrence probability of magnitude number i on logic tree branch j is $w_{l,i,j}$ and the earthquake occurrence frequency on logic tree branch j is o_j , then the frequency at which water level H^{th} is exceeded at fault l , logic tree branch j and monitoring point k is:

$$Q_{l,j,k}(H^{th}) = \sum w_{l,i,j} q_{l,i,j,k}(H^{th}) o_j$$

The hazard curve (=annual probability of exceedance) $f_{l,j,k}(H^{th})$ for logic tree branch j in relation to fault l and monitoring point k is:

$$f_{l,j,k}(H^{th}) = 1 - e^{-Q_{l,j,k}(H^{th})}$$

The annual probability of exceedance $F_{(j_1, j_2, \dots, j_L), k}(H^{th})$ for all (L units) combinations (j_1, j_2, \dots, j_L) of logic trees related to faults is:

$$F_{(j_1, j_2, \dots, j_L), k}(H^{th}) = \sum f_{l, j_1, k}(H^{th})$$

5.3.2 Calculation of Earthquake Occurrence Probability

(1) Methods of Assessing Average Recurrence Interval of Characteristic Earthquakes

Modeling of recurrence intervals of characteristic earthquakes is described in Section 5.2.1(3) of the main volume. According to Table 5.2.1-2, variance of an earthquake recurrence interval model (logarithmic standard deviation σ_{\ln} in a logarithmic normal distribution and α in a BPT distribution) is about 0.2 ~ 0.4. Based on this result, it is regarded as standard to have about three branches of logic tree for variance of earthquake recurrence intervals: 0.2, 0.3, and 0.4.

1) Case Where Data is Available on Average Recurrence Interval

In cases where the average recurrence interval of a characteristic earthquake is based on data, a branch of logic tree is configured based on error and that is assumed to be the logarithmic normal distribution. In a case where the true value of the distribution is x and the arithmetic mean is x_0 , the mean value of x_0-x is zero and the standard deviation (standard error of the distribution of true value x) is σ/\sqrt{n} . σ is the standard deviation of x . Because there is currently a small number of data about average recurrence interval, if the aforementioned standard values ($\sigma_{\ln}= 0.2, 0.3, 0.4$) are used as the standard deviation, then the confidence interval of the estimated values for the number of data units may be assessed. A branch of logic tree for the average recurrence interval is configured based on the confidence interval of the estimated values relating to this earthquake recurrence interval.

In the case of a logarithmic normal distribution, the confidence interval of estimated values for the number of data units pertaining to the recurrence interval is as shown in Table 5.3.2-1.

In an example of a case where the median value of the logarithmic normal distribution is T_m and the number of data units for the earthquake recurrence interval is 1, the confidence level of the values estimated based on variance is as follows.

$$\text{Case where } \sigma_{\ln}=0.2: 0.819 T_m \sim 1.221 T_m$$

$$\text{Case where } \sigma_{\ln}=0.3: 0.741 T_m \sim 1.350 T_m$$

$$\text{Case where } \sigma_{\ln}=0.4: 0.670 T_m \sim 1.492 T_m$$

In a case where the number of data units is 5, the following results are able to be similarly obtained.

$$\text{Case where } \sigma_{\ln}=0.2: 0.914 T_m \sim 1.094 T_m$$

$$\text{Case where } \sigma_{\ln}=0.3: 0.874 T_m \sim 1.144 T_m$$

$$\text{Case where } \sigma_{\ln}=0.4: 0.836 T_m \sim 1.196 T_m$$

It is found that the confidence interval of estimated values is narrower for the case where the number of data units is 5 than for the case where the number of data units is 1.

Table 5.3.2-1 Relationship between variance and confidence interval of estimated values

| No. of data units | Confidence interval | σ_{ln} | | |
|-------------------|---------------------|---------------|-------|-------|
| | | 0.2 | 0.3 | 0.4 |
| 1 | Lower limit | 0.819 | 0.741 | 0.670 |
| | Upper limit | 1.221 | 1.350 | 1.492 |
| 2 | Lower limit | 0.868 | 0.809 | 0.754 |
| | Upper limit | 1.152 | 1.236 | 1.327 |
| 3 | Lower limit | 0.891 | 0.841 | 0.794 |
| | Upper limit | 1.122 | 1.189 | 1.260 |
| 4 | Lower limit | 0.905 | 0.861 | 0.819 |
| | Upper limit | 1.105 | 1.162 | 1.221 |
| 5 | Lower limit | 0.914 | 0.874 | 0.836 |
| | Upper limit | 1.094 | 1.144 | 1.196 |
| 6 | Lower limit | 0.922 | 0.885 | 0.849 |
| | Upper limit | 1.085 | 1.130 | 1.177 |
| 7 | Lower limit | 0.927 | 0.893 | 0.860 |
| | Upper limit | 1.079 | 1.120 | 1.163 |
| 8 | Lower limit | 0.932 | 0.899 | 0.868 |
| | Upper limit | 1.073 | 1.112 | 1.152 |
| 9 | Lower limit | 0.936 | 0.905 | 0.875 |
| | Upper limit | 1.069 | 1.105 | 1.143 |
| 10 | Lower limit | 0.939 | 0.909 | 0.881 |
| | Upper limit | 1.065 | 1.100 | 1.135 |

* σ_{ln} : Logarithmic standard deviation of the logarithmic normal distribution

2) Case Where Data is Not Available on Average Recurrence Interval

When there is no substantial information about the level of activity in submarine active faults, a uniform distribution of 1mm/year (lower limit of activity class A) to 0.1mm/year (upper limit of activity class A) is regarded as the basis.

The mean recurrence interval is obtained by dividing the expected value of the moment release rate per earthquake obtained from the magnitude distribution by the mean moment accumulation rate.

Cases of uniform distribution are simple, but, in the case of the G-R type, if the upper and lower limits of magnitude are m_U and m_L respectively, then the probability density function of the earthquake occurrence frequency in relation to a magnitude m where $m_L \leq m \leq m_U$ is:

$$f(m) = \frac{\beta \exp\{-\beta(m - m_L)\}}{1 - \exp\{-\beta(m_U - m_L)\}} \quad \text{for } m_L \leq m \leq m_U$$

where, $\beta = b \ln 10$ and b are b values. In cases where the b value is unknown, it is assumed to be 0.9 which is the standard value.

3) Confidence Interval for Cases Where recurrence Interval is a Poisson Process

Commensurate with the earthquake sample period (period of time for which records are available) and the number of earthquake occurrences, the confidence interval for the recurrence

frequency is as shown in Table 5.3.2-2. This was prepared based on the table of confidence intervals provided by Weichert (1980), and, when the sample period is T_s , the confidence interval is calculated using the followings:

$$T_s/\mu_U \sim T_s/\mu_L$$

When there is a large number of earthquake occurrences, the confidence interval for recurrence frequency X asymptotes to $X \pm \sqrt{X}$.

Examples of calculations of the confidence interval commensurate with the number of earthquake occurrence in a case where the sample period is 400 years and a case where the sample period is 1,000 years are shown in Table 5.3.2-2. For example, in a case where three earthquakes occurred over a period of 400 years, the upper and lower limits of the number of earthquake occurrences range between 1.37 and 5.92, and it is regarded as sufficient that three earthquakes have occurred during a sample period of 400 years. When this is taken into consideration, the confidence interval for the average recurrence interval is between 68 and 292 years.

Table 5.3.2-2 Confidence interval of Poisson variables (Weichert, 1980)

| Number of earthquakes that occurred N | μ_L | μ_U | 400-year sample period | | 1,000-year sample period | |
|---|---------|---------|------------------------------------|------------------------------------|------------------------------------|------------------------------------|
| | | | Lower limit of confidence interval | Upper limit of confidence interval | Lower limit of confidence interval | Upper limit of confidence interval |
| 0 | 0.00 | 1.84 | 217.39 | ∞ | 543.48 | ∞ |
| 1 | 0.17 | 3.30 | 121.21 | 2,312.14 | 303.03 | 5,780.35 |
| 2 | 0.71 | 4.64 | 86.21 | 564.97 | 215.52 | 1,412.43 |
| 3 | 1.37 | 5.92 | 67.57 | 291.97 | 168.92 | 729.93 |
| 4 | 2.09 | 7.16 | 55.87 | 191.39 | 139.66 | 478.47 |
| 5 | 2.84 | 8.38 | 47.73 | 140.85 | 119.33 | 352.11 |
| 6 | 3.62 | 9.58 | 41.75 | 110.50 | 104.38 | 276.24 |
| 7 | 4.42 | 10.8 | 37.04 | 90.50 | 92.59 | 226.24 |
| 8 | 5.23 | 12.0 | 33.33 | 76.48 | 83.33 | 191.20 |
| 9 | 6.06 | 13.1 | 30.53 | 66.01 | 76.34 | 165.02 |
| 10 | 6.89 | 14.3 | 27.97 | 58.06 | 69.93 | 145.14 |

* μ_L and μ_U : Upper and lower limits of the confidence interval for the number of earthquake occurrences

(2) Probability (Frequency) of Earthquake Occurrence in Hazard Analysis of Long-Term Mean

In the case of a hazard analysis of the long-term mean, the Poisson process is followed for earthquake occurrences. When this focuses on certain seismic region, it is postulated that earthquakes occur in a random manner chronologically. In cases where the latest period of activity is unknown and the properties of the earthquake recurrence time series are not able to be determined, the Poisson process is applied because a probability model that takes into consideration time renewal elements may not be applicable.

When the mean occurrence number per unit of time for earthquakes in accordance with the Poisson process is given as ν , then probability p_k that earthquakes will occur k times or more within time period t is given using the following equation.

$$p_k = \frac{e^{-\nu} (\nu t)^k}{k!}$$

Therefore, the probability that an earthquake will occur 1 or more times during time period t is:

$$1 - p_0 = 1 - e^{-\nu t}$$

The probability of multi-segment rupture is used for regions where it is taken into consideration such as Tokachi-oki (off the shore of Tokachi), Nemuro-oki (off the shore of Nemuro), Miyagi-ken-oki (off the shore of Miyagi Prefecture), close to the trench in Southern Sanriku-oki, and other such regions. The long-term probability of multi-segment rupture is able to be estimated based upon actual past earthquakes (multi-segment rupture rate).

In the region of both Tokachi-oki and Nemuro-oki, it has been estimated that multi-segment earthquakes occurred during the 17th century and in the 12th to 13th centuries, and such earthquakes have been estimated to recur at an interval of between 400 and 500 years (Central Disaster Prevention Council, 2006). The average recurrence interval for the respective segments of Tokachi-oki and Nemuro-oki is about 80 years, and the ratio of multi-segment rupture is regarded as being about 1 in 6.

In the area of Miyagi-ken-oki and close to the trench in Southern Sanriku-oki, there has been one multi-segment rupture earthquake that occurred of the two earthquakes that struck close to the trench in Southern Sanriku-oki (1897 and 1793), and the ratio of multi-segment rupture is regarded as being about 1 in 2.

(3) Probability of Earthquake Occurrence in Hazard Analysis at Current Time

When the logarithmic normal distribution and BPT distribution taking into account the periodicity of earthquakes to individually assess the probability of earthquake occurrences in the future over t period of years, the assessment needs to be carried out in the following method.

BPT distribution takes into account irregularity in the stress accumulation process, and

corresponds to a model where an earthquake occurs when the accumulation of stress reaches a certain level, and the probability of an earthquake occurrence is calculated using variance α pertaining to the seismic interval and mean seismic interval \bar{T} pertaining to earthquakes.

$$f(t) = \left\{ \bar{T} / (2\pi\alpha^2 t^3) \right\}^{1/2} \exp \left\{ - (t - \bar{T})^2 / (2\bar{T}\alpha^2 t) \right\}, t \geq 0$$

In so doing, the probability of the next earthquake occurrence from time T to ΔT years later is:

$$P(T, \Delta T) = \int_T^{T+\Delta T} f(t) dt / \int_T^{\infty} f(t) dt$$

Below, an example is shown where the BPT distribution is used to assess the probability of the earthquake occurrence over a period of 50 years beginning with 2015 as the first year.

Ex.: If the average recurrence interval is 75 years and the time of latest activity is September 26, 2014, then:

- There are 0.2657 years from the time of latest activity through the initial year of 2015, so $T=0.2657$ is assumed.
- If $\alpha=0.3$ is assumed, then when the aforementioned equation is solved based on $\Delta T=50$ and $T=0.2657$, $P(T, \Delta T)=0.11$ is given. In other words the probability of the earthquake occurrence over a period of 50 years beginning from the initial year of 2015 is calculated to be 11%.

In cases where the BPT distribution is used to calculate the rupture probability of each segment and the multi-segment rupture is taken into consideration, then the rupture probability of multi-segment is calculated using the method discussed in Section 5.2.1 of the main volume and is different from the case of a long-term mean. An example is given below.

Ex.: In a case where the rupture probability over the next 30 years for two segments (A and B) is 20% for both and the two segments have ruptured at a rate of 1:6 times in the past.

1) Method described in a preliminary version by the Headquarters for Earthquake Research Promotion:

- (i) The probability of earthquakes simultaneously during the target period is calculated.

$$0.2 \times 0.2 = 0.04$$

- (ii) The resulting probability is multiplied by the rate of multi-segment rupture.

$$0.04 \times 1/6 = 0.007 = 0.7(\%)$$

2) Revised WGCEP method

- (i) In the case of multi-segment earthquakes, half of the mean recurrence probability of past

earthquakes is assumed (=1/12).

$$0.2 \times 1/12$$

(ii) In the case of single earthquake, the recurrence probability \times rate of single earthquake is assumed.

$$0.2 \times 5/6 = 0.17$$

(iii) The remaining portion is allocated so that the number of earthquakes is the minimum.

So that the number of earthquakes for the remaining portion is set at the minimum, multi-segment earthquakes is assumed for all. Accordingly, the probability of multi-segment rupture is: $0.2 \times 1/12 + 0.2 \times 1/12 = 0.033 = 3.3(\%)$.

5.3.3 Configuration of Earthquake Occurrence Model and Tsunami Propagation Model

(1) Occurrence Region

The tsunami sources region that are subject to assessment are appropriately configured by taking into account the impact on assessment points. When variance in the tsunami height estimates is taken into account, it is sufficient that tsunami sources having a significant impact on the probability of exceedance of the targeted water level be regarded as subject to assessment, so it is possible that the composition of the tsunami group reflected in the analysis may change according to the targeted water level. For example, there is an approach where, when calculations are performed using a case where a tsunami becomes the largest within a seismic region (dip angle and rake angle), seismic regions where the maximum water level ascent (descent) H in front of the assessment point is:

$$|X| > |H| \cdot \kappa^{2.3}$$

are not subject to assessment because the only influence on the probability that the water level will be exceeded is on the order of -2 or less of the earthquake occurrence frequency. Where, X is the water level subject to assessment (site height and height at which water may be drawn), and κ is the variance included in the tsunami height. In such a case, even if variance included in tsunami height is assessed, the ultimate impact on the probability of tsunami water level exceedance is regarded as being minuscule. Also, if there is a dominant tsunami source in relation to the hazard, then it is also possible that the relative importance of other occurrence regions or tsunami sources may decrease.

(2) Earthquake Occurrence Model

The basic approach to configuring tsunami source models is shared with the deterministic tsunami hazard analysis presented in Chapter 4 of the main volume. However, in cases where uncertainty in the parameters dominant in the probability of the targeted water level being

exceeded is reflected in the analysis, uncertainty about other parameters whose impact is minimal does not need to be included in the analysis.

(3) Tsunami Propagation Model

In the assessment of phenomenon where tsunami propagate and phenomenon where tsunami inundate, calculation accuracy and other such elements are taken into account so that such hydraulic phenomena are able to be appropriately expressed in selecting the governing equation and numerical scheme as well as configuring the initial conditions and boundary conditions. The basic approach to these elements is presented in Chapter 6 of the main volume.

In cases where the purpose is to design structures, which includes conducting assessments for the purpose of designing the height of seawalls or other such structures on the basis of probabilistic tsunami hazard analyses, it is not necessary that the area around the assessment point reflect the current topography, and it is possible to construct a model, including one where the boundary conditions of the coastline are a vertical wall of unlimited height.

5.3.4 Calculation of Tsunami Height Distribution

(1) Implementation of Tsunami Simulations

The median value of the tsunami height in front of the power plant is needed for all scenarios comprising the branches of a logic tree. The median value is the maximum water level ascent (descent) in front of the power plant that is able to be obtained from numerical simulations of tsunami in accordance with the scenarios.

(2) Consideration of Variance

When the median value has been obtained, various types of errors contained in tsunami simulations are taken into account in calculating the probability distribution of true values (tsunami height that actually strikes the power plant when an earthquake occurs that is in keeping with the scenario). For this, variance κ of the tsunami height included in the scenarios is used. The probability distribution obtained at this stage is a conditional probability when an earthquake as described in the scenario occurs.

The formula for the probability density function of logarithmic normal distribution is given in the following equation, so it is sufficient to apply the logarithm for the median value to μ and the logarithm for κ to σ . For example, in a scenario where a branch of logic tree is selected that holds that “a phenomenon that reaches 1% on both sides of the distribution does not actually occur”, 1% from both sides of the distribution is cut.

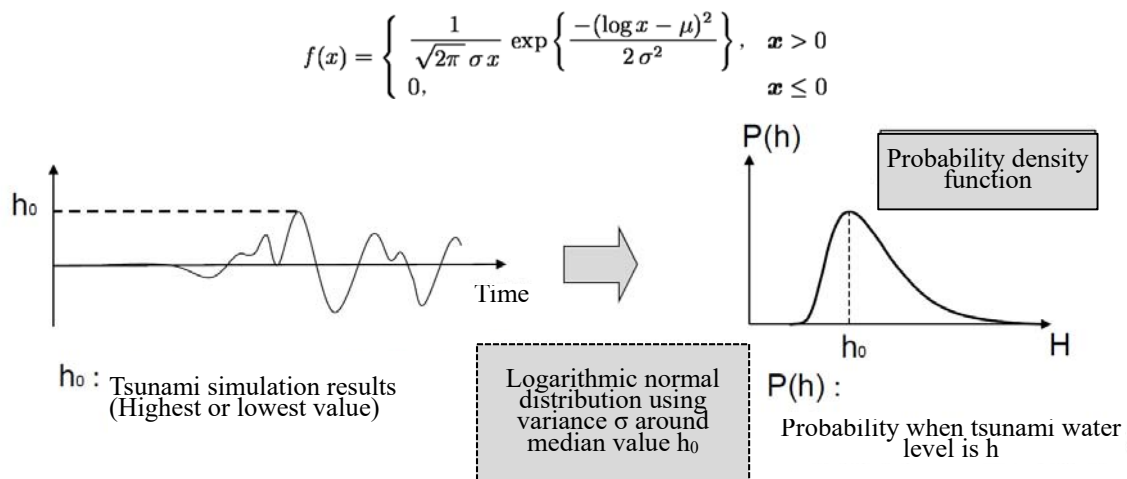


Figure 5.3.4-1 Illustration of consideration of variance in median value

Furthermore, the distribution of the probability of exceedance may be computed by calculating the probability of exceedance for each tsunami height based on the probability density function (Figure 5.3.4-2).

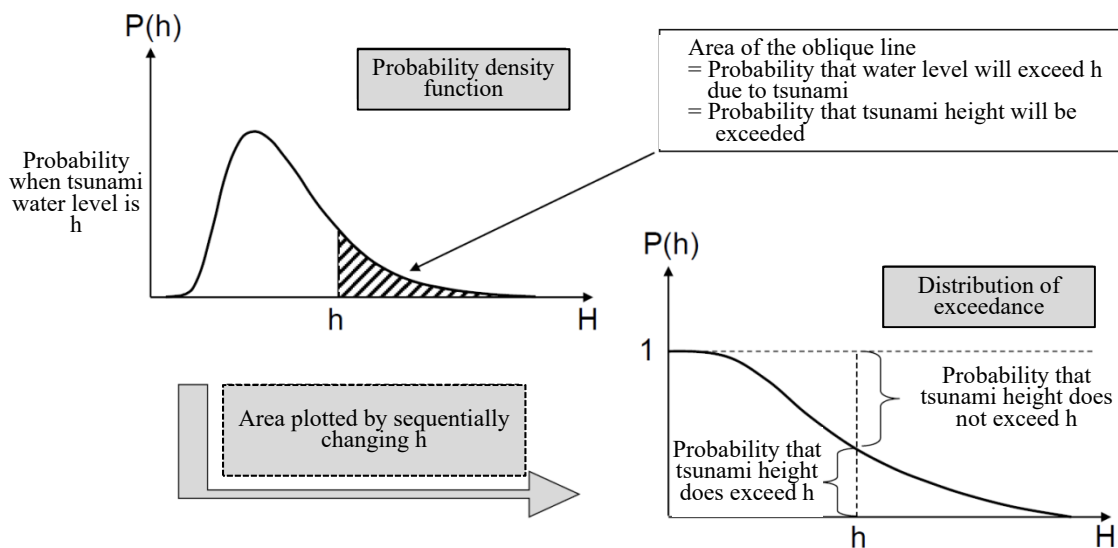


Figure 5.3.4-2 Concept of distribution of probability of water level exceedance

5.3.5 Consideration of Tide Level Distribution

(1) Configuration of Tidal Data

Tide level may be regarded as a random variable that follows a frequency distribution. The probability density function of the tide level may be calculated by using appropriately obtained tide level records of the area around the power plant and processed in the following method.

Specific details on the impact that high tide has on the results of a probabilistic tsunami hazard analysis are given in Section 5.4 of the appendix volume.

1) Case Where Tide Level Records are Available for a Long Period of Time

In a case where records are available about tide levels over a long period of time for the area around the power plant, the tide levels are divided into segments to create a distribution of tide level frequency for each segment from the time history data. If the ratio is multiplied so that the area of the tide level frequency distribution diagram is 1, then this will be the probability density function for tide levels.

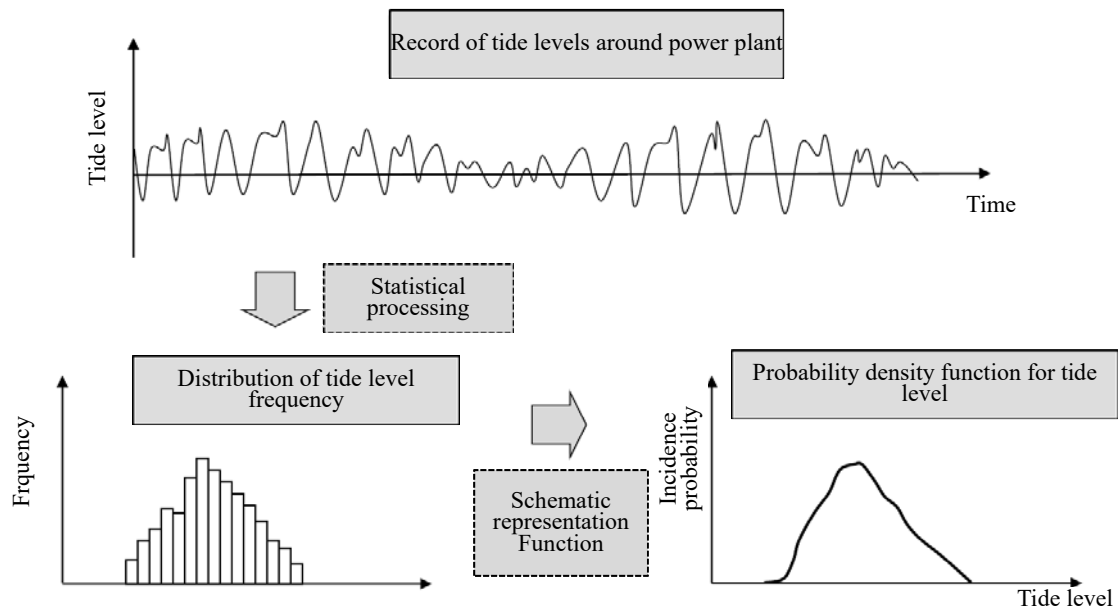


Figure 5.3.5-1 Procedure for converting time history records of tide levels to a probability density function

2) Case Where Only Tidal Harmonic Constant is Available

Tide level records include both astronomical tides that occurred on account of the positional relationship of the earth, moon and sun, as well as meteorological tides which mainly include the effects of atmospheric pressure, and the former are periodical. With tide levels used in probabilistic tsunami hazard analysis, it is desirable to include meteorological tides in order to represent actual tide levels in the area around the power plant. However, in cases where appropriate records of tide levels over the long term are not able to be acquired, it is possible to re-create time history data for astronomical tide levels based on the tidal harmonic constant found from automatic tide-gauge stations near the power plant. However, in such a case,

attention needs to be given so that meteorological tides are not included.

The equation for re-creating tide levels based on the harmonic decomposition value is shown below (Japan Coast Guard, 1992).

$$\text{Tide level } \eta(t) = \sum f_i H_i \cdot \cos([V_i + u_i] - \kappa_i) + Z$$

$$[V_i + u_i] = \{(V_{0i} + u_i) - n \cdot L + \sigma_i \cdot S\} + \sigma_i \cdot t$$

Subscript i represents the types of component tide, and Σ indicates the sum of the component tides.

where,

- f_i, u_i : Correction for amplitude and phase
- H_i, κ_i : Amplitude and lag calculated based on measured values of tides
(harmonic decomposition value)
- V_i : Astronomical parameter
(subscript 0 represents 0:00UT)
- n : Subscript for component tide symbol (ex. $n = 2$ when there are M_2 component tide)
- L : Longitude (west longitude+, east longitude-)
- σ_i : Angular velocity of component tide
- S : Time difference ($S = -9$ at Japan standard time)
- Z : Mean water surface height (height based on basic level surface)

(2) Synthesis of Tide and Calculation Results

In an ordinary tsunami hazard analysis, it is possible to finally take into consideration tide level distribution after a tsunami hazard curve has been obtained. A method for considering tide level distribution in a tsunami hazard curve is shown in Figure 5.3.5-2. Tide level distribution is given as (a), the tsunami hazard curve in a case where the tide level distribution is not taken into account is given as (b), and each of these converted to the segment frequency is shown as (c) and (d), respectively. Adding together the (c) and (d) distributions gives (e), and, when this is converted into a cumulative form, the result is (f).

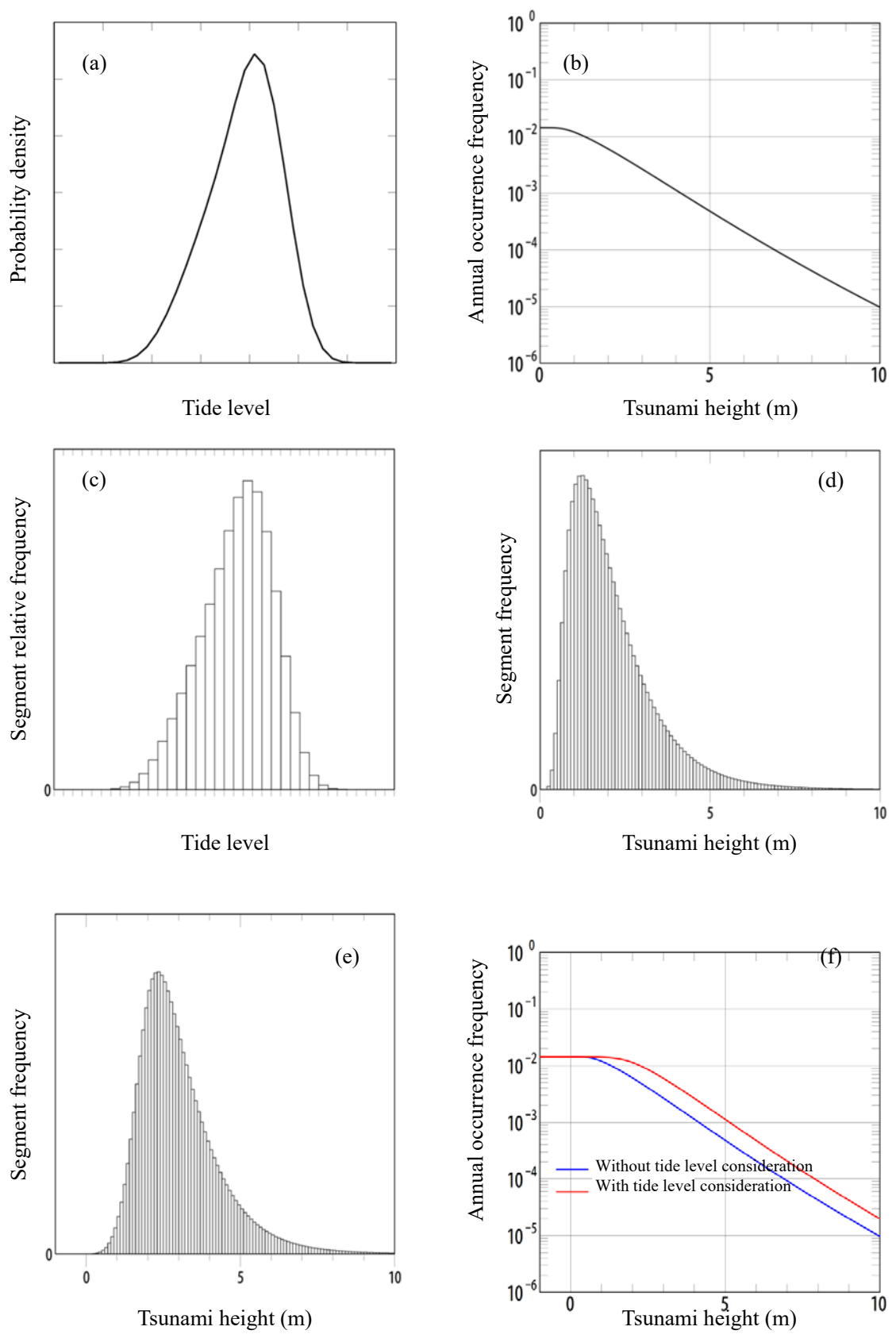


Figure 5.3.5-2 Method of considering tide level distribution in assessment of tsunami hazard curve

5.3.6 Creation of Fractile Curve

The final result of probabilistic tsunami hazard analysis is the frequency that reaches a specific tsunami height (annual probability of exceedance) at a specific site, and the percentage to which a consensus can be reached among experts, who view this level as not being exceeded, is arranged as a parameter (for example, a curve that indicates an annual probability of exceedance where 80% of the experts find that it will be smaller than this is referred to as 80% fractile).

In other words, the abscissa of a fractile hazard curves is the tsunami height (maximum water level or minimum water level), and the ordinates is the annual probability of exceeding this tsunami height (1/year(s)), and several curves are drawn using the ratio (%) of the consensus as a parameter.

It is also possible to draw mean hazard curve by determining the weighted arithmetic mean for each scenario. In the case of the weighted arithmetic mean, sometimes a scenario with very small weight but extremely high probability of exceedance will significantly raise the probability. However, because there is also the advantage that results are easy to intuitively understand and the issue of what should be appropriate fractile is unavoidable, both fractile and mean hazard are calculated in the case of a probabilistic tsunami hazard analysis.

Although the method to calculate fractile hazard curves from hazard curves is shown in Figure 5.3.6-1, fractile curves may actually be calculated according to the following procedure.

- Curves of the annual exceedance probability (hazard curves) are rearranged in descending order for each targeted tsunami height.
- Counting from the largest, the exceedance probability of hazard curves at N% is given as the N% fractile.

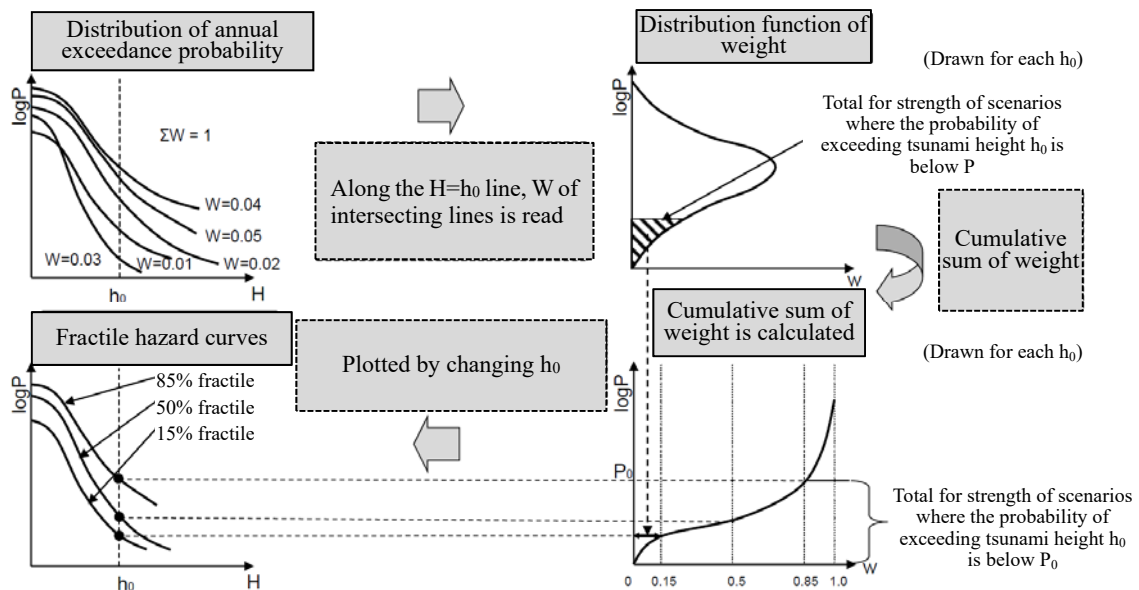


Figure 5.3.6-1 Method to calculate fractile hazard curves from hazard curves

The specifics of the algorithm for calculating fractile curves are shown below, and two methods for randomly creating branches of logic tree (brute-force method and Monte Carlo method) are also indicated.

(1) Brute-Force Method

The reordering of $F_{(j_1, j_2, \dots, j_l), k}(H^{th})$ from lowest to highest value is expressed as $F'_{j', k}(H^{th})$, and the weight of logic tree branch j' is given as $v'_{j'} = \prod_l v_{l, j'_l}$. J is adopted so that to satisfy (Figure 5.3.6-2):

$$\sum_{j'=1}^{J-1} v'_{j'} < V \leq \sum_{j'=1}^J v'_{j'}$$

Then, the $V \times 100\%$ fractile curves $G_k(H^{th})$ are given as:

$$G_k(H^{th}) = F'_{J, k}(H^{th})$$

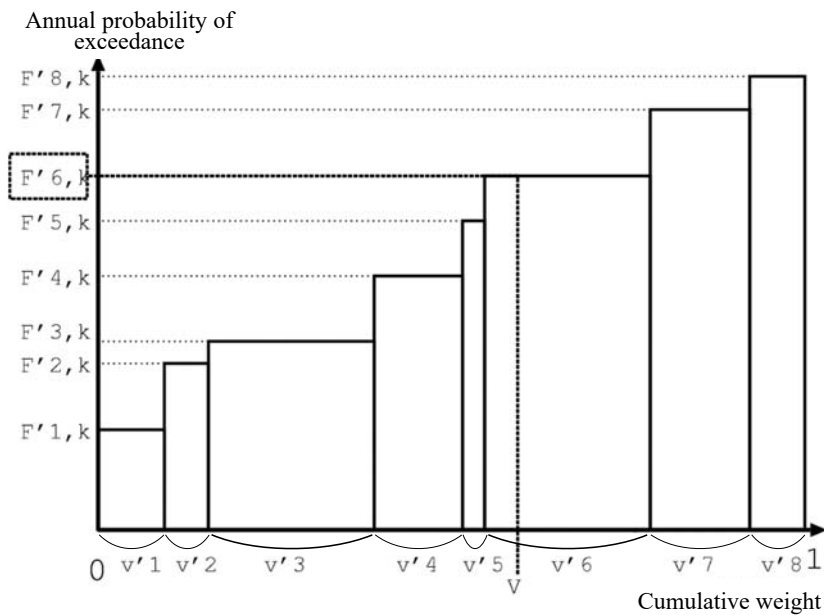


Figure 5.3.6-2 Concept using the brute-force method to convert annual probability of exceedance to fractiles

(2) Monte Carlo method

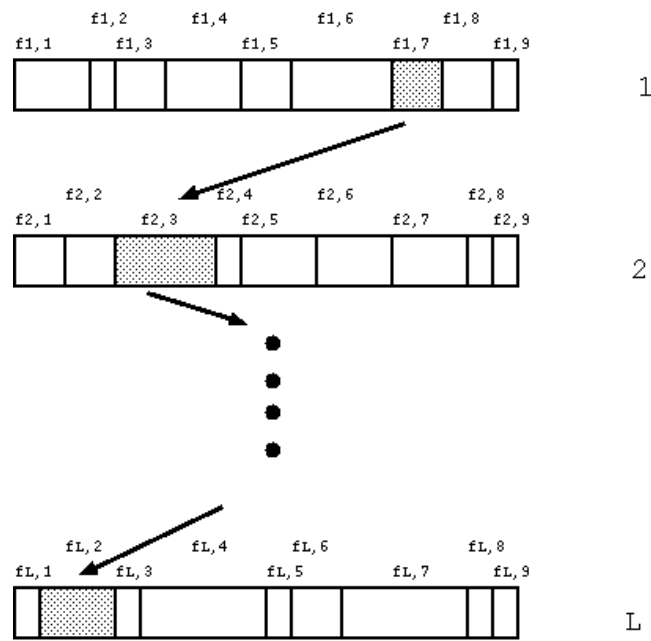
For each fault l , uniform random numbers are produced so that logic tree branch j_l is adopted with probability v_{l, j_l} . (If $\sum_{i=1}^{j_l-1} v_{l, i} \leq$ uniform random number $< \sum_{i=1}^{j_l} v_{l, i}$, then logic tree branch j is adopted)

This is repeated for all faults, and

$$F_{(j_1, j_2, \dots, j_L), k}(H^{th}) = \sum_l f_{l, j_l, k}(H^{th})$$

is calculated.

By repeating this operation, the values of $F_{(j_1, j_2, \dots, j_L), k}(H^{th})$ will be assembled. Because the generated combinations of (j_1, j_2, \dots, j_L) have taken into account weight, $F_{(j_1, j_2, \dots, j_L), k}(H^{th})$ may be regarded as having a uniform weight (see Figure 5.3.6-4). Accordingly, for example, if 100 units are calculated for $F_{(j_1, j_2, \dots, j_L), k}(H^{th})$ using the Monte Carlo method, the value of the 20th, counting from the larger side will be the value for the 80% fractile.



$$F = f_{1,7} + f_{2,3} + \dots + f_{L,2}$$

Figure 5.3.6-3 Monte Carlo method

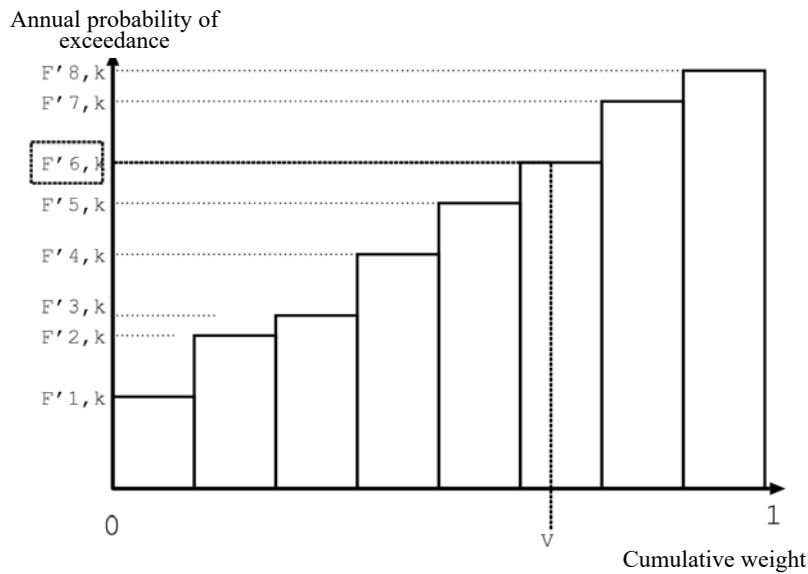


Figure 5.3.6-4 Concept using the Monte Carlo method to convert annual probability of exceedance to fractiles

[Chapter 5 References]

- Aida, I. (1977): Simulation of Large Tsunamis Occurring in the Past off the Coast of the Sanriku District, Bulletin of the Earthquake Research Institute, The University of Tokyo, Vol. 52, pp. 71-101 (in Japanese).
- Annaka, T. and H. Yashiro (2000): Uncertainties in a probabilistic model for seismic hazard analysis in Japan, Risk Analysis II, WITPRESS, Boston, pp. 369-378.
- Annaka, T., M. Shimada and T. Hiroshige (2001): Uncertainty Assessment Method for Earthquake Hazard Curves Based on the Monte Carlo Method, Japan Society of Civil Engineers 56th Annual Scholarly Lecture Meeting, I-A016, pp. 32-33 (in Japanese).
- Annaka, T., T. Suehiro and T. Hiroshige (2002): Uncertainty Assessment Method for Earthquake Hazard Curves Based on the Monte Carlo Method, The 11th Japan Earthquake Engineering Symposium, No. 15, pp. 73-78 (in Japanese).
- Annaka, T., K. Satake, T. Sakakiyama, K. Yanagisawa and N. Shuto (2006): A Method of Probabilistic Tsunami Hazard Analysis, The 12th Japan Earthquake Engineering Symposium, No. 13, pp. 158-161 (in Japanese with English abstract).
- Annaka T., K. Satake, T. Sakakiyama, K. Yanagisawa and N. Shuto (2007): Logic-tree Approach for Probabilistic Tsunami Hazard Analysis and its Applications to the Japanese Coasts, Pure and Applied Geophysics, Vol. 164, pp. 577-592.
- Atomic Energy Society of Japan (2012): Implementation Standard Concerning the Tsunami

- Probabilistic Risk Assessment Due to Tsunami on Nuclear Power Plants: 2011 (in Japanese).
Cabinet Office Nankai Trough Massive Earthquake Model Review Committee (2012): Nankai Trough Massive Earthquake Model Review Committee (Second Report) Tsunami Fault Model Compilation: Tsunami Fault Models and High Tsunami and Flooding Areas, etc. (in Japanese).
http://www.bousai.go.jp/jishin/nankai/model/pdf/20120829_2nd_report01.pdf (Accessed on August 2016)
- Central Disaster Prevention Council Expert Panel on Subduction-Zone Earthquakes Near the Japan and Kuril Trenches (2006): Report of the Expert Panel on Subduction-Zone Earthquakes Near the Japan and Kuril Trenches (in Japanese).
- Ellsworth, W.L., M.V. Matthews, R.M. Nadeau, S.P. Nishenko, P.A. Reasenberg and R.W. Simpson (1999): A Physically-based Earthquake Recurrence Model for Estimation of Long-term Earthquake Probabilities, Workshop on EARTHQUAKE RECURRENCE: STATE OF THE ART AND DIRECTIONS FOR THE FUTURE, Istituto Nazionale de Geofisica, Rome, Italy, pp. 22-25.
- Geist, E. and T. Parsons (2006): Probabilistic Analysis of Tsunami Hazards, Natural Hazards, Vol. 37, pp. 277-314.
- Gutenberg, B. and C.F. Richter (1944): Frequency of earthquakes in California, Bulletin of the Seismological Society of America, Vol. 34, No. 4, pp. 185-188.
- Headquarters for Earthquake Research Promotion Earthquake Research Committee (2001): Methods for Assessment of Long-Term Earthquake Occurrence Probability (June 8, 2001, in Japanese).
- Headquarters for Earthquake Research Promotion Earthquake Research Committee (2005): Long-Term Assessment of Nobi Fault Zone (January 12, 2005, in Japanese).
- Headquarters for Earthquake Research Promotion Earthquake Research Committee (2011): Long-Term Assessment of Earthquake Activity from Area Offshore of Sanriku to Area Offshore of Boso (Second Edition) (November 25, 2011, revised on February 9, 2012, in Japanese).
- Headquarters for Earthquake Research Promotion Earthquake Research Committee (2014): Nationwide Seismic Ground Motion Prediction Map 2014 Version: Survey of Seismic Ground Motion Hazards Nationwide (December 19, 2014, in Japanese).
- Japan Coast Guard (1992): Japan Coastline Tidal Harmonic Constant Table (in Japanese).
- Japan Nuclear Energy Safety Organization (2014): Guide to Formulation of Reference Tsunami Based on the Probabilistic Method.
- Japan Society of Civil Engineers Nuclear Civil Engineering Committee (2011): Methods for Probabilistic Tsunami Hazard Analysis (in Japanese).
<http://committees.jsce.or.jp/ceofnp/node/39>
(Accessed on August 2016)

- Kurita, T., M. Matsuyama and D. Uchino (2013): Uncertainty of Numerical Tsunami Simulation Evaluated in Comparison with the Field Survey Results of the 2011 Tohoku Earthquake Tsunami, *Journal of Japan Society of Civil Engineers B2 (Coastal Engineering)*, Vol. 69, No. 2, pp. I-216 - I-220 (in Japanese with English abstract).
- Mabuchi, H., M. Ohtake and H. Sato (2002): Possibility of Estimating the Maximum Earthquake Magnitude Based on a Modified G-R Model for Magnitude-Frequency Distribution: Spatial Distribution of M_c East off Northeast Japan, *Zisin, Journal of the Seismological Society of Japan, Second Series*, Vol. 55, pp. 261-273 (in Japanese with English abstract).
- Matthews, M.V., W.L. Ellsworth and P.A. Reasenberg (2002): A Brownian Model for Recurrent Earthquakes, *Bulletin of the Seismological Society of America*, Vol. 92, No. 6, pp. 2233-2250.
- Ministry of Construction's Public Works Research Institute Earthquake Hazard Department Earthquake Vibration Research Office (1983): Survey of Frequency and Magnitude of Foreshocks and Aftershocks, *Public Works Research Institute Material*, No. 1995 (in Japanese).
- Murotani, S., K. Satake and Y. Fujii (2013): Scaling Relations of Seismic Moment, Rupture Area, Average Slip, and Asperity Size for $M \sim 9$ Subduction Zone Earthquakes, *Geophysical Research Letters*, Vol. 40, pp. 5070-5074.
- Odagiri, S., and K. Shimazaki (2000): Size of the Historical Earthquake Which Occurred on an Active Fault in Japan, *Zisin, Journal of the Seismological Society of Japan, Second Series*, Vol. 53, pp. 45-56 (in Japanese with English abstract).
- Shimazaki, K., K. Kawase and G. Aoki (1998): One Model for Configuration of Activity Segments in Long and Highly Active Fault System, *Seismological Society of Japan Fall Meeting Proceedings*, C52, p. 112 (in Japanese).
- Sugino, H., Y. Iwabuchi, N. Hashimoto, K. Matsusue, K. Ebisawa, H. Kameda and F. Imamura (2014): The Characterizing Model for Tsunami Source regarding the Inter-plate Earthquake Tsunami, *Journal of Japan Association for Earthquake Engineering*, Vol. 14, No. 5, pp. 1-18 (in Japanese with English abstract).
- Sugino, H., Y. Iwabuchi, M. Nishio, H. Tsutsumi, M. Sakagami and K. Ebisawa (2008): Development of Probabilistic Methodology for Evaluating Tsunami Risk on Nuclear Power Plants, *The 14th World Conference on Earthquake Engineering*, October 12-17, 145 2008, Beijing, China.
- Sugiyama, Y., (1998): Current State of Research on Active Faults and Ancient Earthquakes and Future Issues, *Geology News*, No. 523, pp. 12-20 (in Japanese).
- Utsu, T. (1971): Aftershocks and earthquake statistics (III) - Analyses of the Distribution of Earthquakes in Magnitude, Time, and Space with Special Consideration to Clustering Characteristics of Earthquake Occurrence (1)-, *Journal of the Faculty of Science, Hokkaido University*, Vol. VII, No. 5, pp. 379-441.

- Weichert, D. H. (1980): Estimation of the earthquake recurrence parameters for unequal observation periods for different magnitudes, *Bulletin of the Seismological Society of America*, Vol. 70, No. 4, pp. 1337-1346.
- Wesnousky (1994): The Gutenberg-Richter or Characteristic Earthquake Distribution, Which Is It?, *Bulletin of the Seismological Society of America*, Vol. 84, No. 6, pp. 1940-1959.
- WGCEP (1995): Seismic hazards in southern California: probable earthquakes, 1994 to 2024, *Bulletin of the Seismological Society of America*, Vol. 85, No. 2, pp. 379-439.

Chapter 6 Numerical Simulation Methods

6.1 Simulation of Tsunami Propagation and Run-up

6.1.1 Basic Concepts

(1) Selection of Numerical Model

For assessing the phenomenon of tsunami propagation and run-up, it is important to take into account calculation accuracy and other such elements so that hydraulic phenomena may be appropriately expressed and to select the governing equations and numerical scheme, as well as to configure the initial conditions and boundary conditions.

The method of selecting the numerical model will be discussed in detail in Section 6.1.2 of the main volume.

(2) Execution of Numerical Simulation

The computation domain, grid size, computation time step, bathymetry data, structure data, coefficients in governing equations, and simulating time are appropriately determined according to the spatial tsunami shape and topography of the sea areas along with the sources and target site.

The execution method of the numerical simulation will be discussed in detail in Sections 6.1.3 and 6.1.4 of the main volume.

6.1.2 Selection of Numerical Model

6.1.2.1 Governing Equations and Numerical Scheme

(1) Governing Equations for Tsunami evaluation

Since the tsunami has a longer wavelength as compared to the water depth, the long-wave theory is applied. The theories often used for calculating tsunami propagation are governing equations for two-dimensional field derived by integrating three-dimensional governing equations in the vertical direction from the bottom to the surface of the water, and are divided into three types: linear long-wave theory and nonlinear long-wave theory integrated on the assumption of hydrostatic approximation, and the dispersive wave theory integrated by taking into account wave curvature but not assuming hydrostatic approximation. When calculating tsunami propagation, the characteristics of the following theories need to be understood and then appropriately selected in accordance with the objective phenomena.

In recent years, as fluid analysis technology has developed it is becoming increasingly

possible to also apply three-dimensional fluid analysis models (hereinafter, “three-dimensional models”) that directly calculate a three-dimensional governing equation. Because it is conceivable that in the future there will be a practical three-dimensional model thanks to further advances made with computers, a summary is also provided of three-dimensional models in Section 6.1.4 of the main volume.

1) Linear Long-wave Theory

This is applied under the condition that the ratio of the wave height to the water depth is sufficiently small. The momentum equation comprises an unsteady term and a pressure term (hydrostatic distribution). When the bottom friction cannot be ignored, a friction term should be considered.

2) Nonlinear Long-wave Theory (Shallow Water Wave Theory)

This is applied under the condition that the ratio of the wave height to the water depth is not small (the nonlinearity cannot be ignored). The momentum equation comprises an unsteady term, an advection term, and a pressure term (hydrostatic distribution); with these terms, the steepening of the wave front in shallow water can be considered. In general, since friction with the sea bottom cannot be ignored, a friction term is expressed. The horizontal eddy viscosity term may be considered if necessary.

3) Dispersive Wave Theory

This is applied under the condition that the curvature of the tsunami wave increases with propagation, the vertical acceleration of the water particles cannot be ignored, and wave variance appears. The momentum equation comprises the unsteady term, the advection term, the pressure term, and the variance term, and the variance term is derived by not utilizing hydrostatic approximation in the process of integration. The dispersive wave theory includes a linear dispersive wave theory that focuses on deep sea areas such as calculation of the far-field tsunami propagation, and nonlinear dispersive wave theory that focuses on shallow sea areas such as calculation of near-field tsunami. However, linear long wave theory may be applied in cases where the effect of variance is small even for far-field tsunami (Yanagisawa et al., 2012).

As the tsunami propagates in a shallow water area, depending on the conditions such as wave shape and water depth, the synergetic effect of the nonlinear effect in which the wave peak is inclined forward and the variance effect in which short waves of the cycle are left behind from the wave body as a result, the phenomenon that the tsunami body splits into multiple waves with a short period and the wave height is amplified may occur. This is called soliton fission. If a tsunami is accompanied by soliton fission, wave breaking occurs before or

after run-up. Even if the soliton fission had forced an increase in the run-up heights, this factor is accordingly taken into account by setting the slip of the fault model to be larger, provided the run-up heights were derived from calculations using the same governing equations and numerical scheme employed in setting the fault. Consequently, in discussing the water level, the nonlinear dispersive theory might not be needed in principle. The variance term has the effect of suppressing the leaning of wave front. Therefore, there is also an idea that using dispersive wave theory more consistently than deep water region without limiting to the soliton fission wave generation region can more accurately evaluate the water level change in the coast area including the split start position (Iwase et al., 1998; Hara et al., 1998). There are also examples where the usefulness of this theory has been verified by including a damping term due to wave breaking and applying this to practical numerical simulations (Nuclear Civil Engineering Committee Tsunami Evaluation Subcommittee, 2007).

The index of variance effect by Iwase et al. (2002) serves as an evaluation criterion that takes into consideration the impact of the variance effect in deep sea regions, and examples of detailed reviews are given in Section 4.1.4.2 of the appendix volume.

(2) Governing Equations and Numerical Scheme for Near-field Tsunami Propagation

1) Nonlinear Long-wave Theory

For nearshore tsunami propagation, where the water depth is shallower than 200m, the governing equations of the nonlinear wave theory should be selected (Shuto, 1986). In such a case, an explicit finite difference scheme with a staggered leapfrog method is generally adopted because the analysis method of the numerical error caused by the finite difference scheme is nearly established.

In actual practice, either the method of Goto and Ogawa (1982) (hereinafter referred to as the Goto method, see Section 4.1.1 of the appendix volume) or the method of Tanaka (1985) (hereinafter referred to as the Tanaka method) is applied. Both are nonlinear wave theories, but have slight differences as shown in Table 6.1.2-1.

However, since it has been verified that there is very little difference between both methods except under special conditions when the sea bottom slope is less than 1/100 and the period is less than 5 minutes, the use of either method does not pose a practical problem.

In addition, it is possible to apply the finite element method or other numerical simulation method. In such a case, it should be verified that the accuracy of the method is equal to or better than that of the abovementioned method by a prior analysis of the numerical error.

2) Nonlinear Dispersive Wave Theory

In the design of structures in cases where the structure is subject to the impact of an increase in tsunami force due to soliton fission, such as breakwaters erected in the offing, a nonlinear dispersive wave theory is used to take into consideration such impact.

In the “Tsunami-Resistant Design Guideline for Breakwaters” (Ministry of Land, Infrastructure, Transport and Tourism, 2013), it is stated, “The condition to consider this is that the incident tsunami height is generally at least 30% of the water depth (the tsunami height by numerical simulation is at least 60% of the water depth) and the sea bottom slope is shallow at about 1/100 or less”.

Table 6.1.2-1 Comparison between Goto method and Tanaka method

| | | Goto method | Tanaka method |
|--------------------|--|--|--|
| Governing equation | Advection term | Conservation type | Non-conservation type |
| | Friction term | Manning type | General friction type |
| | Horizontal eddy viscosity term | Introduced if necessary | Introduced |
| Numerical scheme | Alignment of variables | Staggered scheme | Staggered scheme |
| | Difference in pressure term | Leapfrog scheme (Discretization error has accuracy to the second degree because both space and time are from a central difference.) | Leapfrog scheme (Discretization error has accuracy to the second degree because both space and time are from a central difference.) |
| | Difference in advection term | 1 st -order upstream difference scheme with accuracy of 1 st -order | Lax-Wendroff scheme with accuracy of 2 nd -order |
| | Difference in friction term | Approximated implicitly | Approximated explicitly (time forward difference) |
| | Difference in horizontal eddy viscosity term | - | Approximated explicitly (time forward difference) |

(3) Governing equations and numerical scheme for the far-field propagation of tsunamis

In the case of the far-field propagation of a tsunami, the linear theory can be applied because the wave height is small when compared to the water depth. However, when the initial tsunami profile has a wide range with respect to the frequency components, the wave velocity varies slightly for each frequency at the deep water; further, since it propagates for a long time, the delay of the shorter wave is larger. Therefore, in order to reproduce this effect, it becomes necessary to apply governing equations that include the variance term. Furthermore, for far-field tsunamis, the Coriolis force must be considered in the momentum equation. In addition, since the effects of the

spherical earth cannot be ignored, a spherical coordinate system must be adopted. For a numerical scheme, the alignment of variables is performed by a staggered leapfrog scheme while the explicit difference method is adopted for the equation of continuity. An implicit difference calculus is generally adopted for the momentum equation (see Section 4.1.2 of the appendix volume).

6.1.2.2 Initial Conditions

(1) Distribution of vertical displacement on the Sea Bottom

The distribution of vertical displacement on the sea bottom - the initial condition for the numerical simulation of the tsunami - is generally evaluated by using the Mansinha and Smylie (1971) method (see Section 4.2 of the appendix volume) and the Okada (1985) method. These methods are based on the theory of elasticity under the conditions of isotropy and homogeneity. Therefore, it is often the case that calculation of distribution of vertical displacement is performed by these methods for both near-field tsunami and far-field tsunami.

The aforementioned methods treat ground structures as homogeneous, when examining the influence of the three-dimensional underground structure on the tsunami, the method by the seafloor crustal movement analysis that can consider the three-dimensional heterogeneous structure can be applied (see Section 4.2.2 of the appendix volume) (Tsuchiya et al., 2013).

(2) Continuance time of displacement

The duration of the fault movement that generates a tsunami is assumed to be approximately several 10s to 120s. In such a case, the continuance time of displacement has no significant effect on the results of the numerical simulation of the tsunami as compared to the case in which the sea bottom is displaced instantaneously (Aida, 1969; Iwasaki and Yang, 1974). Consequently, both the methods - with and without a consideration of the continuance time of displacement - may be applicable.

When an instantaneous distribution of vertical displacement is assumed on the water surface, a short-period oscillation might occasionally occur in the numerical results. This oscillation can be ignored if it disappears when the continuance time of displacement is considered. Also, as seen in the 2011 Tohoku earthquake, 2004 Sumatra earthquake, when some large earthquakes may have the capability of generating tsunamis due to multiple large fault breaks, the rupture time of fault reaches several hundred seconds or more. For example, in the Cabinet Office (2012), fault rupture velocity propagated from the rupture point and the continuance time of fault displacement (rise time) have been taken into consideration in heterogeneous tsunami source models.

(3) Setting the Initial Conditions

The distribution of vertical displacement on the sea bottom in Section (1) is generally given for the initial water surface as an initial condition. When considering the time change of seabed ground fluctuation, the hydrostatic surface is taken as the initial water level condition. Also, because the dip angle of faults around the trench is quite small, horizontal displacement is larger than vertical displacement. For this reason, tsunami resulting from horizontal displacement in the seafloor slope can no longer be disregarded. Tanioka and Satake (1996) took into consideration the effect on the water level attributable to horizontal displacement in the seafloor slope.

In any of the above cases, there is no initial velocity due to the tsunami.

6.1.2.3 Setting the Boundary Conditions

(1) Offshore Boundary Conditions

Since the computational region is finitely determined, open boundaries are artificially provided on the offshore and lateral sides. Appropriate boundary conditions need to be applied so that the behavior of the tsunami is free from the artificial reflection from the boundaries. The offshore boundary and twolateral side boundaries are referred to as the offshore boundaries.

1) Boundary conditions for a tsunami propagating from the inner to the outer areas of the computational region:

As the boundary conditions in a case where there is a wave source region within the analysis region, free transmission conditions (Goto and Ogawa, 1982) may be assumed, which are derived based on the method of characteristics. Also, by configuring appropriate parameters, nonreflecting boundary conditions (ex., Cerjan et al., 1985) and other such conditions may be applied.

The other free transmission conditions can be considered by setting a virtually complete reflecting wall at the open boundary. The transmitted wave height at this boundary is assumed to be one half of the standing wave height at the virtually complete reflecting wall (Hino and Nakaza, 1988). In such a case, if the wall is properly positioned, results can be obtained with high accuracy (Imamura et al., 2001).

Both the methods, i.e., the method of characteristics and that of the virtually complete reflection wall, can be applied to the case in which the tsunami propagates from the outer to the inner areas of the computational region.

2) Method of inputting a tsunami at the offshore boundary in the near-field ocean:

In case of the calculation of a far-field tsunami in the coasts of Japan, the tsunami motion

is calculated in accordance with the linear long-wave theory or the linear dispersive wave theory formulated using the spherical coordinates system under the initial condition that was obtained using the tsunami source model. The incident tsunami component may be used for the offshore boundary of the computational region in the near-field domain.

The time series of tsunami estimated from tide observation data can be used as an input for the offshore boundary condition.

(2) Onshore Boundary Conditions

The boundary conditions between the sea and land should be applied in accordance with the following conditions.

1) Full Reflection Conditions

When the tsunami run-up onto land is not considered, a vertical wall with an infinite height should be positioned on the coastal line, and the flow rate per unit width in the direction perpendicular to the coastal line should be assumed to be zero. In other words, a complete reflection condition should be applied. However, when this condition is applied, the water depth must be sufficient so that the sea bottom at the seaside region adjacent to the coastal line is not exposed during the run-down of the tsunami. If the water depth is low, the boundary conditions at the run-up front, which are discussed in the following section, can be used by taking the exposure of the sea bottom during the run-down into account.

2) Wave front Conditions

When considering the tsunami run-up onto sloping land or run-down into a shallow sea exposing the sea bottom, the topography is approximated in the form of steps with the mesh size, and the existence of water in the topography at the tsunami front is judged at every time step. Kotani et al. (1998) proposed a method that improved on that of Iwasaki and Mano (1979), and has been extensively used in practical works (see Section 4.3 of the appendix volume). This method can be summarized as follows:

- The tsunami front is located at the boundary between the cell in which the sum of the water depth and maximum still water depth at the cell boundaries (four sides) is positive, and the cell in which the sum is either zero or negative.
- The total water depth for calculating the flow rate per unit width is given as the difference between the water level of the wave front and the bottom height in the neighboring cell. When this difference is negative, the flow rate per unit width should be assumed to be zero (no run-up).
- When calculating advection term, in cases where the total water depth is zero or less

than a certain minimum value, only term where the total water depth has a denominator are omitted in calculating the advection term.

(3) Overflow Boundary Conditions

The boundary conditions for the case in which the tsunami flows over the breakwater, sea dike, seawall revetment, and other structures should be applied according to the following conditions.

1) When the breakwater, etc., are modeled by the ground height as a part of the topography:

In this case, the boundary conditions at the run-up front described in the previous section can be applied to the boundary conditions in which the tsunami flows over the breakwater, etc.

2) When the breakwaters, etc., are modeled by the boundaries between cells:

[1] Honma Model (Honma, 1940)

When breakwaters or sea dikes exist in the computational region and the water level exceeds the crest elevation, the overflow rate per unit width is estimated using the following formulae in accordance with the overflow conditions (Iwasaki et al., 1981; Goto and Ogawa, 1982).

(Complete and incomplete overflows)

$$q = \mu h_1 \sqrt{2gh_1} \quad h_2 \leq \frac{2}{3} h_1$$

(Submerged overflows)

$$q = \mu' h_2 \sqrt{2g(h_1 - h_2)} \quad h_2 > \frac{2}{3} h_1$$

where h_1 and h_2 are the water depths in front of and behind the structure on the top of the structure, respectively, $\mu = 0.35$, $\mu' = 2.6$, and g is the gravitational acceleration. If the water does not flow over the breakwater and sea dike, the complete reflection condition setting of the vertical wall is assumed and the flow rate per unit width in the direction perpendicular to the structures is assumed to be zero.

[2] Aida Model (Aida, 1977a)

When a seawall exists on the coastal line, the volume of overflow onto the dry bed of the seawall can be estimated using the following broad-crested weir formula and the flow rate coefficient as is the case with a submerged breakwater.

$$q = C_1 H_1 \sqrt{g \Delta H}$$

where H_1 is the water level on top of the revetment; ΔH is the water level difference at the discontinuous position; and $C_1=0.6$.

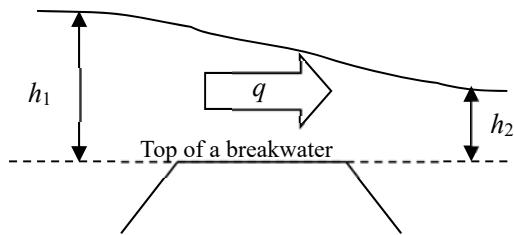


Fig. 6.1.2-1 Description of Honma model

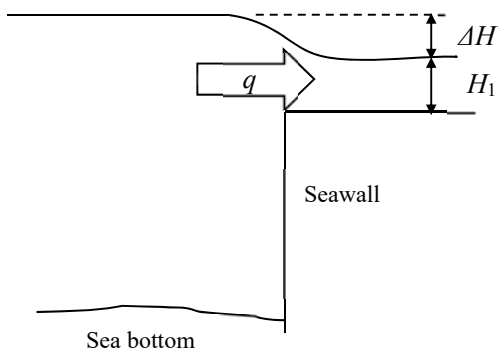


Fig. 6.1.2-2 Description of Aida model formula

6.1.3 Execution of Numerical Simulation

6.1.3.1 Setting the Computational Region

It is important that the size of the tsunami source region, spatial waveform of the tsunami, characteristics of the seafloor and coastal topography, structures and other such elements are taken into account in the calculation region in a numerical simulation of a tsunami so as to appropriately configure the calculation region so that the behavior of the tsunami, which includes refraction, reflection, diffraction, seiche, run-up and so on, is able to be calculated with good precision.

6.1.3.2 Setting the Grid Size

In numerical simulations of tsunami, a method is used to connect and simultaneously calculate regions of the calculation grid size which differ depending on the spatial waveform of the tsunami or topography conditions. In other words, the length of one wave of a tsunami spatial waveform in a sea area is on an order between several kilometers to several hundred kilometers and the wavelength becomes shorter as the water depth becomes less in coastal regions. Therefore, in line with this, a finer grid size will be needed. In addition, because in many cases the topography of areas near the coastline is intricate, the grid size needs to be appropriately configured in keeping with the scale of artificial structures or the distinctive topography of the target coastline, in addition to the spatial waveform of the tsunami.

The following points need to be kept in mind in configuring and connecting the grid sizes.

(1) Grid Size

Grid sizes are set as follows so that accurate calculation results can be obtained in each partial region. However, what is shown below is a target value for the most general case where a numerical simulation model is applied that is based upon the staggered grid and leapfrog difference method. With respect to grid sizes and element dimensions in a case where the finite element method or other numerical simulation model is applied, the appropriate values need to be configured after sufficiently examining the relationship between those and calculation error.

1) Tsunami Source Region

For the tsunami source region, the grid size is configured by focusing on the size of the tsunami source region and the spatial waveform of the tsunami.

As the criterion when configuring the grid size based on the spatial waveform of the tsunami, there is a method proposed by Hasegawa et al. (1987), which is a technique for configuring $1/20$ or less of one wavelength of the tsunami spatial waveform as the grid size.

2) Sea Area in Propagation Process

For a sea area in a propagation process, the grid size is configured by focusing on refraction phenomena that have occurred due to the effect of submarine topography, in addition to the tsunami spatial waveform.

In cases where the submarine topography is simple, the criterion when configuring the grid size is the same as numeral 1), but there are also cases where the grid size is needed that is $1/100$ or less of one wavelength of the tsunami spatial waveform in regions where it is determined that the impact of refraction phenomena is great (see Section 4.3.2.1 of the appendix volume).

3) Sea Area around the Target Site

For sea areas around the target site, the grid sizes are configured by focusing on the tsunami spatial waveform, submarine slope inclination, sea floor and coastal topography, size and shape of seawalls and other structures.

In conditions where the coastal topography is not complex and there is almost no impact from structures, the grid size from a depth of 50m or shallower to the shoreline is made gradually smaller from about 100m to 10m as the criterion.

In cases where there are ports or other such structures, it is known that, if a grid size that is about 1/5 or less of the port opening width is used for the area around the port opening, then the water level in the port will be able to be calculated with good precision (see Section 4.3.2.2 of the appendix volume). Also, in cases where the area near the target site is a V-shaped port, the grid size needs to be configured commensurate with ratio L_V/λ between the port interior mean wavelength L_V and the port length λ . In this case, there are also situations where when $L_V/\lambda < 6$, a grid size needs to be 1/100 or less of one wavelength of an induced seiche or a tsunami in the closed-off section of the port (see Section 4.3.2.2 of the appendix volume).

4) Land Area

For land areas under conditions where the topography is not complex, the grid size (Δx) may be configured by means of the following equation which uses slope gradient α , cycle T , and gravitational acceleration g (see Section 4.3.2.2 of the appendix volume).

$$\frac{\Delta x}{\alpha g T^2} \leq 7 \times 10^{-4} \quad (\text{Case where Manning's coefficient of roughness } n=0.03\text{m}^{-1/3}\text{s})$$
$$\frac{\Delta x}{\alpha g T^2} \leq 4 \times 10^{-4} \quad (\text{Case where friction not considered, Goto and Shuto, 1983})$$

(2) Connection of Regions with Different Grid Size

In numerical simulations of tsunami, the methods of connecting the regions with different grid sizes according to the tsunami spatial waveform and topographic conditions are often used so as to calculate these simultaneously (nesting). In such connection calculations, it is often the case that the grid size is reduced to a ratio of 1/3 or 1/2 in order to alleviate the impact of part of the short wavelength component that occurs in a small region, which does not propagate to a large region and is re-reflected.

The computation may become unstable if the connecting boundary on the lateral side intersects the coastline at an acute angle. This is because the reflected wave from the coastline reaches the lateral side boundary immediately; further, the difference between the actual and

calculated results for a region with a larger grid size is large when the numerical results are obtained for an outer region with a rough topography. It is desirable to take such cases into account in configuring connection regions so that the lateral connection boundaries and land coastline do not intersect at acute angles.

6.1.3.3 Preparation of Topographic Data

(1) Sea Area Topographic Data

The technology for measuring water depth distribution has dramatically improved thanks to the development in recent years of sonic depth finding technology and satellite position measuring technology covering a broad range. For this reason, in numerical simulations of tsunami, it is desirable that the water depth data is prepared based on the latest measurement results from the standpoint of improved accuracy.

For the sea area topographic data, the bathymetric digital data and other information presented in Section 3.2 of the main volume may be utilized. Also, soundings and other specific measurement data may also be used after verifying such accuracy.

(2) Land Area Topographic Data

It is also desirable that land area topographic data are prepared based on the latest topographic maps and other such sources, and the material presented in Section 3.2 of the main volume may be utilized as land area topographic data. Also, specific measurement data may be utilized after verifying such accuracy.

(3) Data of Past Topography

In case where artificial modifications (erection of structures, land reclamation, etc.) that did not exist at the time of the past tsunami incident is reflected in the latest topographic data, when comparing the run-up height of past tsunami at the target site with the tsunami height or reproducing the past tsunami height at the time of simulation, it is possible to utilize topographic data such as the ancient map shown in Section 3.2 of the main volume in which the topography before modification is described.

6.1.3.4 Preparation of Structure Data

(1) Buildings or Other Structures and Two-Dimensional Structures (Linear Structures)

Structures such as buildings that exist in the process of tsunami propagation and run-up, and two-dimensional structures such as sea embankments and breakwaters may affect the behavior of the tsunami. Two-dimensional structures, in particular, need to be given sufficient attention in the

preparation of structure data due to their comparatively large impact, such as obstructing the tsunami flow or changing its direction. Two-dimensional structures include sea embankments, tide embankments, breakwaters, and river levees.

In tsunami calculations, there are many cases where these structures are treated as described below commensurate according to the size of the structure.

1) Cases Where Structures Treated as Topographic Data

In cases of sea embankments, breakwaters and other two-dimensional structures where the width of the structure is wider than the grid size, the height of the structure is assumed in the grid and treated as topographic data.

2) Cases Where Structures Treated as Overflow Boundary Conditions

In cases of sea embankments, breakwaters and other two-dimensional structures where the width of the structure is narrower than the grid size, the structure is arranged as if there is a wall in between grids and the height is taken into account in overflow boundary conditions.

3) Cases Where Structures Addressed by Combining Topographic Data and Overflow Boundary Conditions

In cases where a parapet or other structure, which has a narrow width, has been erected on a breakwaters or other structure that has a wider width than the grid size, the structure may also be addressed by combining 1) topographic data and 2) overflow boundary conditions.

4) Cases Where Structures Treated as if No Structure Present

Detached breakwaters and other such permeable structures for which wave-dissipating concrete blocks have been stacked up are in many cases treated as though there is no structure present at all.

(2) Consideration of Earthquake Resistance and Tsunami Resistance

Because the tsunami often comes after the earthquake, it may be necessary to consider the situation after the earthquake depending on the earthquake resistance of the structure. Also, with embankments and other such structures, scouring may also be anticipated when the tsunami overflows, so there are also cases where scouring of such structures is reflected in numerical simulations as necessary.

(3) Gates, Curtain Walls and Other Structures with Underwater Openings

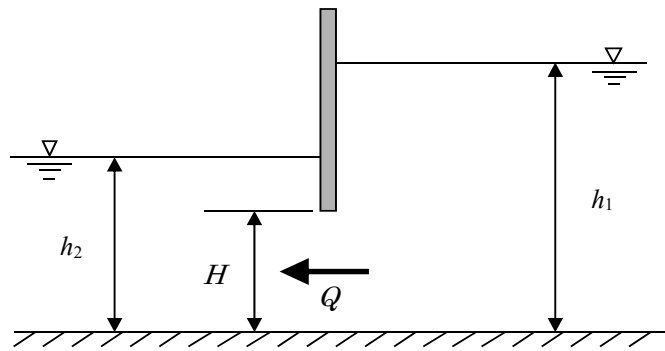
In cases where there are gates, curtain walls or other structures with openings underwater, these are modeled by using a method capable of appropriately computing the flow rate through the opening, as necessary. The calculation formula set forth by Kuriki et al. (1996), which is shown

below, is a method for calculating this pass-through flow rate.

In cases where the tsunami exceeds the crown of a gate or curtain wall, the overflow volume, which is determined based upon Honma (1940) presented in Section 6.1.2.3 of the main volume, is added to the flow rate passing through this opening.

Table 6.1.3-1 Calculation formula for pass-through flow rate for structures having an opening underwater (Kuriki et al., 1996)

| | Water level relationship | | Calculation formula | Flow rate coefficient C |
|-----|--------------------------|-------------------------|--|---------------------------|
| i | $h_2 < H$ | $h_1 < \frac{3}{2}H$ | Free outflow : $Q = CBh_2\sqrt{2g(h_1 - h_2)}$ However, in case of $\frac{h_1}{h_2} \geq \frac{3}{2}$, then $h_2 = \frac{2}{3}h_1$ | 0.79 |
| ii | | $h_1 \geq \frac{3}{2}H$ | Intermediate outflow : $Q = CBH\sqrt{2gh_1}$ | 0.51 |
| iii | $h_2 \geq H$ | | Submerged outflow : $Q = CBH\sqrt{2g(h_1 - h_2)}$ | 0.75 |



h_1, h_2 : Water level in facility (m), H : Opening height (m), Q : Flow rate (m^3/s),
 B : Opening width (m), C : Flow rate coefficient, g : Gravitational acceleration (m/s^2)

Figure 6.1.3-1 Diagram of calculation formula proposed by Kuriki et al. (1996)

6.1.3.5 Setting Various Coefficients, etc.

(1) Coefficients Relating to Friction term

Coefficients assigned to friction term may be configured with reference to the literature and other sources indicated in Table 6.1.3-2.

Table 6.1.3-2 Coefficients assigned to friction term

| Name of coefficient | Values presented in literature | Values often utilized in assessments of tsunami water levels for design of nuclear power plants |
|--|---|---|
| Manning's coefficient of roughness n ($m^{-1/3}s$) | Iwasaki and Mano (1979) : Sea area 0.03 Goto and Sato (1993) : Sea area 0.025 Kotani et al. (1998) : Run-up area(As given below) High-density residential area: 0.08 Medium-density residential area: 0.06 Low-density residential area: 0.04 Forest area: 0.03 Rice/vegetable fields: 0.02 | Sea areas: 0.025, 0.03 Run-up area: 0.025, 0.03 Run-up area near the target site: Configured in accordance with the topography |
| Friction coefficient k_b | Tanaka (1985) : Deep sea area: 0.0026 Shallow sea area: 0.005 to 0.01 Run-up area: 0.01 ~ 0.5 | Deep sea area : (15m or deeper): 0.0026 Shallow sea area : (15m or shallower): 0.00637 Run-up area: 0.01 |

However, in cases where the friction coefficient is modified according to the water depth, it is desirable that it be configured so that it changes smoothly because there are also cases where the results of calculation of the velocity field at such location becomes unnatural when a change is made in a discontinuous manner.

(2) Horizontal Eddy Viscosity Coefficient

If the horizontal eddy viscosity coefficient is $10m^2/s$ ($10^5cm^2/s$) or less, then the rate of water level decline will be about 5% or less in comparison to a zero case (see Section 4.3.3.2 of the appendix volume), so in cases where a change in the water level is subject to assessment, $10m^2/s$ ($10^5cm^2/s$) may be set as the criterion for the maximum value.

With the Tanaka method, $10m^2/s$ ($10^5cm^2/s$) has been empirically adopted as the horizontal eddy viscosity coefficient.

(3) Wave Depth Relating to Tsunami Head

In theory, when the water depth at the tsunami head becomes zero, that location turns into a newly exposed area. However, in actuality, there are cases where meaningless calculations are continued at minute water depths caused by numerical simulation error. Also, because water depth of the run-up tsunami head is very small, denominators for friction and advection term become smaller and numerical simulation becomes easy to diverge.

Therefore, the two methods are used. The first method sets "Minimum water depth" so as not to carry out calculation by regarding the water depth at the tip as zero, and the second method sets "Virtual water depth" so as not to make the water depth, which is substituted for the friction term and advection term, smaller than a certain water depth. Imazu et al. (1996) conducted research on minimum water depth and virtual water depth, and this study may be referenced in such setting.

6.1.3.6 Setting Simulation Time and Computation Time Interval

(1) Simulation Time

The first wave of a tsunami is not always the largest, and the time when the largest wave rises changes depending on the initial water level of the tsunami, topographic conditions near the target site and other factors. For example, in cases where the resonant oscillation inside the bay are excited and cases where reflective waves and succeeding waves overlap, the maximum water level may also occur after several waves, and it is important to set a sufficient simulation time to grasp these.

(2) Setting Computation Time Interval

For grid size appropriately set according to the concept described in Section 6.1.3.2 of the main volume, computation time intervals are set to satisfy the Courant-Friedrichs-Lewy (CFL) condition (a general condition of stability in numerical simulations of wave motion, and, the conditions for cases of plane two-dimensional numerical simulation are indicated below) shown below, taking account of the stability of the simulation.

$$\Delta t \leq \frac{\Delta x}{\sqrt{2gh_{max}}}$$

where, Δx : Grid size

Δt : Computation time interval

h_{max} : Maximum water depth

g : Gravitational acceleration.

Ordinarily, calculation regions with different mesh sizes are connected and the numerical simulation is carried out all together with the time intervals set to be constant. Firstly, Δt is found

so that the CFL condition is satisfied for each region where Δx is the same, and, finally, the minimum Δt or less is adopted as the computation time interval.

However, in cases where actual calculations are performed, numerical error and nonlinearity of phenomena interfere, so Δt needs to be configured smaller with some margin in comparison to $\Delta x / \sqrt{2gh_{max}}$. In particular, when performing calculations in a case where high velocity flow is present in coastal or other such areas where the inundation depth become smaller, there are also cases where the flow velocity value will become greater than tsunami propagation velocity $\sqrt{gh_{max}}$ and this leads to calculation divergence.

6.1.4 Three-Dimensional Model

6.1.4.1 Basic Approach

Three-dimensional models may be used as a useful means when reproducing the three-dimensional flow of a tsunami around a structure or other such location, and when assessing the tsunami wave force more precision. However, tremendous computational resources are necessary to effectuate all three processes of tsunami occurrence, ocean propagation and land run-up in a three-dimensional model. Accordingly, it is necessary to devise measures such as limitation of calculation region, appropriate configuration of reproduction time of phenomenon, proper coupling with plane two-dimensional model, etc.

6.1.4.2 Typical Three-Dimensional Model

In the application of a three-dimensional model, it is desirable to use an analysis code that has been verified for assessment of tsunami wave force and three-dimensional fluid behavior having a water surface. An overview of typical three-dimensional fluid analysis codes and case studies verifying their validity are given in Table 6.1.4-1.

6.1.4.3 Perform of Numerical Simulation

Ordinarily, calculation grid sizes in a horizontal direction of a three-dimensional model need to be made even smaller than those of a plane two-dimensional model. Also, there are cases where the calculation accuracy of the hydraulic quantity decreases when the calculation grid sizes in a vertical direction are rough. Nevertheless, a well-defined index for grid division of three-dimensional models has not been proposed as of the current point in time, so it is desirable to verify that appropriate calculation accuracy is able to be obtained in comparison with proven analysis results and hydraulic

model experiment results by performing preliminary calculations or other such techniques.

Case studies of analyses of hydraulic model experiments, which are given in Section 4.1.6 of the appendix volume, may be referenced with respect to verifying the validity of three-dimensional models.

Table 6.1.4-1(1) Previous case studies of typical three-dimensional fluid analysis codes

| Name of analysis code (source) | Summary | Case study verifying validity |
|---|--|--|
| CADMAS-SURF/3D (Coastal Development Institute of Technology, 2010) | <ul style="list-style-type: none"> • Non-hydrostatic three-dimensional model for which the governing equation is continuity equation and the Navier-Stokes equation enhanced for porous model, which focus on three-dimensional incompressible viscous fluid. • For discretization over time, the Euler method, coupling of the momentum equation is used, and the SMAC^{*1} method is used for continuity equation, and the VOF^{*2} method is used for the free surface analysis model. • In addition to calculations of wave pressure and behavior of tsunami running up on land, coupling is also possible with gas, ground and solids. | Validity was verified based on a comparison with the results of model experiments on run-up tsunami with respect to fluid behavior and wave pressure (Arikawa et al., 2005) |
| OpenFOAM (OpenFOAM Foundation) | <ul style="list-style-type: none"> • Analysis code for two-phase flow of immiscible fluid incompressible of water and air (interFoam solver). • Using the continuity equation and Navier-Stokes equation for incompressible fluids as the governing equation, the finite volume method is employed to perform discretization and the PISO^{*3} method is used to calculate flow velocity and pressure. • The VOF method is used for tracking gas-liquid interface. • Tsunami behavior along the coastline, including run-up tsunami, may be calculated. | Verified by applying OpenFOAM calculations for reproducing water column collapse issues and run-up tsunami hydraulic experiments, and compared with the results of tests on fluid behavior and water pressure (Pham et al., 2012; Kawasaki et al., 2013) |

Table 6.1.4-1(2) Previous case studies of typical three-dimensional fluid analysis codes

| Name of analysis code (source) | Summary | Case study verifying validity |
|---|---|--|
| <p>Storm Surge and Tsunami Simulator (STOC^{*4})</p> <p>(Tomita and Kakinuma, 2005; Takahashi and Tomita, 2013)</p> | <ul style="list-style-type: none"> • Hybrid model capable of connecting, as necessary, the quasi-three-dimensional hydrostatic multilevel model STOC-ML with the three-dimensional non-hydrostatic flow model STOC-IC. • Capable of analyzing propagation and run-up of far-field tsunami and near-field tsunami, soliton fission, interference with structures, and tsunami debris. <p>STOC-IC</p> <ul style="list-style-type: none"> • Non-hydrostatic three-dimensional model, which uses as its governing equation the Reynolds equation and continuity equation applying the porous model to discretize space over a staggered mesh and uses the leapfrog method to evolve over time. • Correspondingly applies the time evolution-type bore model to the wave breaking model. <p>STOC-ML</p> <ul style="list-style-type: none"> • Calculation may also be performed in single layers using a quasi-three-dimensional model that divides the calculation region into multiple phases in a vertical direction and assumes hydrostatic pressure at each phase. • Other than the fact that pressure is not solved and wave breaking is not taken into consideration, it is the same as STOC-IC. | <p>Model validity and precision has been verified based on a comparison with model experiments of tsunami on inclined planes, experiments on overflow of rectangular weirs, model experiments on tsunami breakwaters, and model experiments based on actual topography (Tomita and Kakinuma, 2005; Tomita and Honda, 2008; Takahashi and Tomita, 2013)</p> |
| <p>DOLPHIN-3D</p> <p>(Kawasaki and Hakamada, 2007)</p> | <ul style="list-style-type: none"> • Three-dimensional multiphase flow turbulence numerical model which is based on the expanded SMAC method and CIP^{*6} method which adopts irregular interval grids, kinematic analysis techniques for multiple rigid bodies, and the dynamic bivariate mixing model DTM^{*5}. • The governing equation is comprised of a mass conservation method for compressible viscous fluid, momentum equation, pressure equation, advection equation with density function indicating the interphase ratio, and equation of state for barotropic fluid. • The behavior of run-up tsunami and other such waves, interaction between structures and tsunami, and the dynamic behavior of tsunami debris are able to be calculated. | <p>Verified in a comparison with results of model experiments on collisions and drifting of rectangular rigid bodies with bore following water column collapse with respect to fluid behavior and wave pressure (Kawasaki et al., 2006; Kawasaki and Hakamada, 2007)</p> |

Table 6.1.4-1(3) Previous case studies of typical three-dimensional fluid analysis codes

| Name of analysis code (source) | Summary | Case study verifying validity |
|---|--|--|
| <p>Tsunami complex disaster forecasting model</p> <p>(Yoneyama and Nagashima, 2009)</p> | <ul style="list-style-type: none"> • Non-hydrostatic three-dimensional model for incompressible fluid in which the VOF method is used for predicting surface behavior and the FAVOR^{*7} method is used for handling boundary profiles. • The governing equation is comprised of the continuity equation, the Reynolds equation, advection equation for fluid volume and the turbulent flow valuation formula, and these are discretized on an orthogonal coordinate system and analyzed based on the SIMPLE^{*8} method. • In addition to fluid movement, vessel movement and mooring line tension may also be calculated. | <p>The validity of run-up tsunami and tsunami debris behavior have been validated based on a comparison with the results of model experiments (Yoneyama et al., 2008; Yoneyama and Nagashima, 2009)</p> |
| <p>C-HYDRO3D</p> <p>Kihara and Matsuyama, 2010; Kihara et al., 2013; Kihara et al., 2012)</p> | <ul style="list-style-type: none"> • Three-dimensional numerical model where hydrostatic approximation is assumed in which partial continuity equation based on topographic frame of reference, continuity equation that is vertically integrated from subgrade to water surface, and a momentum equation with a horizontal direction in which hydrostatic approximation used are used as the basic equations. • For the turbulence model, the Mellor and Yamada level 2 model has been adopted for the vertical direction and the Smagorinsky model for the horizontal direction. • The finite difference method is used for discretization, a staggered arrangement for arrangement of variables, and the FSC method, which is a semi-implicit method, for time evolution of the governing equation. • In addition to calculating tsunami propagation from the tsunami source region to the coastline as well as overflow and the run-up flow, calculations may also be made of geomorphic change due to the tsunami and the movement of tsunami debris. | <ul style="list-style-type: none"> • Validated reproducibility of tsunami behavior and geomorphic change for the area around ports in Sri Lanka using model experiments and the 2004 Sumatra earthquake tsunami • Using a comparison with moving-bed open channel experiments, vertical distribution of suspended sediment concentrations has been validated (Kihara and Matsuyama, 2010; Kihara et al., 2012) |

*1 SMAC: Simplified Marker and Cell

*2 VOF: Volume of Fluid

*3 PISO: Pressure-Implicit with Splitting of Operators

*4 STOC: Storm Surge and Tsunami Simulator in Oceans and Coastal Areas

*5 DTM: Dynamic Two-parameter mixed model

*6 CIP: Cubic Interpolated Propagation

*7 FAVOR: Fractional Area/Volume Obstacle Representation

*8 SIMPLE: Semi-Implicit Method for Pressure-Linked Equation

6.2 Numerical Methods for Tsunami Generated by Submarine Landslides, Slope Failure, Flank Collapse, etc.

6.2.1 Basic Approach

There are several triggers for generation of tsunami: submarine landslide, slope failure, flank collapse caused by volcanic activity or other such events (hereinafter, referred to as “landslides, etc”). In the numerical simulations of tsunami we should take into account the requirements for its propagation and run-up calculations described in Section 6.1 of the main volume. It is particularly necessary to keep these requirements in mind in determining computational conditions and modeling the process of tsunami generation.

6.2.2 Selection of Numerical Model

Although various numerical methods have been proposed with respect to tsunami due to landslides, etc., there are few cases of such application in comparison with tsunami occurring due to fault movement. For this reason, in selecting a method, attention needs to be given to phenomena anticipated by each method and the scope of such application.

Considering uncertainty with the numerical method, it is conceivable that multiple methods may be selected and applied to anticipated phenomena. The selection of a method and the validity of the configuration need to be verified by, for example, comparing multiple calculation results against each other.

Table 6.2.2-1 shows numerical simulation methods for tsunami due to landslides, etc. The methods are described in Section 4.4.1 of the appendix volume.

6.2.3 Execution of Numerical Simulation

6.2.3.1 Setting the Computational Region and Grid Size

Based on the spatial waveform of the tsunami, characteristics of the topography from the tsunami source to the evaluation points and other elements, computational region and grid size are appropriately determined as with tsunami due to fault movements. In tsunami source regions where

landslides and other such events may occur, considering the size of the depletion zone and accumulation zone as well as the wavelength of the tsunami, we need to determine an appropriate grid size. For example, with the Kinematic Landslide model where the distribution profile and movement of landslide bodies are input and the two-layer flow model where the initial distribution profile of landslide bodies is input and the subsequent distribution and movement can be calculated, in cases where a model the distribution profile and movement of landslide bodies are input and calculated is utilized, a computational region is configured so that the region comprising movement of landslide bodies that give rise to tsunami (=tsunami source region) is included, and then a grid interval needs to be configured that is appropriate for representing the distribution profile and movement of landslide bodies.

Reference information concerning grid intervals appropriate for tsunami source regions is given in Section 4.4.2 of the appendix volume.

6.2.3.2 Setting the Computation Time Interval

In determining computation time interval, in addition to satisfying the CFL condition, it is necessary to satisfy the conditions that accord with the selected numerical simulation model for the process of tsunami generation. However, there are few methods for which the conditions for computation time interval are clearly defined and, moreover, numerical error, nonlinearity, and other issues are involved, so a determination needs to be made on verifying validity and convergence as to whether or not the computation time interval has been appropriately set for the actual calculation.

6.2.3.3 Topographic Conditions

As for input conditions for numerical simulation of tsunami due to landslides, etc., there are cases where it is necessary to have topographic conditions for landslides, etc. such as the disintegrated sediment volume, topography before and after collapse, and topography of slip planes. With respect to landslides, etc. that generated in the past, Hiraishi et al. (2001) (submarine landslides) and Satake and Kato (2001) (flank collapse) provide case studies that reconstruct the pre-occurrence topography based upon data about the topography in the vicinity of the generation area. The Express Highway Research Foundation of Japan (1985) offers a method for preparing the collapsed surface of a slope failure. Also, reference for configuring topographic conditions have been described in Section 3.3.1 of the main volume.

6.2.3.4 Various Coefficients, etc.

Various coefficients and other constants need to be appropriately determined on the basis of the numerical method and the phenomena. Values of various coefficients from previous studies are given in Section 4.4.1 of the appendix volume. Also, with respect to several numerical methods, studies of the relationship between simulation conditions and computed tsunami heights are given in Section 4.4.3 of the appendix volume.

Many previous studies have determined coefficients through a process of trial and error by comparing calculation results and the run-up height of past tsunamis. In the determination of various coefficients, the characteristics of events need to be taken into account in examining the difference between the values considered while, at the same time, continuing to reference setting values for which reproducibility has been verified in past reviews. In determining the various coefficients related to topography after landslides and landslide movements, it is considered effective to reference the results of analyses based on models used for analyzing landslide movement (LSFLOW, TITAN2D, FLOW3D, etc.). For example, Sasahara (2004) used LSFLOW to perform a flank collapse simulation and verify consistency by comparing the results interpreted from submarine topography maps and calculation results with respect to the range of distribution of collapse sediment.

Table 6.2.2-1(1) Numerical models for tsunami occurring due to landslides, etc.

| Name of model | Summary | Input conditions | Examples of application |
|-----------------------------------|--|---|--|
| Flow rate model | Method to give the inflow of depleted mass into the sea as the seawater flow rate along the coastline | Volume of depleted mass, position and width of coastline to which depleted mass flows into, duration of inflow, etc. | Numerical Experiments of the Tsunami Associated with the Collapse of Mt. Mayuyama in 1792 (Aida, 1975), and Tsunamis Generated by Eruptions from Komagatame Volcano, Hokkaido, Japan (Nishimura and Shimizu, 1993) |
| Circular slip method | Method to give the topography before and after landslides on unstable slopes derived using the circular slip method and reflect this in the sea surface water level | Landslide profile topography, landslide volume magnification factor, landslide duration, etc. | 1771 Meiwa Yaeyama (Hiraishi et al., 2001) |
| Kinematic Landslide model | Method to find the submarine geomorphic change based on the topography before and after landslide, movement velocity of the landslide, and duration of the landslide and give this in a time series as sea surface change | Topography before and after landslide, movement velocity of the landslide, duration of landslide, etc. | 1741 Oshima-Oshima flank collapse (Satake and Kato, 2002), Volcanic origin of the 1741 Oshima-Oshima tsunami in the Japan Sea (Satake, 2007) and submarine landslides off Oahu Island (Satake et al., 2002) |
| Landslide movement analysis model | Method to give the change in bed thickness of depleted mass, which is obtained by using an analytical model (for example, LSFLOW, TITAN2D or FLOW3D) to solve for landslide movement, in a time series as sea surface change | Initial depleted mass distribution, coefficients necessary for landslide kinematic analysis (friction angle of slip plane, density and viscosity coefficient for depleted mass, etc.), etc. | Numerical Simulation of the Tsunami caused by the sector Collapse of Mt. Mayuyama, Shimabara Peninsula, Kyushu in 1792 (Sasahara, 2004) |

Table 6.2.2-1(2) Numerical models for tsunami occurring due to landslides, etc.

| Name of model | Summary | Input conditions | Examples of application |
|---|--|---|--|
| Two-layer flow model submarine mass failure | Method to solve a shallow water equation with two vertical layers where sediment is the bottom layer and seawater is the upper layer by taking into consideration the interaction between layers | Initial sediment bed thickness distribution, sediment density, various coefficients relating to inter-layer interaction (coefficient of interfacial resistance force, etc.), etc. | 1998 Papua New Guinea submarine landslides (Hashi and Imamura, 2000), and Model of tsunami generation by collapse of volcanic eruption: the 1741 Oshima-Oshima tsunami, in Tsunamis: Case Studies and Recent Developments (Kawamata et al., 2005), etc.(However, only the prediction equation for maximum amplitude has been verified based on a comparison with past tsunami) |
| Predictive empirical equations describing tsunami generation by submarine mass failure by Watts et al. (2005) | Method to estimate the initial water level distribution by combining an equation that gives the plane two-dimensional distribution of tsunami water level and a prediction equation that gives the maximum amplitude and wavelength of tsunami in the tsunami source region for submarine landslides | Characteristic values of the landslide topography (length, thickness, width, etc.), characteristic values of the tsunami source region (water depth, slope gradient, etc.), etc. | Tsunami Generation by Submarine Mass Failure. II: Predictive Equations and Case Studies (Watts et al., 2005) (However, only the prediction equation for maximum amplitude has been verified based on a comparison with past tsunami) |
| Distinct element method | Method where a two-phase flow model that treats solid phase with the distinct element method and fluid resistance force as interaction in coupling with fluid phase (particle method) is used | Physical properties of solid phase particles (particle size, resistance coefficient, porosity of particle fluidized bed), and the physical properties of fluid (density, viscosity coefficient) | Reproduction of water tank experiments (Goto et al., 2011) |

6.3 Water Level Fluctuation Simulation of Sea Water Intake and Discharge Facilities

6.3.1 Basic Approach

(1) Purpose of Simulation

Of the risks anticipated when a tsunami reaches a nuclear power plant, the risks relating to sea water intake and discharge facilities include inundation from above such a facility due to the rise of the water level within the sea water intake and discharge facilities, and inundation of pump motors, and impossibility of water intake due to lowering of the water level of water tank, etc. (Figure 6.3.1-1). In order to examine the impact that these risks have on a nuclear power plant, it is necessary to ascertain the degree of water level fluctuation within the facility, but there are also cases where the water level fluctuation within the facility is amplified when components are included that are the same degree as the eigen period for the target facilities in the waveform of the tsunami arriving at the water intake or discharge. Accordingly, in cases where it is conceivable that a tsunami will cause the water level within a sea water intake and discharge facilities to fluctuate, it is necessary to simulate the water level fluctuation within the sea water intake and discharge facilities.

If it is obvious that the target site is not affected by the tsunami (eg, the amplitude of the tsunami at the water intake or discharge position is small and there is a large difference in the predominant period of the target tsunami and the eigen period of the facility, it is possible to omit simulating the change in the water level at the corresponding water discharge facilities.

(2) Selection of Numerical Simulation Method

The method for simulating fluctuation in the water level due to tsunami for water intake facilities (intake - intake channel - intake tank) and discharge facilities (discharge tank - discharge channel - discharge) is generally performed using the calculation tsunami waveform at the water intake or discharge as the water level boundary condition. The flow within the water intake and discharge channels may be treated as a one-dimensional flow along a water channel, and, in cases where there is only open channel flow, cases where there is only pipeline flow (flow in a completely filled state without a free water surface), and, moreover, cases where both of these situations coexist, an appropriate basic equation and simulation method are applied which are able to simulate these with good precision.

(3) Modeling of Sea Water Intake and Discharge Facilities and Implementation of Numerical Simulation

In performing the water level fluctuation simulation for a sea water intake and discharge facilities, the eigen period of the tsunami which is an external force and the hydraulic response characteristics (eigen period) of the sea water intake and discharge facilities overlap, and it results in the cases where fluctuation in the water level of the water intake and water discharge tanks is amplified, so it is important that the sea water intake and discharge facilities be modeled with good precision.

In modeling a sea water intake and discharge facilities, the water channel flow path length and water flow cross-section, water tank shape and other such elements be configured based on structural diagrams of the facility and other such sources, and the water channel friction loss and shape loss (refraction, bending, etc.) as well as facility internal structures (screens, overflow weirs, etc.) are appropriately configured.

Also, with respect to the impact of shells and other marine organisms attaching to wall surfaces, it is desirable that such effects be appropriately reflected in keeping with the assessment object. In addition, because there is the possibility that water intake or discharge volume, tide conditions, and crustal movements from earthquakes may also have an impact on the hydraulic response characteristics or other such attributes, these are included as simulating conditions as necessary.

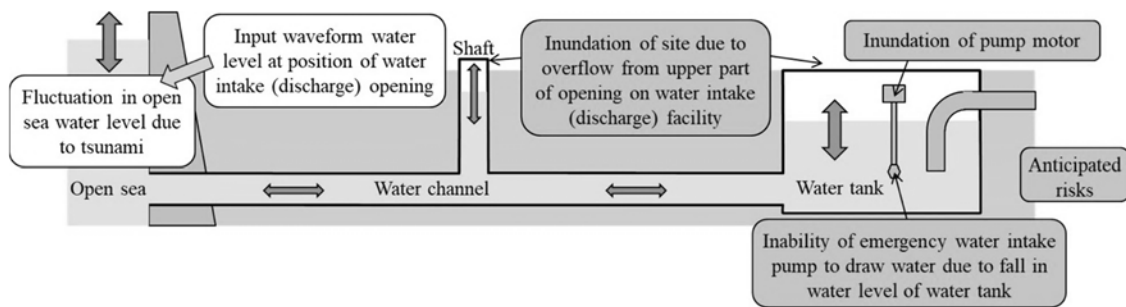


Figure 6.3.1-1 Overview of water level fluctuation simulation and risks related to sea water intake and discharge facilities

6.3.2 Selection of Numerical Simulation Method

6.3.2.1 Simulation Methods for Water Channel Portion

The flow through the water channel portion is classified depending on the water channel structure and fluctuation in the water level when a tsunami strikes into (1) cases where all sections are pipeline flow (flow in a completely filled state), (2) cases where all sections are open channel flow, and (3) cases where there are both sections with an open channel flow and sections with a pipeline flow (section in a completely filled state), and the simulation method applicable to the respective flow situation needs to be selected.

(1) Cases Where All Sections Are Pipeline Flow

In cases where the water channel portion has a pipeline flow through all sections (flow in a completely filled state), a free water surface does not develop within the water channel, so the intake (or discharge) water level and the intake tank (or discharge tank) water level serve as the boundary conditions, and an equation for one-dimensional unsteady flow through the pipeline may be used to simulate the flow rate through the water channel section. The intake tank (or discharge tank) water level is sequentially simulated using the calculated flow rate for the water channel section in the previous step (see Section 6.3.2.2 of main volume).

(2) Cases Where All Sections Are Open Channel Flow

In cases where all sections are open channel flow, either of the following simulation methods is often used.

- Method of applying an equation for one-dimensional unsteady flow through an open channel used in simulation of river flood flow and other such situations
- Method of modeling the water channel using a plane two-dimensional grid and applying nonlinear long-wave theory or other such scheme

(3) Cases of Both Sections with Open Channel Flow and Sections with Pipeline Flow

In cases where there are both sections with an open channel flow and sections with a pipeline flow (section in a completely filled state) within a water channel, either of the following two simulation methods is often used.

- Simulation method based on the slot model

As shown in Figure 6.3.2-1, the slot model (for example, Ohtani et al., 1998) is able to configure a virtual slot above a pipe so that the pipeline section may also be treated as open channel flow. Accordingly, it is no longer necessary to distinguish between open channel

sections and pipeline sections and the method is applied to an equation for one-dimensional unsteady flow through an open channel in all sections. The slot width is configured dependent upon the pipeline cross-section and pressure wave velocity (about 100m/s).

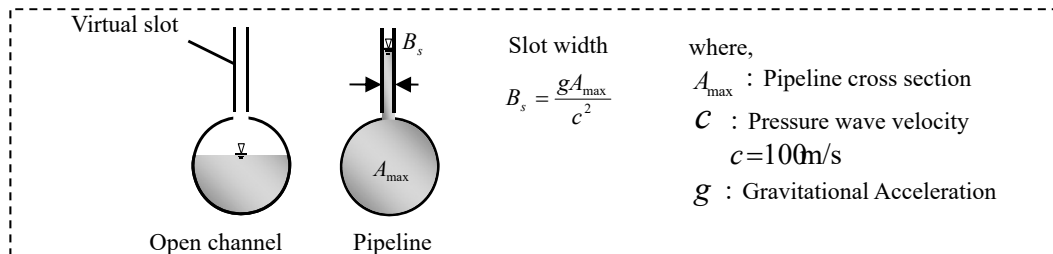


Figure 6.3.2-1 Overview of slot model

- Simulation Method Separating Open Channel Section and Pipeline Section

As shown in Figure 6.3.2-2, each portion of the water channel separated into minute sections is sequentially assessed to determine whether it is in an open channel state or a pipeline state, and the flow rate for the pipeline sections is simulated by using the water level of the open channel sections at both ends (water level of the free water surface) as the boundary conditions (in the pipeline sections, the wave velocity of the pressure wave is assumed to be infinity, and the cross-section flow rate within the pipeline section is regarded as the same). Just as with the slot model, an equation for one-dimensional unsteady flow in the open channel is applied to the open channel sections.

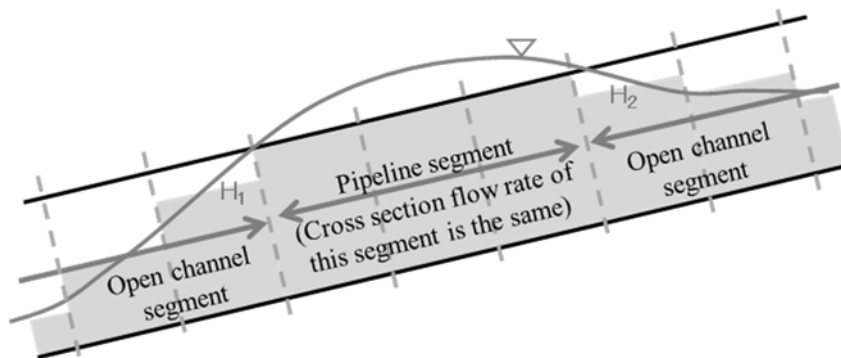


Figure 6.3.2-2 Overview of simulation method separating open channel section and pipeline section

6.3.2.2 Simulation Method for Water Intake/Discharge Tanks and Pits

For intake and discharge tanks as well as pits (hereinafter, these are collectively referred to as “water tanks”), the appropriate simulation method is to be selected from among the methods indicated

below in accordance with the simulating conditions and shape of the water tank to be modeled. In all of these methods, the flow rate through the water channel connecting to the water tank is used as the boundary condition, and the water level and flow velocity inside the water tank, volume of overflow from upper part of opening on water tank are computed. However, the computed water level of the water tank interior is used for computing the flow rate of the water channel portion in the next step, so all of these methods also need to be treated as issues coupled with the water channel portion.

- Simulation method based on model taking into consideration only change in water volume within the water tank

This method is used with the relationship between water level and volume that integrates the water surface area in the water tank interior in a vertical direction so as to compute the water volume and water level within the water tank based upon the total flow rate value for water channels connected to the water tank.

- Simulation method based on one-dimensional water channel model

This method models the water tank interior using an open channel and then utilizes a one-dimensional unsteady flow continuity equation and momentum equation to compute the water level and flow rate of the flow direction inside the water tank.

- Simulation method based on plane two-dimensional model

This method is similar to the numerical model used in plane two-dimensional tsunami simulations. The method models the water tank interior using a plane two-dimensional grid so as to compute the water level and flow velocity distribution within the water tank using the nonlinear long-wave theory or other such scheme.

- Simulation method based on three-dimensional model

This method models the water tank interior using a three-dimensional grid (structured grid or non-structured grid) so as to compute the water level, pressure and flow velocity inside the water tank three-dimensionally.

6.3.3 Modeling of Sea Water Intake and Discharge Facilities and Implementation of Numerical Simulation

(1) Modeling of Sea Water Intake and Discharge Facilities

Sea water intake and discharge facilities are modeled based on the specifications taken below from structural diagrams and other such drawings.

- Water channel portion
: water channel elevation, water channel inclination, water channel length, water channel cross-section profile, etc.
- Water tank portion

: cross-section profile of ponding area, water surface area or water volume according to height, height of overflow from upper part of water tank, etc.

When simulating fluctuation in the water level of a sea water intake and discharge facilities, the modeled water channel portion and water tank portion are connected and, ordinarily, the simulation is made comprehensively for the entire system.

The events subject to assessment in the simulation of fluctuation in the water level of a sea water intake and discharge facilities are the lowering of the water level at the location where the water intake pump is installed, overflow from above the water tank, and other events. Along with this, it is necessary to compute the water level fluctuation at the assessment point, and the hydraulic response characteristics (eigen period) of the sea water intake and discharge facilities come to be closely involved in the magnitude of the water level fluctuation. In cases where loss is disregarded with a single water channel and simple structure in the intake tank, the eigen period for the facility with a pipeline flow (all sections in a completely filled state) is expressed below (see for example, Tsubaki, 1974).

$$T = 2\pi \sqrt{\frac{AL}{ga}}$$

where, T : Eigen period (s), A : Water tank plane area (m²), a : Completely filled pipe cross section (m²), L : Water channel length of completely filled section (m), g : Gravitational Acceleration (m/s²).

In a case where the eigen period of the facility and the predominant period of the tsunami input at the water intake or discharge are at the same degree, the water level fluctuation within the facility is amplified. Also, in cases where a pump bearing slab or other such component is installed within the water tank or other such cases involving a structure where there are sudden changes in the water surface area of the water tank, the eigen period of the facility will also fluctuate according to the water level, so the structure may also become the factors which amplify water level fluctuation. Accordingly, it is important that an appropriate model be constructed based on structural diagrams and other such information about the facility.

(2) Application of Water Channel Friction Loss and Shape Loss

Ordinarily, Manning's law is applied to friction loss in water intake channels and water discharge channels. The friction loss of head, which is based on Manning's law, is expressed using the following equation (Electric Power Civil Engineering Association Compilation, 1995).

$$h_f = n^2 \cdot V^2 \frac{L}{R^{4/3}}$$

where, h_f : Friction loss of head (m), n : Manning's coefficient of roughness (m^{-1/3}s), V : Cross-section flow velocity (m/s), L : Water channel length (m), R : Hydraulic radius (m).

Tables 6.3.3-1, 6.3.3-2 and 6.3.3-3 show examples of configurations of Manning's coefficient

of roughness and the thickness of shellfish adhesion along water intake channels as given by the Electric Power Civil Engineering Association Compilation (1995) (Figure 6.3.3-1 is presented as reference material for water intake and discharge channel profiles in Table 6.3.3-1 and Table 6.3.3-2). These need to be appropriately configured in accordance with the assessment target.

The formulas presented in the Electric Power Civil Engineering Association Compilation (1995), Japan Society of Civil Engineers Compilation (1999) and other sources are applied to curvature, refraction and other shape loss, and simulations are necessary that appropriately model such shape loss in the numerical simulations as well.

Table 6.3.3-1 Thickness of shellfish adhesions, etc. on intake channel and coefficient of roughness
(Electric Power Civil Engineering Association Compilation, 1995)

| Type of water intake channel | Cross-section flow velocity | Thickness of shellfish adhesions, etc. | Coefficient of roughness |
|------------------------------|-----------------------------|--|---------------------------------------|
| Culvert | 0.8 ~ 2.2 m/s | 0 ~ 20cm (Often 0, 5 or 10cm) | 0.014 ~ 0.027 (Often 0.015, 0.020) |
| Pipeline | 2.0 ~ 3.6 m/s | 0 ~ 10cm | 0.015 ~ 0.018 |

Table 6.3.3-2 Thickness of shellfish adhesions, etc. on discharge channel and coefficient of roughness
(Electric Power Civil Engineering Association Compilation, 1995)

| Type of water discharge channel | Cross-section flow velocity | Thickness of shellfish adhesions, etc. | Coefficient of roughness |
|---------------------------------|-----------------------------|--|--------------------------|
| Culvert | 1.6 ~ 3.6 m/s | 0 ~ 20cm (Often 0cm) | 0.014 ~ 0.027 |
| Tunnel | 1.8 ~ 3.0 m/s | 0 ~ 20cm (Often 0cm) | 0.014 ~ 0.027 |

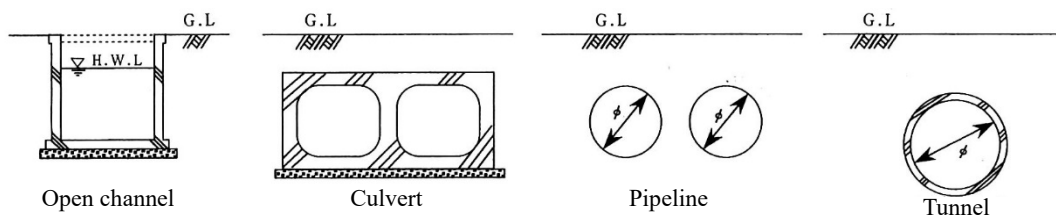


Figure 6.3.3-1 Examples of types of intake and discharge channel structures

(Electric Power Civil Engineering Association Compilation, 1995)

Table 6.3.3-3 Manning's coefficient of roughness n

(Electric Power Civil Engineering Association Compilation, 1995)

| Material | Range of n |
|--|---------------|
| Good concrete lined water channel constructed using steel form | 0.011 ~ 0.014 |
| Ordinary concrete lined water channel | 0.012 ~ 0.016 |
| Unlined tunnel with only poured concrete foundation | 0.020 ~ 0.030 |
| Total cross-section unlined tunnel | 0.030 ~ 0.040 |
| Welded steel pipe | 0.010 ~ 0.014 |
| Revit connection pipe | 0.013 ~ 0.017 |
| Ordinary concrete water channel with shellfish adhesion | 0.017 ~ 0.020 |

(3) Treatment of Overflow Weirs and Other Structures

In cases where there are overflow weirs, gates or other such structures, a numerical simulation is needed that includes models representing the hydraulic characteristics of these structures. The overflow formula, flow rate coefficient and so on are basically configured with reference to the Japan Society of Civil Engineers Compilation (1999), but, in cases where measured values are able to be obtained in hydraulic model experiments or other such testing, it is desirable to prepare the configuration based on such results.

(4) Implementation of Water Level Fluctuation Simulations Considering Water Intake/Discharge Flow Rate, Tide Conditions, etc.

The water intake and discharge flow rate affect the initial water level prior to a tsunami strike as well as hydraulic response characteristics, so boundary conditions need to be configured and the impact ascertained.

Fluctuation in the water level within the tank attributable to tides may have an effect on hydraulic response characteristics, so it is necessary to simulate the initial water level in the facility and the tsunami waveform of the intake and discharge considering tidal conditions. Moreover, in cases where the amount of crustal movement occurring due to an earthquake in the surrounding area may not be disregarded with respect to a sea water intake and discharge, the water level fluctuation simulation is necessary for which the change in the height of the target facility resulting from crustal movement is taken into account. In the consideration of crustal movement, it is necessary to select an appropriate technique in keeping with the assessment method, such as setting up an arrangement so that the assessment will be on the safe side for the target facility.

(5) Inundation Simulation of Site Considering Overflow from Sea Water Intake and Discharge Facilities

In simulating water level fluctuation of a sea water intake and discharge facilities, in cases where the water tank water level rises higher than the height of the opening on the water tank top, the amount of overflow from the water tank is calculated, and an inundation simulation within the power plant site is performed as necessary. When performing the inundation simulation of the site, a method is generally used that models the site interior using a plane two-dimensional model or other such scheme and gives the calculated overflow amount as a flow rate boundary condition along the corresponding grids of places where there is overflow from the sea water intake and discharge facilities. However, in cases where the state of drainage from the site after inundation is examined, the amount of drainage from inside the site to the sea water intake and discharge facilities varies depending on the water level within the sea water intake and discharge facilities, so the examination needs to be performed as a coupled simulation that simultaneously performs simulations for inside the site and simulations of the water level fluctuation of the sea water intake and discharge facilities.

6.4 Setting Fault Model Capable of Explaining Run-up Height Record of Past Tsunami

6.4.1 Evaluation of Goodness of Fit of Numerical Model

The goodness of fit of the numerical model is evaluated by using the appropriate topographic conditions and tsunami source model to conduct an analysis of the tsunami, and then using highly accurate data of the run-up height of past tsunami to conduct an evaluation based on geometric average K and geometric standard deviation κ put forth by Aida (1977b).

(1) Evaluation Criteria

Aida (1977b) evaluates the goodness of the fault model based on the geometric average K and geometric standard deviation κ . The indexes K and κ by Aida (1977b) have been applied as indexes of fitness in space between the run-up height records and calculated heights of tsunami. The defining equations of K and κ are given as follows.

$$\log K = \frac{1}{n} \sum_{i=1}^n \log K_i$$

$$\log \kappa = \left[\frac{1}{n} \left\{ \sum_{i=1}^n (\log K_i)^2 - n (\log K)^2 \right\} \right]^{1/2}$$

n : number of points for evaluation

$$K_i = R_i / H_i$$

R_i : run-up height of past tsunami at i

H_i : calculated height of tsunami at i

Since the estimated error of κ depends on the number of points, the number of points should be stated for reference in calculating K and κ .

(2) Necessity for Reproduction of Topography

The topography of the area around run-up point records of tsunami which are used for verification of reproducibility should be a model that reflects the actual topography when the tsunami occurred to the extent feasible. It is desirable to conduct surveys of transformations of the topography along the coastline, the state of development of harbors and fishing ports and other such features so as to configure the topographic conditions present at the time when the tsunami occurred.

(3) Method of Selecting Calculation Run-up Height to Contrast with Run-up Point Records of Tsunami

In principle, in cases where the run-up height records of tsunami and the calculation run-up height of tsunami that ran up onto land are contrasted, the value that is near the grid in which the run-up point record of tsunami is included is used for the calculation run-up height. However, in cases where the tsunami run-up area in the calculation does not extend to the run-up point record of tsunami and in cases where there are limitations in terms of the topographic representation in the modeling, a substitution may be made using a calculation run-up height near the run-up point record of tsunami.

In cases where tsunami inundation simulations are not performed, values are used around the grid of the coastline which serves as the estimated inrush path to the run-up point records of tsunami. Also, in cases where there is regional deviation in the number of the data distribution for run-up height records of tsunami and overall reproducibility is regarded as unattainable, it is desirable to figure out a way to exclude such effects.

(4) Points to be noted

When verifying reproducibility, run-up height records of tsunami which are obtained through surveys of past tsunami as presented in Section 3.1 of main volume may be utilized. However, when the reliability of the run-up height records of tsunami is doubtful, the accuracy of the records must be re-examined based on the original document. If their reliability is determined to be low, they can be eliminated when evaluating the goodness of fit (see Section 4.8.1 of the appendix volume).

Since the tide gauge records may provide smaller amplitudes than the run-up height records of tsunami depending on the period of the tsunamis and the response characteristics of the tide gauges (see Section 4.8.2 of the appendix volume), when the highest tide gauge record is adopted as a substitute for the run-up height of past tsunami in the evaluation of fit of the fault model, the

systematic differences between the tide gauge records and run-up height records of tsunami must be carefully considered.

In performing a confirmation of the reproducibility with respect to the results of tsunami deposits, there is no need to apply the geometric standard deviation κ and geometric mean K put forth by Aida (1977b). However, the results of tsunami deposits provide information relating to the height of the minimum level of past tsunami and the extension of the run-up area, so the calculation results need to exceed these.

6.4.2 Setting Fault Model Capable of Explaining Run-up Height Records of Tsunami of Past Tsunami

The tsunami source parameters of the tsunami source model of the past tsunamis should be set in such a way to reproduce the distribution of run-up height records of tsunami along the coast.

In General, in cases of tsunami resulting from earthquakes, a source model that can explain the seismic waves is not always consistent with a model which can explain the run-up height records of tsunami. Needless to say, it aims at the evaluation of the tsunamis considered in this paper. When the tsunami source model of the past tsunami is set, it is important to also set the tsunami source parameters in order to effectively explain the distribution of the run-up height records of tsunami along the coast well.

(1) General

When the tsunami source model of the past tsunami is set, the tsunami source parameter is set in such a manner that the run-up height records of tsunami along the coast can be satisfactorily explained. In other words, the tsunami source parameters should be set so that geometric average K by Aida (1977b) becomes nearly 1.0, and the geometric standard deviation κ may acquire as low as possible.

It is recommended to use the following conditions as a good rule of thumb for K and κ of wide areas (Japan Society of Civil Engineers, 2002).

$$0.95 < K < 1.05$$

$$\kappa < 1.45$$

These conditions are essential in order to enable an explanation of the overall trend of the distribution of the run-up height records of tsunami over a wide area; further, they are also important for ensuring satisfactory reproducibility in the vicinity of the target site.

When the run-up height records of tsunami for evaluating the reproducibility are selected taking the target site into careful consideration, the following criteria should be considered.

- 1) The distance from the site is short.
- 2) The number of run-up height records of tsunami necessary for calculating K and κ is

statistically reliable.

If the tide gauge records can be referred, the parameters should be set so that the wavelength, phase, etc., of the tsunami can be expressed.

When abundant records are available for recent tsunamis as well as the earthquakes that caused them, various characteristics of the earthquake can be referred. These characteristics include aftershock distribution, focal mechanism solution, crustal deformation before and after the earthquake, etc.

On the other hand, in cases of historical tsunami for which the reliability of run-up height records of tsunami is low, reproducibility on a level equivalent to recent tsunami is not able to be expected.

(2) Fault Models Proposed in Literature

In the case of major past tsunamis, fault models that can explain tsunami phenomena have been proposed in literature, and it is possible to refer to these models when evaluating such tsunamis. The literature edited by Sato (1989) has a collection of such fault models.

Among these models, the ones from particularly old sources may be inaccurate in the light of recent seismological findings in terms of consistency of the depth of plate boundaries, etc. Also, the grid sizes are roughly drawn leading to a tsunami simulation with poor precision. Therefore, the parameters of the fault model should be corrected as necessary.

Among the fault models that can explain tsunamis proposed in literatures, there are the models that can explain not run-up height records of tsunami but tide gauge records. Since the tide gauge records may provide smaller amplitudes than the run-up height records of tsunami depending on the period of the tsunamis and the response characteristics of the tide gauges, when the fault model set by using the tide gauge records is adopted, the systematic differences between the tide gauge records and run-up height records of tsunami must be carefully considered.

(3) Setting Fault Models Based on Tsunami Inversion Analysis

In cases where a fault model that is appropriate for past tsunami has not been proposed, an effective method is to set a fault model by means of tsunami inversion analysis. Some typical methods are given below.

1) Nonlinear Inversion Analysis

This is a linear approximation iterative solution for a nonlinear model based on the Gauss-Newton method (see, for example, Nakagawa and Koyanagi, 1991), and, although nonlinear long-wave theory may be utilized as the numerical model, the simulating time is extensive. The Central Disaster Management Council (2003) used this method as its application (the ratio of the water level between coarse-mesh and fine-mesh was used as the conversion coefficient).

2) Linear Inversion Analysis

A linear inversion analysis where the numerical model is a linear long-wave theory allows for high-speed and easy simulation but is not able to take into consideration nonlinearity. In response to the method proposed by Satake (1987), Tanioka and Baba (2004) set forth a method in which smoothing of the estimation parameters and constraint conditions are given.

3) Linear Inversion Analysis Considering Shallow Water Deformation Effect

This is the tsunami inversion method proposed by Annaka et al. (1999). In the method, the measured values, excluding the shallow water deformation effect, are regarded as the target values, and, through repetition of inversion analysis utilizing Green's function, the method combines a forward analysis based on nonlinear long-wave theory to converge the results down into a tsunami source model that considers nonlinear effects.

The parameter, which is estimated by tsunami inversion analysis, is generally magnitude of slip. Strike direction, dip angle, slip angle and other elements are configured in advance based on seismological knowledge and the region enveloping the anticipated tsunami source region is divided into multiple small faults so that the slip distribution of the individual small faults is able to be found using inversion analysis. In cases where there are a high number of small faults, the unknown quantity (number of groups estimating slip) may be reduced by dividing the region into groups where the slip is assumed to be the same.

Records of tsunami tidal observations, run-up height records of tsunami, records of crustal movements and other such elements are used as the objects of reproduction in the tsunami inversion analysis and the fault slip, for which the residual sum of squares of these observed values and the calculated values are the smallest, is found as the optimal solution. However, with historical tsunami for which tidal observation records or other measurement records are insufficiently available, the solution becomes unstable when the number of the unknown number increases, so creative schemes are necessary such as limiting the unknown number or assuming constraints and smoothing as proposed by Tanioka and Baba (2004).

For tsunami inversion analysis of the 2011 Tohoku Earthquake, sufficient observation records are available, and Satake et al. (2013), Sugino et al. (2013), Takao et al. (2012) and others have reported case studies in which inversion analyses where fault rupture propagation and time lag are taken into consideration have been performed.

6.5 Assessment of Tsunami Wave Force

6.5.1 Basic Approach

In cases where a tsunami reaches seawalls, buildings or other such structures, the tsunami wave force (hereinafter, “tsunami wave pressure” is included in the term “tsunami wave force”) needs to be appropriately calculated so as to ascertain the impact to the facility. With respect to the tsunami wave force, after taking into account the location where the structures to be assessed are located (maritime or land), the appropriate assessment formula is utilized to calculate the tsunami wave force based on tsunami water level, inundation depth, temporal change in flow velocity and other such data.

Although sufficient knowledge has not become available about tsunami wave forces acting on the ground in the vicinity of structures, research case studies on this issue are given in Section 8.1.3 of appendix volume. Also, in cases where application of previous assessment formula is considered difficult or other such similar situations, hydraulic model experiments and three-dimensional numerical simulation can be performed.

6.5.2 Calculation of Tsunami Wave Force

The hydraulic quantity (water level, inundation depth, flow velocity) obtained from the tsunami propagation and run-up simulations is used to calculate, using the appropriate assessment formula, the tsunami wave force acting on a structure in accordance with the type of tsunami wave pressure, conditions of the tsunami impact (presence of soliton fission, etc.), profile of the targeted structure, etc. The points noted below should be kept in mind for appropriately selecting the formula for assessment of tsunami wave force.

(1) Hydraulic Quantity Used for Calculation of Tsunami Wave Force

For calculation of tsunami wave force, there are hydraulic quantity in which water level (in the case of maritime structures) or inundation depth (in the case of land structures) obtained from tsunami propagation and run-up simulations are used, and hydraulic quantity where flow velocity is used, in addition to these. For this reason, it is necessary to calculate the appropriate hydraulic quantity in accordance with the assessment formula utilized.

(2) Type of Tsunami Wave Pressure

Arikawa et al. (2005) classified the tsunami wave pressure acting on an upstanding wall using a time series as shown in Figure 6.5.2-1. In other words, the tsunami wave pressure is classified by the wave pressure that develops during the action of the tsunami head (hydro dynamic pressure)

and the wave pressure that develops due to the continuous arrival of incident waves (continuous pressure). Among the assessment equations that have been proposed, there are the equations that can estimate hydro dynamic pressure and continuous pressure in a time series, those that focus only on maximum continuous pressure, and those that estimate the maximum tsunami wave pressure regardless of the type of tsunami wave pressure. For this reason, after closely scrutinizing the process through which each assessment formula is derived, the appropriate assessment formula needs to be selected in keeping with the type of tsunami wave pressure to be estimated.

With respect to inclined-type maritime structures, the classification of tsunami wave pressure is more complicated as, in addition to the classifications shown in Figure 6.5.2-1, there is tsunami wave pressure that develops when there is run-up over a slope, tsunami wave pressure that develops when incident waves and reflective waves collide on a slope, and other types of tsunami wave pressures. Mizutani and Imamura (2000) and Mizutani and Imamura (2002) classified tsunami wave pressures acting on inclined-type structures and proposed assessment formulas for each (see Section 8.1.1 in the appendix volume).

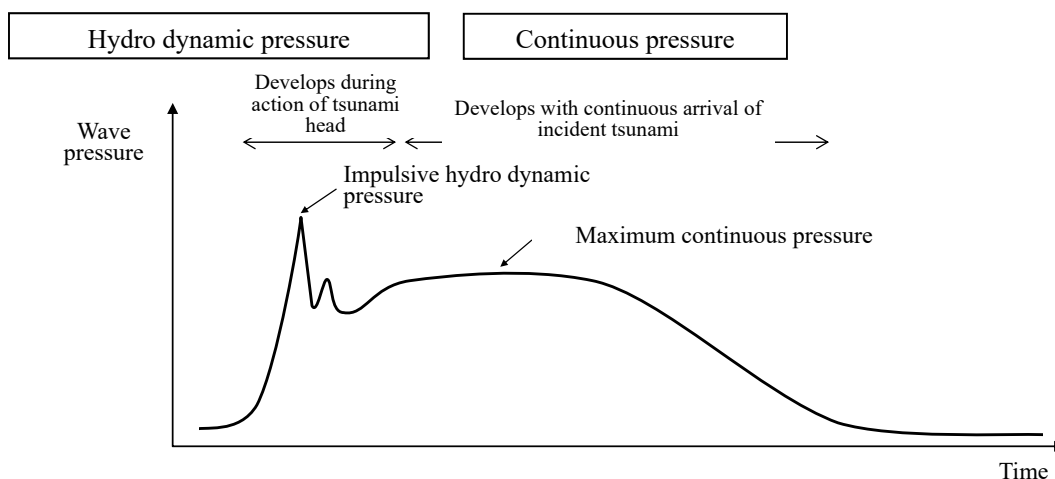


Figure 6.5.2-1 Classification of tsunami wave pressure (Arikawa et al., 2005)

(3) Presence of Soliton Fission

In cases where undular bore develops, which has a bore shape at the head of a tsunami with a long wavelength and splits into multiple short wavelength waves (soliton fission), the impulsive force is increased. Accordingly, an assessment is performed for whether or not soliton fission develops, and an assessment formula where this is taken into account needs to be used in cases where the development of soliton fission is anticipated.

(4) Profile of Target Structures

The profile of structures can be classified into three-dimensional structures such as buildings where a tsunami flows into the back through both sides of the structure, and two-dimensional structures (linear structures) such as seawalls that are homogenous in a cross direction and there is no inflow of the tsunami into the back except for overflow. In the calculation of tsunami wave force, assessment formula needs to be utilized that is appropriate in keeping with the profile of the target structure (three-dimensional structure, two-dimensional structure).

6.5.3 Features of Tsunami Wave Force Assessment Formulas

Separated into those for a tsunami wave force acting on maritime structures and tsunami wave force acting on land structures, previous assessment formulas and their features are presented. The specific details of the respective assessment formulas are given in Sections 8.1.1 and 8.1.2 of the appendix volume. In addition, case studies verifying the validity of tsunami wave force assessment formulas are presented in Section 8.1.4 of the appendix volume.

6.5.3.1 Tsunami Wave Force Acting on Maritime Structures

(1) Classification of Assessment Formulas for Tsunami Wave Force Acting on Upright Maritime Structures

In the Ministry of Land, Infrastructure, Transport and Tourism (2013), the experience of the 2011 Tohoku Earthquake was taken into account and a classification was worked out as shown in Table 6.5.3-1 for tsunami wave forces used in verification of the stability of the upright portion of composite-type breakwaters, and respective assessment formulas have been proposed.

Table 6.5.3-1 Classification of formulas for assessing tsunami wave force acting on upright maritime structures

| Tsunami wave force assessment formula | Presence of target structures subject to tsunami simulation | Hydraulic quantity used in tsunami wave force calculation | Type of tsunami wave pressure | Presence of soliton fission | Profile of target structure | Presence of overflow |
|--|---|---|----------------------------------|-----------------------------|-----------------------------|---------------------------|
| Ikeno et al. (2005) | With structures | Maximum tsunami water level | Impulsive hydro dynamic pressure | Fission | Two-dimensional structure | Overflow and non-overflow |
| Tanimoto et al. (1984) | With structures | Maximum tsunami water level | Impulsive hydro dynamic pressure | Non-fission | Two-dimensional structure | Non-overflow |
| Ministry of Land, Infrastructure, Transport and Tourism (2013) | With structures | Maximum water level difference | Maximum continuous pressure | Non-fission | Two-dimensional structure | Overflow |

(2) Classification of Assessment Formulas for Tsunami Wave Force Acting on Inclined Maritime Structures

With respect to formulas for assessing tsunami wave force acting on inclined maritime structures, a classification of the assessment formulas that have been proposed is shown in Table 6.5.3-2.

Table 6.5.3-2 Classification of formulas for assessing tsunami wave force acting on inclined maritime structures

| Tsunami wave force assessment formula | Presence of target structures subject to tsunami simulation | Hydraulic quantity used in tsunami wave force calculation | Type of tsunami wave pressure* | Presence of soliton fission | Profile of target structure | Presence of overflow |
|---|---|---|---|-----------------------------|-----------------------------|----------------------|
| Fukui et al. (1962) Mizutani and Imamura (2000) Mizutani and Imamura (2002) | No structure | Incident wave height and wave velocity | Hydro dynamic pressure and impulsive hydro dynamic pressure | Non-fission | Two-dimensional structure | Non-overflow |
| Mizutani and Imamura (2000) | No structure | Incident wave height and wave velocity | Run-up pressure | Non-fission | Two-dimensional structure | Non-overflow |
| Mizutani and Imamura (2000) | No structure | Incident wave height and wave velocity | Impact continuous pressure and impulsive impact continuous pressure | Non-fission | Two-dimensional structure | Non-overflow |
| Mizutani and Imamura (2002) | With structure | Crown maximum flow velocity | Overflow pressure and impulsive overflow pressure | Non-fission | Two-dimensional structure | Overflow |

* Classification based on Mizutani and Imamura (2000) and Mizutani and Imamura (2002) (See Section 8.1.1 in the appendix volume)

6.5.3.2 Tsunami Wave Force Acting on Land Structures

(1) Classification of Assessment Formulas for Tsunami Wave Force Acting on Land Structures

Classification of formulas which have been proposed for assessing tsunami wave force acting on land structures is shown in Table 6.5.3-3. The tsunami wave force assessment formulas are classified depending on whether or not the target structures in the tsunami inundation simulation are taken into consideration, hydraulic quantity used in tsunami wave force calculation, type of tsunami wave pressure, presence of soliton fission, and the profile of target structures.

Table 6.5.3-3 Classification of formula for assessing tsunami wave force acting on land structures

| Tsunami wave force assessment formula | Presence of target structures subject to tsunami simulation | Hydraulic quantity used in tsunami wave force calculation | Type of tsunami wave pressure | Presence of soliton fission | Profile of target structure |
|--|---|---|--|-----------------------------|--|
| Asakura et al. (2000) | No structure | Maximum inundation depth | Impulsive hydro dynamic pressure and maximum continuous pressure | Fission and non-fission | Two-dimensional structure |
| Ikeno et al. (2006) | | Maximum inundation depth | Impulsive hydro dynamic pressure and maximum continuous pressure | Fission and non-fission | Two-dimensional structure Three-dimensional structure |
| Cabinet Office (2005) | | Maximum inundation depth | Impulsive hydro dynamic pressure and maximum continuous pressure | Non-fission | Three-dimensional structure |
| Ministry of Land, Infrastructure, Transport and Tourism (2012) | | Maximum inundation depth | Impulsive hydro dynamic pressure and maximum continuous pressure | Non-fission | Three-dimensional structure |
| Fire and Disaster Management Agency (2009) | | Maximum inundation depth | Impulsive hydro dynamic pressure and maximum continuous pressure | Non-fission | Two-dimensional structure (Dike) |
| | | Maximum inundation depth and flow velocity | Impulsive hydro dynamic pressure and maximum continuous pressure | Non-fission | Three-dimensional structure (Cylindrical tank) |
| Asakura et al. (2002) | | Maximum inundation depth and flow velocity | Impulsive hydro dynamic pressure and maximum continuous pressure | Non-fission | Two-dimensional structure Three-dimensional structure |
| Sakakiyama (2012) | | Maximum inundation depth and flow velocity | Impulsive hydro dynamic pressure and maximum continuous pressure | Non-fission | Two-dimensional structure |
| Omori et al. (2000) | | Inundation depth and flow velocity | Hydro dynamic pressure and continuous pressure (time series) | Non-fission | Three-dimensional structure |
| Iizuka and Matsutomi (2000) | | With structure | Maximum inundation depth | Maximum continuous pressure | Non-fission |
| Arimitsu et al. (2012) | Inundation depth and flow velocity | | Hydro dynamic pressure and continuous pressure (time series) | Non-fission | Two-dimensional structure Three-dimensional structure |
| Kihara et al. (2012) | Inundation depth and flow velocity | | Continuous pressure (time series) | Non-fission | Three-dimensional structure |
| Takabatake et al. (2013) | Inundation depth and flow velocity | | Continuous pressure (time series) | Non-fission | Two-dimensional structure |

(2) Presence of Target Structures in Tsunami Inundation Simulation and Method of Applying Assessment Formula

The formulas that have been proposed for assessment of tsunami wave force are categorized into equations assessing tsunami wave force based on the specifications of incident tsunami under conditions where there is no structural impact, and equations assessing tsunami wave force based on the specifications of tsunami under conditions where structural impact is taken into consideration.

In the tsunami inundation simulation, major structures within the target site are considered as topographic data, so, in cases where the results of tsunami inundation simulations without any structures are used to calculate the tsunami wave force, the tsunami inundation simulation is performed under conditions where the target structures or all structures have been removed. In the assessment formulas, where the results of tsunami inundation simulations with structures are used, the hydraulic quantity that has sustained structural impact is used to calculate tsunami wave force, so the results of tsunami inundation simulations where structures have been taken into consideration.

Cases focusing on structures in water channels are the examples where application of the former assessment formula is not easy. At this time, the greater the width of a structure becomes in proportion to the water channel width, the higher the blockage ratio of the water channel becomes and the greater the water depth in front of the structure. As a result, even if the specifications of inflowing tsunami and pass-through tsunami are constant, the tsunami wave pressure acting in front of the structure will become greater. In other words, tsunami wave pressure does not depend only on the specifications of inflowing tsunami and pass-through tsunami, and application of the former assessment formula may be difficult.

An example where application of the latter assessment formula is not simple may be seen in a case where the grid size for numerical simulations is larger than the size of the target structure. At this time, the impact that the structure has on flow is not able to be appropriately expressed in numerical simulations. Accordingly, in such a case, the accuracy of the data input into the latter assessment formula becomes lower and the precision of the tsunami wave pressure estimated as a result decreases. For this reason, the latter assessment formula is suited to the calculation of tsunami wave force acting on structures that is able to be represented using a certain number of grids. For example, numerical simulation solving for tsunami flow within a power plant site using a grid resolution of several meters is suited to the computation of tsunami wave force with respect to seawalls, buildings of tens of meters in width and other such structures.

6.6 Sediment Transport Simulation

6.6.1 Basic Approach

The impact that the transport of sediment due to a tsunami may have on a nuclear power facility includes, for example, a decline in water intake function resulting from deposits of sand in front of the water intake opening as well as structures collapsing and being swept away by scouring from sand around a breakwater or other such structure. In cases where the impact of such phenomena is assessed, it is necessary to use the appropriate topography change prediction model to simulate sediment transport so as to assess deposits of sand in front of water intake openings, scouring around structures and other such effects.

Erosion, sedimentation and scouring due to the transport of sediment on the seafloor when a tsunami occurs affects the safety of port and coastal facilities such as revetments, so a topography change prediction model allowing for a high level of reproducibility is required, and research has been conducted on the development of such models as well as verification of their validity.

Takahashi et al. (1992), Takahashi et al. (1999) and Fujii et al. (1998) have conducted research on the prediction of topography change due to tsunami and developed prediction models. Also, Ikeno et al. (2009) has proposed a new pickup rate equation of suspended sediment where the effect of sand grain size dependence is taken into consideration based on data about flow velocity and suspended sediment concentration obtained from the experiments of sediment transport model. Takahashi et al. (2011) used hydraulic model experiments to find a pickup rate equation and bed load equation where sand grain size dependency is taken into account. Morishita and Takahashi (2014) focused on the factors that have a dominant effect on sediment transport and suggested the possibility of improvement the model.

From the standpoint of model verification, Fujii et al. (1998) and Takahashi et al. (1999) conducted the assessments of field applicability by numerical simulating topography change in Kesenuma bay when the 1960 Chile tsunami struck. Also, Fujii et al. (2009) carried out the verification by numerical simulating of topography change, which was obtained from the experiments conducted by Ikeno et al. (2009).

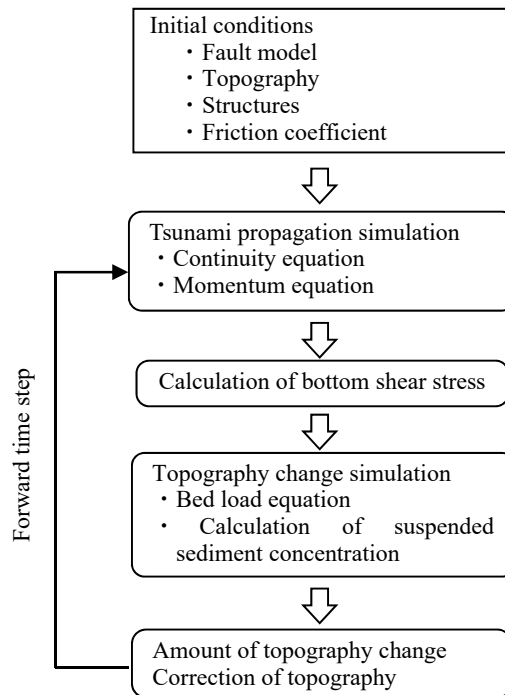


Figure 6.6.2-1 Flowchart of sediment transport simulation attributable to tsunami

6.6.2 Selection of Numerical Model

In the selection of a numerical model for sediment transport simulation, an appropriate numerical model is selected that is able to calculate with even better precision erosion, sedimentation and scouring from sand attributable to tsunami.

Flowchart showing the course of the sediment transport simulation caused by tsunami is shown in Figure 6.6.2-1. The sediment transport simulation is performed by separating into a fluid layer and sand layer. First, a tsunami propagation simulation is performed to calculate shear stress in the fluid layer. Next, topography change is simulated in the sand layer. The topography change simulation of the sand layer solves the continuity equation for sediment and the bed load equation, and the bed load equation estimates the bed load sediment rate by using the bottom shear stress transferred from the fluid layer. With the continuity equation for sediment, topography change due to the estimated sediment transport rate is found to update the topography.

Although the process commonly employed in the sediment transport simulation is as described above, the following three points differ significantly depending on the model applied.

- Assessment of bottom shear stress
- Bed load equation
- Pickup rate equation and deposition rate equation

The methods proposed by Fujii et al. (1998), Ikeno et al. (2009), Takahashi et al. (1999) and

Takahashi et al. (2011) are the major models where bed load and suspended sediment are taken into consideration. With respect to these methods, the continuity equation for bed load sediment, continuity equation for suspended sediment concentration, bed load equation, pickup rate equation, deposition rate equation and friction velocity equation are shown in Table 6.6.2-1 (see Section 8.2.1 of the appendix volume for detailed commentary). Examples of sediment transport simulations are given in Sections 8.2.2 and 8.2.3 of the appendix volume.

Table 6.6.2-1 Summary of sediment transport simulation methods

| | Fujii et al. (1998) method | Takahashi et al. (1999) and (2011) methods | Ikeno et al. (2009) method |
|--|---|--|--|
| Continuity equation for bed load sediment | $\frac{\partial Z}{\partial t} + \alpha \left(\frac{\partial Q}{\partial x} \right) + \frac{E-S}{\sigma(1-\lambda)} = 0$ | $\frac{\partial Z}{\partial t} + \frac{1}{1-\lambda} \left(\frac{\partial Q}{\partial x} + \frac{E-S}{\sigma} \right) = 0$ | $\frac{\partial Z}{\partial t} + \frac{1}{1-\lambda} \left(\frac{\partial Q}{\partial x} + E-S \right) = 0$ |
| Continuity equation for suspended sediment concentration | $\frac{\partial C}{\partial t} + \alpha \left(\frac{\partial UC}{\partial x} \right) - \frac{E-S}{D} = 0$ | $\frac{\partial (C_s D)}{\partial t} + \frac{\partial (MC_s)}{\partial x} - \frac{E-S}{\sigma} = 0$ | $\frac{\partial \bar{C} D}{\partial t} + \frac{\partial \bar{C} M}{\partial x} - E + S = 0$ |
| Bed load equation | Experimental formula by Kobayashi et al. (1996) $Q = 80\tau^{1.5} \sqrt{sgd^3}$ | Experimental formula by Takahashi et al. (1999) $Q = 21\tau^{1.5} \sqrt{sgd^3}$ Experimental formula by Takahashi et al. (2011) $Q = 5.6\tau^{1.5} \sqrt{sgd^3}$ ($d = 0.166mm$) $Q = 4.0\tau^{1.5} \sqrt{sgd^3}$ ($d = 0.267mm$) $Q = 2.6\tau^{1.5} \sqrt{sgd^3}$ ($d = 0.394mm$) | Experimental formula by Ashida et al. (1972) $\frac{Q}{\sqrt{sgd^3}} = 17\tau^{3/2} (1 - \tau_c / \tau) \{1 - (\tau_c / \tau)^{1/2}\}$ |
| Pickup rate equation | $E = \frac{(1-\alpha)Qw^2\sigma(1-\lambda)}{Uk_z \left[1 - \exp\left(\frac{-wD}{k_z}\right) \right]}$ | Experimental formula by Takahashi et al. (1999) $E = 0.012\tau^2 \sqrt{sgd} \cdot \sigma$ Experimental formula by Takahashi et al. (2011) $E = 7.0 \times 10^{-5} \tau^2 \sqrt{sgd} \cdot \sigma$ ($d = 0.166mm$) $E = 4.4 \times 10^{-5} \tau^2 \sqrt{sgd} \cdot \sigma$ ($d = 0.267mm$) $E = 1.6 \times 10^{-5} \tau^2 \sqrt{sgd} \cdot \sigma$ ($d = 0.394mm$) | $\frac{E}{\sqrt{sgd}} = a(v^2 / sgd^3)^{0.2} \{w / \sqrt{sgd}\}^{0.8} (\tau - \tau_c)^{1/2}$ *Coefficient a is a range of 0.1 ~ 0.2 determined based on previous experimental results |
| Deposition rate equation | $S = wC_b$ | $S = wC_s \cdot \sigma$ | $S = wC_b$ |
| Friction velocity equation | Calculated using the formula calculated by intergrating the log-wake law vertically | Calculated using Manning's law $u_* = \sqrt{gn^2 U^2 / D^{1/3}}$ | Calculated using the formula calculated by intergrating the log-wake law vertically |

Guide to symbols

- Z : Amount of change in water depth [m]
 Q : Bed load sediment rate per unit width and unit time [$\text{m}^3/\text{s}/\text{m}$]
 τ : Shields number
 τ_c : Critical shields number
 s : Underwater specific gravity of sediment ($\sigma/\rho-1$)
 g : Gravitational acceleration [m/s^2]
 U : Flow velocity [m/s]
 M : Flow rate per unit width $U \times D$ [m^2/s]
 n : Manning's coefficient of roughness [$\text{m}^{-1/3} \cdot \text{s}$]
 α : Ratio that component whose movement is dominated only by localized external force accounts for of all sediment transport rate (=0.1; based on Fujii et al., 1998)
 w : Settling velocity of sand grains (Rubey, 1993) [m/s]
 Z_0 : Roughness height ($=k_s/30$) [m]
 k_z : Vertical diffusion coefficient ($=0.2\kappa u_* h$; based on Fujii et al., 1998) [m^2/s]
 k_s : Equivalent roughness [m]
 κ : Karman constant (=0.4; based on Fujii et al., 1998)
 h : Water depth [m]
 C_s, C_b : Suspended sediment concentration, bottom suspended sediment concentration [kg/m^3]
 \bar{C} : Mean suspended sediment concentration
 C_s : Suspended sediment volume concentration
log-wake law: Equation adding wake function (Fujii et al., 1998) to logarithmic law
$$u_* / U = \kappa / [\ln(h / Z_0) - 1]$$

 t : Time [s]
 x : Plane coordinates
 σ : Density of sand [kg/m^3]
 d : Sand grain size [m]
 ρ : Density of seawater [kg/m^3]
 D : Total water depth [m]
 λ : Porosity
 ν : Kinematic viscosity coefficient [m^2/s]

6.6.3 Simulating Conditions and Coefficients

When simulating sediment transport, the simulating conditions and other parameters are set by collecting and analyzing information such as boring survey results and geologic distribution charts about the vicinity of the assessment points as presented in Section 3.4 of main volume.

(1) Initial Sand Distribution and Sediment Thickness

Based on the results of surveys of bottom sediment in the surrounding sea areas and other such data, the planar sand layer distribution is confirmed. In cases where information is available about sediment thickness, the erosion and scouring maximum limit of thickness is configured. Also, in cases where information is not available about sediment thickness, the erosion and scouring maximum limit of thickness may also be configured as an infinite thickness.

(2) Grain Size and Density

Based on the results of surveys of bottom sediment in the surrounding sea areas and other such data, the median grain size and density of sand is configured.

(3) Upper Concentration Limit for Suspended Sediment

The characteristics of method are taken into account to appropriately configure the upper concentration limit for suspended sediment based on the results of previous research. Examples of previous research on the upper concentration limit for suspended sediment are given in Section 8.2.3.3 of the appendix volume.

Configurations of the upper concentration limit for suspended sediment have been verified in actual sea areas, and these research results may be referenced. Fujita et al. (2010) used the methods proposed by Takahashi et al. (1999) and Ikeno et al. (2009) to verify the extent of topography change in Hachinohe port that resulted from the 1960 Chile tsunami, and obtained results showing good reproducibility in the case that an upper concentration limit for suspended sediment is 1 to 2%. Also, Imai et al. (2015) formulated the saturated suspended sediment concentration as a function of flow velocity in order to take into account that the saturated suspended sediment concentration changed following water turbulence.

(4) Porosity

The porosity of sediment is configured based on a general value. Takahashi et al. (1992) used 0.4 for it.

(5) Settling Velocity

The settling velocity of sand grains is calculated based on Rubey (1933) and other sources.

(6) Grid Size

An appropriate grid size is configured so that the tsunami flow velocity, which is important for the sediment transport simulation, is able to be reproduced.

6.7 Assessment of Debris

6.7.1 Behavior of Debris

6.7.1.1 Basic Approach

With regard to debris that is generated by tsunami, the behavior of debris needs to be understood in cases where it is conceivable there is the possibility of debris colliding with structures, equipment or other such items or the debris blocking water intake channels and other such pathways.

The behavior of debris during tsunami is based on the appropriate configuration which is in accordance with the temporal change of inundation depth, flow velocity, flow direction and other such characteristics, which are determined from a plane two-dimensional model that is based on the nonlinear long-wave theory. In recent years, research has been advanced on methods to analyze the behavior of tsunami and the behavior of debris (floating, collision, submersion, etc.) at the same time, and these methods may also be utilized after verifying the applicability of them.

6.7.1.2 Examples of Past Research Studies on Debris Numerical Methods

With regard to wood and lumber, Goto (1983) proposed a movement simulation where the inertia, the pressure gradient of water flow, additional mass, drift wood resistance and diffusion are taken into consideration in the movement of wood and lumber in a horizontal direction.

With respect to ships and vessels, Fujii et al. (2005) used the Distinct Element Method (DEM) to calculate the debris behavior of vessels and compared these with the results of hydraulic model experiments. This method is not only applicable to ships and vessels but also to other types of debris. In addition, Kobayashi et al. (2005), Honda et al. (2009) and Hashimoto et al. (2010) have proposed methods for calculating the behavior of ships and vessels using a momentum equation where surging, swaying and yawing are taken into consideration. Also, in recent years, the methods have been proposed that include a method in which a solid-gas-liquid multi-phase model for conducting flow simulation including solid phase is used (Kawasaki et al., 2007), a method to solve a momentum

equation where three translational degrees of freedom and three rotational degrees of freedom are taken into consideration (Yoneyama and Nagashima, 2009), a method in which the particle method is applied to calculate behavior of debris (Goto et al., 2009), and a method coupling the Distinct Element Method (DEM) to the gas-liquid two-phase model to calculate behavior of debris (Ikeda and Arikawa, 2014).

Examples of calculations of debris numerical methods are given in Section 8.3.3 of the appendix volume.

6.7.2 Calculation of Impact Force Attributable to Debris

6.7.2.1 Selection of Debris and Collide Objects

In calculating the impact force due to debris, objects which becomes debris are selected on the basis of the results of surveys of debris as presented in Section 3.5 of main volume as well as tsunami water level, flow velocity and other hydraulic quantity. The assessment method proposed by Ikeno and Tanaka (2003) is referenced with respect to the selection of objects which becomes debris. Also, in cases where the specifications of objects collided with are necessary for the calculation of impact force, objects collided with, which are object to assessment, are determined along with the selection of objects which becomes debris.

6.7.2.2 Calculation Method for Impact Force

In the assessment of the impact force of debris, calculations are performed by using the appropriate impact force calculation equation based on specifications of debris and drifting speed. The drifting speed is appropriately configured based on the hydraulic quantity (tsunami water level, inundation depth, flow velocity, flow direction, etc.) obtained from the results of numerical simulations based on nonlinear long-wave theory.

Specific details about impact force calculation equations for major debris, which have been proposed, are given in Section 8.3.1 of the appendix volume. With respect to impacts of debris, calculation equations to assess such impacts using “force” and calculation equations to assess such impacts using “energy” have been proposed, but, in this publication, calculation equations to assess impact of debris by means of “force” are compiled in Section 8.3.1 of the appendix volume.

6.7.2.3 Selection of Impact Force Calculation Equations

With regard to the impact force of debris, a variety of calculation equations have been proposed

for drift wood and containers. However, there are currently many points that have not been sufficiently clarified, and cases of verification and practical application are limited, and quantitative assessment methods have not been established. Accordingly, in the calculation of impact force attributable to debris, it is desirable to utilize a calculation equation after closely examining the underlying assumptions of various calculation equations with respect to debris, drifting, impact and other such elements. Examples of impact force calculation equations whose validity has been verified are given in Section 8.3.2 of the appendix volume.

[Chapter 6 References]

- Aida, I. (1969): Numerical Experiments for the Tsunami Propagation - the 1964 Niigata Tsunami and the 1968 Tokachi-oki Tsunami, Bulletin of the Earthquake Research Institute, University of Tokyo, Vol.47, pp. 673-700.
- Aida, I. (1975): Numerical Experiments of the Tsunami Associated with the Collapse of Mt. Mayuyama in 1792, Zisin: Journal of the Seismological Society of Japan, Second Series, Vol. 28, pp. 449-460 (in Japanese).
- Aida, I. (1977a): Numerical Experiments for Inundation of Tsunamis: Susaki and Usa, in Kochi Prefecture, Bulletin of the Earthquake Research Institute, The University of Tokyo, Vol.52, pp. 441-460 (in Japanese).
- Aida, I. (1977b): Simulations of Large Tsunamis Occurring in the Past off the Coast of the Sanriku District, Bulletin of the Earthquake Research Institute, The University of Tokyo, Vol. 52, pp. 71-101 (in Japanese).
- Annaka, T., K. Ota, H. Motegi, I. Yoshida, M. Takao and H. Soraoka (1999): Tsunami Inversion Based on the Shallow Water Theory, Proceedings of Coastal Engineering, JSCE, Vol. 46, pp. 341-245 (in Japanese).
- Arikawa, T., M. Ikebe, F. Yamada, K. Shimosako and F. Imamura (2005): Large-Scale Experiments of Tsunami Wave Force on Revetments and Land Structures, Annual Journal of Coastal Engineering, JSCE, Vol. 52, pp. 746-750 (in Japanese).
- Arikawa, T., F. Yamada and M. Akiyama (2005): Study of Applicability of Tsunami Wave Force in Three-Dimensional Numerical Wave Tank, Annual Journal of Coastal Engineering, JSCE, Vol. 52, pp. 46-50 (in Japanese).
- Arikawa, T. and M. Washizaki (2010): Large scale tests on concrete wall destruction by tsunami with driftwood, Journal of the Japan Society of Civil Engineers, Ser. B2 (Coastal Engineering), Vol. 66, No. 1, pp. 781-785 (in Japanese).
- Arimitsu, T., K. Ooe and K. Kawasaki (2012): Proposal of Evaluation Method of Tsunami Wave

- Pressure Using 2D Depth-Integrated Flow Simulation, Journal of the Japan Society of Civil Engineers, Ser. B2 (Coastal Engineering), Vol.68, No.2, pp. I_781-I_785 (in Japanese).
- Asakura, R., K. Iwase, T. Ikeya, M. Takao, T. Kaneto, N. Fujii and M. Ohmori (2000): Empirical Study of Wave Force Caused by Tsunami Overflowing Revetments, Proceedings of Coastal Engineering, JSCE, Vol. 47, pp. 911-915 (in Japanese).
- Asakura, R., K. Iwase, T. Ikeya, M. Takao, N. Fujii and M. Ohmori (2002): THE TSUNAMI WAVE FORCE ACTING ON LAND STRUCTURES, Proceedings of 28th International Conference on Coastal Engineering, Vol. 28, pp. 1191-1202.
- Ashida, K. and M. Michiue (1972): Study on Hydraulic Resistance and Bed-load Transport Rate in Alluvial Streams, Japan Society of Civil Engineers Collection of Papers and Reports, No. 206, pp. 59-69 (in Japanese).
- Cabinet Office (2005): Guidelines on Tsunami Evacuation Buildings, etc. (in Japanese).
- Cabinet Office (2012): Mega Earthquake Model conference for the Nankai Trough (Second Report) Tsunami Fault Model Compilation: Tsunami Fault Models and Tsunami Height and Inundation Areas, etc. (in Japanese).
http://www.bousai.go.jp/jishin/nankai/model/pdf/20120829_2nd_report01.pdf (Accessed on August 2016)
- Cerjan, C., D. Kosloff, R. Kosloff and M. Reshef (1985): A nonreflecting boundary condition for discrete acoustic and elastic wave equations, Geophysics, Vol. 50, No. 4, pp. 705-708.
- Central Disaster Management Council (2003): Calculation Method of Tsunami Source Area Using Inversion, Committee for Technical Investigation on Countermeasures for the Tonankai and Nankai Earthquakes (16th), Reference Material 2-7 (in Japanese).
- Coastal Development Institute of Technology (2010): Research and Development on CADMAS-SURF/3D, Report of Study Group on Application of Three-Dimensional Numerical Wave Tank to Maritime Structures Design, Coastal Technology Library, No. 39 (in Japanese).
- Electric Power Civil Engineering Association, Editor (1995): Design of Civil Engineering Structures for Thermal and Nuclear Power Plants; Supplemental Revised Edition, pp. 786-833 (in Japanese).
- Express Highway Research Foundation of Japan (1985): Research Report on Stability Assessment of Landslide Terrain, Japan Highway Public Corporation (in Japanese).
- Fire and Disaster Management Agency (2009): Investigative Report on Tsunami and Inundation Countermeasures for Hazardous Material Facilities (in Japanese).
- Fujii, N., M. Omori, M. Takao, S. Kanayama, H. Otani (1998): Study on Numerical Model of Topography Change due to Tsunami, Proceedings of Coastal Engineering, JSCE, Vol. 45, pp. 376-380 (in Japanese).

- Fujii, N., M. Omori, T. Ikeya, R. Asakura, T. Takeda, and K. Yanagisawa (2005): Numerical Analysis of Tsunami Debris in Ports, Annual Journal of Coastal Engineering, JSCE, Vol. 52, pp. 296-300 (in Japanese).
- Fujii, N., M. Ikeno, T. Sakakiyama, M. Matsuyama, M. Takao and T. Mukohara (2009): Hydraulic Experiment on Flow and Topography Change in Harbor due to Tsunami and Its Numerical Simulation, Journal of the Japan Society of Civil Engineers, Vol. 56, pp. 291-295 (in Japanese).
- Fujita, N., K. Inagaki, N. Fujii, M. Takao and T. Kaneto (2010): Study on Field Applicability of Estimation Model for Topography Change due to Tsunamis, Annual Journal of Civil Engineering in the Ocean, JSCE, Vol. 26, pp. 213-218 (in Japanese).
- Fukui, Y., H. Shiraishi, M. Nakamura and Y. Sasaki (1962): Tsunami Research (II) Bore-Type Tsunami Impact on Coastal Dike, 9th Coastal Engineering Committee Proceedings, pp. 50-54 (in Japanese).
- Goto, C. and Y. Ogawa (1982): Numerical Calculation Method Using the Leapfrog Method, Tohoku University of Engineering Department of Civil and Environmental Engineering Material, 52p. (in Japanese).
- Goto, C. (1983): Calculation of Outflow of Timber due to Tsunami, Proceedings of the 30th Japanese Conference on Coastal Engineering, pp. 594-597 (in Japanese).
- Goto, C. and N. Shuto (1983): Numerical Simulation of Tsunami Propagation and Run-up, Tsunamis: Their Science and Engineering, pp. 439-451.
- Goto, C. and K. Sato (1993): Development of Tsunami Numerical Simulation System for Sanriku Coast in Japan, Port and Harbour Research Institute, Vol. 32, No. 2, pp. 3-44 (in Japanese).
- Goto, H., H. Ikari, K. Tonomo, T. Shibata, Tomoya Harada and Atsunori Mizoe (2009): Numerical Analysis on Drifting Behavior of Container on Apron due to Tsunami by Particle Method, Journal of the Japan Society of Civil Engineers, Ser. B2 (Coastal Engineering), Vol. B2-65, No.1, pp. 261-265 (in Japanese).
- Goto, H., H. Ikari, T. Matsubara and T. Ito (2011): Numerical Simulation on Tsunami due to Sector Collapse by Solid-Liquid Two-Phase Flow Model Based on Accurate Particle Method, Journal of the Japan Society of Civil Engineers, Ser. B2 (Coastal Engineering), Vol. 67, No. 2, pp. I_196-I_200 (in Japanese).
- Hara, N., H. Iwase and C. Goto (1998): Multi-step Mixed Finite Difference Scheme for Nonlinear Dispersive Long Wave Theory, Proceedings of Coastal Engineering, JSCE, Vol. 45, pp. 26-30 (in Japanese).
- Hasegawa, K., T. Suzuki, K. Inagaki and N. Shuto (1987): A Study on the Mesh Size and Time Increment in the Numerical Simulation of Tsunamis, Proceedings of Japan Society of Civil Engineers, No. 381/II-7, pp. 111-120 (in Japanese).
- Hashi, K. and F. Imamura (2000): Study on Multi-Tsunami Source in the Case for the 1998 Papua

- New Guinea Tsunami, Proceedings of Coastal Engineering, JSCE, Vol. 47, pp. 346-350 (in Japanese).
- Hashimoto, T., S. Koshimura, E. Kobayashi, N. Fujii and M. Takao (2010): Development of Hazard Map in Waterfront Area by Ship Drifting and Grounding Model in Tsunami, Journal of the Japan Society of Civil Engineers, Ser. B2 (Coastal Engineering), Vol. 66, No. 1, pp. 236-240 (in Japanese).
- Hino, M. and E. Nakaza (1988): Application of New Non-Reflective Boundary Scheme to Plane Two-Dimensional Problems in Numerical Wave Motion Analysis, Proceedings of the 35th Japanese Conference on Coastal Engineering, pp. 262-266 (in Japanese).
- Hiraishi, T., H. S. and N. Hara (2001): Reproduction of Meiwa Yaeyama Earthquake-Tsunami with Landslide Tsunami Source Using Circular Slip Method, Proceedings of Coastal Engineering, JSCE, Vol. 48, pp. 351-355 (in Japanese).
- Honda, K., T. Tomita, D. Nishimura and A. Sakaguchi (2009): Numerical Modeling of Tsunami Drifted Bodies, Annual Journal of Civil Engineering in the Ocean, JSCE, Vol. 25, pp. 39-44 (in Japanese).
- Honma, M. (1940): Flow Rate Coefficient for Low-Overflow Dams, Journal of the Japan Society of Civil Engineers, Vol. 26, No. 6, pp. 635-645, No. 9, pp. 849-862 (in Japanese).
- Iizuka, H. and H. Matsutomi (2000): Estimation of Damage from Tsunami Inundated Flow, Proceedings of Coastal Engineering, JSCE, Vol. 47, pp. 381-385 (in Japanese).
- Ikeda, T. and T. Arikawa (2014): Study on the Drifting Container Motion by using Solid-Gas-Liquid Coupled CADMAS-SURF/3D, Journal of the Japan Society of Civil Engineers, Ser. B2 (Coastal Engineering), Vol. 70, No. 2, pp. I_331-I_335 (in Japanese).
- Ikeno, M. and H. Tanaka (2003): Experimental study on impulsive force due to collision of drifted body and Tsunami Run-up on Land, Proceedings of Coastal Engineering, JSCE, Vol. 50, pp. 721-725 (in Japanese).
- Ikeno, M., M. Matsuyama, T. Sakakiyama and K. Yanagisawa (2005): Empirical Research on Assessment of Tsunami Wave Force Acting on breakwater Accompanied by Soliton Fission and Breakers, Annual Journal of Coastal Engineering, JSCE, Vol. 52, pp. 751-755 (in Japanese).
- Ikeno, M., M. Matsuyama, Tsutomu Sakakiyama and Ken Yanagisawa (2006): Experimental study on Soliton Fission Tsunami Wave Force which Running up on Land, Annual Journal of Coastal Engineering, JSCE, Vol. 53, pp. 776-780 (in Japanese).
- Ikeno, M., T. Yoshii, M. Matsuyama and N. Fujii (2009): Estimation of Pickup Rate of Suspended Sand by Tsunami Experiment and Proposal of Pickup Rate Formula, Journal of the Japan Society of Civil Engineers, Ser. B2 (Coastal Engineering), Vol. 65, No.1, pp. 506-510 (in Japanese).
- Ikeno, M., N. Kihara and D. Takabatake (2013): Simple and Practical Estimation of Movement

- Possibility and Collision Force of Debris due to Tsunami, Journal of the Japan Society of Civil Engineers, Ser. B2 (Coastal Engineering), Vol.69, No.2, pp. I_861-I_865 (in Japanese).
- Imai, K., D. Sugahara, T. Takahashi, S. Iwama and H. Tanaka (2015): Numerical Study for Sediment Transport due to Tsunami Around the Kitakami River Mouth, Journal of the Japan Society of Civil Engineers, Ser. B2 (Coastal Engineering), Vol. 71, No. 2, pp. I_247-I_252 (in Japanese).
- Imamura, F., I. Yoshida and A. Moore (2001): Numerical Study on the 1771 Meiwa Tsunami at Ishigaki Island and the Movement of the Tsunami Stones, Tsunami Engineering Report, No. 18, pp. 61-72 (in Japanese).
- Imazu, Y., F. Imamura and N. Shuto (1996): Study on the Stability Condition at a Front for Flood Simulations, Japan Society of Civil Engineers 51st Annual Meeting Proceedings Part 2, pp. 242-243 (in Japanese).
- Iwasaki, T. and Y. Zemin (1974): Numerical Experiments of Sanriku Big Tsunami, Proceedings of the 21st Japanese Conference on Coastal Engineering, pp. 83-89 (in Japanese).
- Iwasaki, T. and A Mano (1979): Two-Dimensional Numerical Computation of Tsunami Run-ups in the Eulerian Description, Proceedings of the 26th Japanese Conference on Coastal Engineering, pp. 70-74 (in Japanese).
- Iwasaki, T., A. Mano and T. Arai (1981): Numerical Calculation of Tsunami at Ayasato-Minato, Proceedings of the 28th Japanese Conference on Coastal Engineering, pp. 79-83 (in Japanese).
- Iwase, H., T. Mikami and C. Goto (1998): Practical Tsunami Numerical Simulation Model by Use of Non-linear Dispersive Long Wave Theory, Journal of Hydraulic, Coastal and Environmental Engineering, JSCE, No. 600/II-44, pp. 119-124 (in Japanese).
- Iwase, H., C. Goto, K. Fujima and K. Iida (2002): The Dispersion Effect on the Propagation of Tsunami in Deep Sea Region, Journal of Hydraulic, Coastal and Environmental Engineering, JSCE, No. 705/II-59, pp. 101-114 (in Japanese).
- Japan Society of Civil Engineers, Editor (1999): Hydraulic Formula (1999 Edition), pp. 373-377 (in Japanese).
- Japan Society of Civil Engineers Nuclear Civil Engineering Committee (2002): Tsunami Assessment Method for Nuclear Power Plants in Japan (in Japanese).
- Kawamata, K., K. Takaoka, K. Ban, F. Imamura, S. Yamaki and E. Kobayashi (2005): MODEL OF TSUNAMI GENERATION BY COLLAPSE OF VOLCANIC ERUPTION: THE 1741 OSHIMA-OSHIMA TSUNAMI, Tsunamis: Case Studies and Recent Developments, pp. 79-96.
- Kawasaki, K., S. Yamaguchi, M. Hakamata, N. Mizutani and S. Miyajima (2006): Wave Pressure Acting on Drifting Body after Collision with Bore, Annual Journal of Coastal Engineering, JSCE, Vol. 53, pp. 786-790 (in Japanese).
- Kawasaki, K. and M. Hakamata (2007): Development of Three-Dimensional Numerical Model of

- Multiphase Flow “DOLPHIN-3D” and Dynamic Analysis of Drifting Bodies under Wave Actions, Annual Journal of Coastal Engineering, JSCE, Vol. 54, pp. 31-35.
- Kawasaki, K., S. Matsuura and T. Sakatani (2013): Validation of Free Surface Analysis Method in Three-Dimensional Computational Fluid Dynamics Tool “OpenFOAM”, Journal of the Japan Society of Civil Engineers, Ser. B3 (Ocean Engineering) Vol. 69, No. 2, pp. I_748-I_753 (in Japanese).
- Kihara, N. and M. Matsuyama (2010): On applicability of the hydrostatic 3-D tsunami analysis system to tsunami-induced sediment transport - Simulations of sediment transport around the Kirinda port induced by the Indian Ocean tsunami -, Central Research Institute of Electric Power Industry Reports, N09004 (in Japanese).
- Kihara, N., N. Fujii and M. Matsuyama (2012): Three-dimensional sediment transport processes on tsunami-induced topography changes in a harbor, Earth Planets Space, Vol. 64, pp. 787-797.
- Kihara, N., D. Takabatake, T. Yoshii, M. Ikeno, K. Ota and N. Tanaka (2012): Tsunami Fluid Force on Land Structures (Part I) - Numerical Study for Structures with Finite Width Under Non-Overflow Condition -, Central Research Institute of Electric Power Industry Reports, N12010 (in Japanese).
- Kihara, N., M. Matsuyama and N. Fujii (2013): A Probabilistic Approach for Debris Impact Risk with Numerical Simulations of Debris Behaviors, Journal of the Japan Society of Civil Engineers, Ser. B2 (Coastal Engineering), Vol. 69, No. 2, pp. I_341-I_345 (in Japanese).
- Kobayashi, A., Y. Oda, T. Toue, M. Takao and N. Fujii (1996): Research on Sediment Transport due to Tsunamis, Proceedings of Coastal Engineering, JSCE, Vol. 43, pp. 691-695 (in Japanese).
- Kobayashi, E., S. Koshimura and M. Kubo (2005): A Basic Study on Ship Drifting by Tsunami, Journal of the Kansai Society of Naval Architects, Japan, No. 243, pp. 49-56 (in Japanese).
- Kotani, M., F. Imamura and N. Shuto (1998): Tsunami Run-up Simulation and Damage Estimation by using GIS, Proceedings of Coastal Engineering, JSCE, Vol. 45, pp. 356-360 (in Japanese).
- Kuriki, M., T. Suetsugi, H. Umino, Y. Tanaka and H. Kobayashi (1996): Flood Simulation Manual (Draft), Public Works Research Institute Document No. 3400, p. 137 (in Japanese).
- Mansinha, L. and D. E. Smylie (1971): THE DISPLACEMENT FIELD OF INCLINED FAULTS, Bulletin of the Seismological Society of America, Vol. 61, No. 5, pp. 1433-1440.
- Ministry of Land, Infrastructure, Transport and Tourism National Institute for Land and Infrastructure Management (2012): Practical Guide on Requirement for Structural Design of Tsunami Evacuation Buildings, Technical Note National Institute for Land and Infrastructure Management, No. 673 (in Japanese).
- Ministry of Land, Infrastructure, Transport and Tourism Ports and Harbours Bureau (2013): Tsunami-Resistant Design Guideline for Breakwaters, 35 p. (in Japanese).
- Mizutani, S. and F. Imamura (2000): Experiments with Bore Wave Force Acting on Structures,

- Proceedings of Coastal Engineering, JSCE, Vol. 47, pp. 946-950 (in Japanese).
- Mizutani, S. and F. Imamura (2002): Proposal for Design External Force Calculation Flowchart Taking into Consideration Overflow and Impulsivity of Tsunami Bore, Proceedings of Coastal Engineering, JSCE, Vol. 49, pp. 731-735 (in Japanese).
- Morishita, Y. and T. Takahashi (2014): Accuracy Improvement of Movable Bed Model for Tsunamis by Applying for Kesenuma Bay when the 2011 Tohoku Tsunami Arrived, Journal of the Japan Society of Civil Engineers, Ser. B2 (Coastal Engineering), Vol. 70, pp. 491-495 (in Japanese).
- Nakagawa, T. and Y. Koyanagi (1991): Experimental Data Analysis Using Least Squares Method, University of Tokyo Press, 206p. (in Japanese).
- Nishimura, Y. and H. Shimizu (1993): Tsunamis Generated by Eruptions from Komagatake Volcano, Hokkaido, Japan, Bulletin of the Natural Disaster Science Data Center, Hokkaido, Vol. 8, pp. 17-28 (in Japanese).
- Nuclear Civil Engineering Committee Tsunami Evaluation Subcommittee (2007): Research for Developing Precise Tsunami Evaluation Methods, Japan Society of Civil Engineers, Ser. B, Vol. 63, No. 2, pp. 168-177 (in Japanese).
- Ohtani, H., M. Sakai, K. Ishino, S. Arakawa and N. Mizumukai (1998): A Control Method of Surging in Discharge Channel with Vertical Shafts, Annual Journal of Hydraulic Engineering, JSCE, Vol. 42, pp. 667-672 (in Japanese).
- Okada, Y. (1985): SURFACE DEFORMATION DUE TO SHEAR AND TENSILE FAULTS IN A HALF-SPACE, Bulletin of the Seismological Society of America, Vol. 75, No. 4, pp. 1135-1154.
- Omori, M., N. Fujii, O. Kyoya, M. Takao, Toshimichi Kaneto and Tsuyoshi Ikeya (2000): Numerical Simulation of Tsunami Water Level, Flow Velocity and Wave Force Overflowing Vertical Seawalls, Proceedings of Coastal Engineering, JSCE, Vol. 47, pp. 376-380 (in Japanese).
- OpenFOAM Foundation: OpenFOAM User Guide.
<http://www.openfoam.org/docs/> (Accessed on April 2016)
- Pham Van Phuc., M. Hasebe and I. Takahashi (2012): A Study on Three-Dimensional Tsunami Analysis Using VOF Method, Journal of the Japan Society of Civil Engineers, Ser. B2 (Coastal Engineering), Vol. 68, No. 2, pp. I_071-I_075 (in Japanese).
- Rubey, W. (1933): SETTLING VELOCITY OF GRAVEL, SAND, AND SILT PARTICLES, American Journal of Science, Vol. 25, pp. 325-338.
- Sakakiyama, T. (2012): Tsunami Inundation Flow and Tsunami Pressure on Structures, Journal of the Japan Society of Civil Engineers, Ser. B2 (Coastal Engineering), Vol. 68, No. 2, pp. I_771-I_775 (in Japanese).
- Sasahara, N. (2004): Numerical Simulation of the Tsunami Caused by the Sector Collapse of Mt. Mayuyama, Shimabara Peninsula, Kyushu in 1792, Report of Hydrographic and

- Oceanographic Researches, Vol. 40, pp. 63-72 (in Japanese).
- Satake, K. (1987): INVERSION OF TSUNAMI WAVEFORMS FOR THE ESTIMATION OF A FAULT HETEROGENEITY: METHOD AND NUMERICAL EXPERIMENTS, *Journal of Physics of the Earth*, Vol. 35, pp. 241-254.
- Satake, K. and Y. Kato, (2001): The 1741 Oshima-Oshima Eruption: Extent and Volume of Submarine Debris Avalanche, *Geophysical Research Letters*, Vol. 28, No. 3, pp. 427-430.
- Satake, K. and Y. Kato (2002): The 1741 Japan Sea tsunami caused by debris avalanche in the Oshima Oshima volcano, *Kaiyo Monthly Special Edition*, No. 28, pp. 150-160 (in Japanese).
- Satake, K. (2007): Volcanic origin of the 1741 Oshima-Oshima tsunami in the Japan Sea, *Earth Planets Space*, Vol. 59, pp. 381-390.
- Satake, K., Y. Fujii, T. Harada and Y. Namegaya (2013): Time and Space Distribution of Coseismic Slip of the 2011 Tohoku Earthquake as Inferred from Tsunami Waveform Data, *Bulletin of the Seismological Society of America*, Vol. 103, No. 2B, pp. 1473-1492.
- Shuto, N. (1986): Tsunamis and Countermeasures, *Proceedings of the Japan Society of Civil Engineers*, No. 369/II-5, pp. 1-11 (in Japanese).
- Sugino, H., Changjiang Wu, M. Korenaga, M. Nemoto, Y. Iwabuchi and K. Ebisawa (2013): Analysis and Verification of the 2011 Tohoku Earthquake Tsunami at Nuclear Power Plant Sites, *Journal of Japan Association for Earthquake Engineering*, Vol. 13, No. 2, pp. 2-21 (in Japanese).
- Takabatake, D., N. Kihara and N. Tanaka (2013): Numerical Study for the Hydrodynamic Pressure on the Front of Onshore Structures by Tsunami, *Journal of the Japan Society of Civil Engineers, Ser. B2 (Coastal Engineering)*, Vol. 69, No. 2, pp. I_851-I_855 (in Japanese).
- Takahashi, T., F. Imamura and N. Shuto (1992): Numerical Simulation of Topographical Change due to Tsunamis, *Proceedings of Coastal Engineering, JSCE*, Vol. 39, pp. 231-235 (in Japanese).
- Takahashi, T., N. Shuto, F. Imamura and D. Asai (1999): A Movable Bed Model for Tsunami with Exchange Rate between Bed Load Layer and Suspended, *Proceedings of Coastal Engineering, JSCE*, Vol. 46, pp. 606-610 (in Japanese).
- Takahashi, T., T. Kurokawa, M. Fujita and H. Shimada (2011): Hydraulic Experiment on Sediment Transport due to Tsunamis with Various Sand Grain Size, *Journal of the Japan Society of Civil Engineers, Ser. B2 (Coastal Engineering)*, Vol. 67, No. 2, pp. I_231-I_235 (in Japanese).
- Takahashi, K. and T. Tomita (2013): Simulation of the 2011 Tohoku Tsunami in Kuji Bay Using Three-Dimensional Non-Hydrostatic Numerical Model, *Journal of the Japan Society of Civil Engineers, Ser. B2 (Coastal Engineering)*, Vol. 69, No. 2, pp. I_166-I_170 (in Japanese).
- Takao, M., T. Tani, T. Kaneto, K. Yanagisawa and T. Annaka (2012): TSUNAMI INVERSION ANALYSIS OF THE GREAT EAST JAPAN EARTHQUAKE, *Proceedings of the International Symposium on Engineering Lessons Learned from the 2011 Great East Japan Earthquake*, pp. 622-631.

- Tanaka, H. (1985): Development of Mathematical Models for Tsunami Behavior on Coastal Zones, Central Research Institute of Electric Power Industry Reports, 385017, 46p. (in Japanese).
- Tanimoto, K., H. Tsuruya and S. Nakano (1984): Study on Tsunami Force and Causes for Damage of reclamation revetment at Nihonkai-Chubu Earthquake in 1983, Proceedings of the 31st Japanese Conference on Coastal Engineering, pp. 257-261 (in Japanese).
- Tanioka, Y. and K. Satake (1996): Tsunami generation by horizontal displacement of ocean bottom, Geophysical Research Letters, Vol. 23, No. 8, pp. 861-864.
- Tanioka, Y. and T. Baba (2004): Re-Estimation of Slip Distribution of the 1944 Tonankai Earthquake using the Tsunami Waveform Inversion, The Earth Monthly, Vol. 26, No. 11, pp. 755-758 (in Japanese).
- Tomita, T. and T. Kakinuma (2005): Storm Surge and Tsunami Simulator in Oceans and Coastal Areas (STOC), Report of the Port and Airport Research Institute, Vol. 44, No. 2, pp. 83-98 (in Japanese).
- Tomita, T. and K. Honda (2008): Application of Three-dimensional Non-hydrostatic Numerical Model to Tsunamis in Coastal Areas, Annual Journal of Coastal Engineering, JSCE, Vol. 55, pp. 231-235 (in Japanese).
- Tsubaki, T. (1974): Encyclopedia of Fundamental Civil Engineering Studies 7: Hydraulics II, 16p. (in Japanese).
- Tsuchiya, S., Y. Sato, M. Matsuyama and Y. Tanaka (2013): The Effect Generated by Calculation Method of the Sea Bottom Displacement on Tsunami Estimation: Three-dimensional Sea Bottom Crustal Movement Analysis, Journal of the Japan Society of Civil Engineers, Ser. B2 (Coastal Engineering), Vol. 69, No. 2, pp. I_441-I_445 (in Japanese).
- Watts, P., S. T. Grilli, D. R. Tappin and G. J. Fryer (2005): Tsunami Generation by Submarine Mass Failure II: Predictive Equations and Case Studies, Journal of Waterway, Port, Coastal, and Ocean Engineering, Vol. 131, No. 6, pp. 298-310.
- Yanagisawa, H., N. Fujii and T. Kaneto (2012): Study on Characteristics of the 1700 Cascadia Earthquake Tsunami along the Pacific Coast of Japan, Journal of the Japan Society of Civil Engineers, Ser. B2 (Coastal Engineering), Vol. 69, No. 2, pp. I_441-I_445 (in Japanese).
- Yoneyama, N., H. Nagashima and K. Toda (2008): Numerical Analysis for the Behavior of the Driftage with Tsunami Run-up Using FAVOR Method, Annual Journal of Hydraulic Engineering, JSCE, Vol. 52, pp. 1399-1404 (in Japanese).
- Yoneyama, N. and H. Nagashima (2009): Development of a Three Dimensional Numerical Analysis Method for the Drift Behavior in Tsunami, Journal of the Japan Society of Civil Engineers, Ser. B2 (Coastal Engineering), Vol. B2-65, No. 1, pp. 266-270 (in Japanese).